MODEL-BASED OPTIMAL CONTROL OF VARIABLE-SPEED AIR CONDITIONERS IN RESPONSE TO DYNAMIC PRICING IN SMART GRIDS

HU MAOMAO

PhD

The Hong Kong Polytechnic University

2019

The Hong Kong Polytechnic University

Department of Building Services Engineering

MODEL-BASED OPTIMAL CONTROL OF VARIABLE-SPEED AIR CONDITIONERS IN RESPONSE TO DYNAMIC PRICING IN SMART GRIDS

Hu Maomao

A thesis submitted in partial fulfillment of the requirements for the degree of Doctor of Philosophy

July 2018

CERTIFICATE OF ORIGINALITY

I hereby declare that this thesis is my own work and that, to the best of my knowledge and belief, it reproduces no material previously published or written, nor material that has been accepted for the award of any other degree or diploma, except where due acknowledgement has been made in the text.

_____ (Signed)

Hu Maomao (Name of student)

ABSTRACT

Abstract of thesis entitled:	Model-based Optimal Control of Variable-speed Air Conditioners in Response to Dynamic Pricing in Smart Grids
Submitted by :	Hu Maomao
For the degree of:	Doctor of Philosophy

at The Hong Kong Polytechnic University in July, 2018

Today's electrical grids are facing great challenges due to the harmful power imbalance between the supply and demand sides. The increasing penetrations of intermittent and unpredictable renewable resources, such as wind and solar energy, exacerbate this imbalance. Demand response (DR) is a cost-effective method to address this imbalance issue. With the assistance of smart grid technologies, such as smart meters and smart home energy manage systems (HEMSs), electricity end-use customers at the demand side are informed and enabled to take DR actions to reduce/shift power consumption and improve the grid reliability. Dynamic electricity pricing is the major DR program adopted by electric utilities and grid operators to encourage electricity end-users to take DR actions.

Buildings, as the major electricity consumers worldwide, have great responsibilities and potential to provide DR resources. Centralized heating ventilation and air conditioning (HVAC) systems and decentralized HVAC equipment, such as air conditioners (ACs) and heap pumps, account for a large proportion of the total electricity use in buildings. Their power consumption has a direct impact on power

grids. In the context of smart grids, building HVAC systems and equipment need to be not only energy-efficient, but also grid-friendly and grid-responsive to address the power imbalance issue effectively.

Unlike centralized HVAC systems in commercial buildings, which are enabled to fulfill automatic DR control by advanced building automation systems (BAS), residential HVAC equipment is still facing challenges to make automatic DR during peak demand periods. Although DR control of residential ACs has been widely studied, the residential ACs in the previous studies were almost all single-speed ACs with on-off control. On-off control carries the great disadvantage of undesired current peaks during state transitions. Single-speed ACs are also being gradually replaced by inverter ACs, which have greater energy efficiency in partial-load conditions. Inverter ACs can operate within a wide range of frequencies (20 to 100 Hz), which is accompanied by large variations in power consumption. The control algorithms of inverter ACs are more complicated than those of single-speed ACs. Two types of dynamic retail electricity pricings are widely used by most utilities in the United States: day-ahead pricing (DAP) and real-time pricing (RTP). For DAP, the prices for specific hourly intervals are announced to the end-consumers 1 day ahead. For RTP, the electricity prices are provided every 5 minutes based on the current electricity supply and demand of grid nodes. To conclude, the present thesis aims to develop model-based DR control methods for residential variable-speed ACs in response to two types of dynamic pricings, i.e. DAP and RTP.

Two types of model-based optimal DR control methods are developed in response to two major dynamic electricity pricings, respectively: 1) Indirect model-based optimal

control method in response to hourly day-ahead prices (DAP) via temperature set-point reset; 2) Direct model predictive control method in response to 5-minute real-time pricing (RTP) via operating frequency adjustment. Both DR control methods are developed based on the system model and the predictions of the influential variables, including the weather conditions, occupancy and RTPs. The system concerned in the present study is an integrated system consisting of an air-conditioned room and a variable-speed AC. Thus, simplified models for both room thermal dynamics and energy performances of AC are needed.

A semi-physical (grey-box) dynamic room thermal model is developed and validated for predicting the indoor air temperature under dynamic operating conditions. For the computational efficiency, the dynamic room thermal model is transformed from the form of ordinary differential equations (ODE) to stochastic discrete-time state-space representation. Random white Gaussian noise is added in the system model considering the uncertainties arising from the exogenous input variables and make the model more realistic. The state space model can be used to formulate convex optimization problems which in general can be conveniently solved by using state-of-the-art optimization techniques. The model parameters can be learnt by making effective use of the data available in the today's smart in-home sensors. Due to the simple structure and moderate computation load, the developed room thermal model is suitable for developing model-based optimal control of residential ACs in response to dynamic DR signals. A simplified energy performance model of variable-speed ACs is developed and validated to characterize the AC performances under various operating frequencies and environmental conditions. The proposed simply structured energy performance model of variable-speed ACs can be readily used by electrical

researchers and engineers for either model-based DR control in smart HEMSs or DR potential estimation of a single variable-speed AC or a large population of variable-speed ACs.

A model-based optimal control method is developed for variable-speed ACs in response to hourly DAP, which adopts a two-level hierarchy structure. The high-level controller, i.e., the supervisory controller, is used to output the optimal set-point scheduling for the low-level local PID controller. The local PID controller is used to track the optimal set-points. Optimal scheduling of indoor air temperature set-points is formulated as a nonlinear programming problem which seeks the preferred trade-offs among electricity costs, thermal comfort and peak power reductions. Genetic algorithm (GA) is used to search the optimal solution of the nonlinear programming problem. The test results show that the proposed model-based optimal control method can reduce the whole electricity costs and the peak power demands during DR hours while meeting thermal comfort constraints. Besides, sensitivity analyses on the trade-off weightings in the optimization objective function demonstrate that electricity costs, occupant comfort and peak power reductions are sensitive to the weightings and the use of the weightings is effective in achieving the best trade-off.

An MPC method is also proposed to directly control the operating frequency of variable-speed ACs in response to 5-minute RTP, which differs from the indirect DR control method (i.e., indoor air temperature set point reset). The major advantage of MPC is to take account of all the influential variables, such as weather conditions, occupancy, and dynamic electricity pricing, at the controller design stage while satisfying the system operating constraints. A simplified room thermal model in the

stochastic state-space representation and performance maps of an inverter AC are integrated into the MPC controller for online prediction of the thermal response of an air-conditioned room. Two types of MPC controllers are designed for comparison, including an ordinary MPC controller without DR function and a DR-enabled MPC controller. The test results show that compared to the conventional PID controller, the MPC controller can implement automatic and optimal precooling based on the predictions of dynamic weather conditions and occupancy. Besides, the DR-enabled MPC controller demonstrates great improvements in both peak power reduction and electricity cost savings and is thus more grid-friendly and cost-efficient.

To conclude, in order to make the residential variable-speed ACs grid-responsive and DR-enabled, two types of model-based optimal control methods are developed in response to two commonly used dynamic electricity pricings, i.e., DAP and RTP. The proposed DR control methods help to reduce the power consumptions during peak demand periods, reduce the electricity costs for end-use customers, and improve the grid reliability.

PUBLICATIONS ARISING FROM THIS THESIS

Journal Papers

2017 **Hu, M.**, Xiao, F., & Wang, L. (2017). Investigation of demand response potentials of residential air conditioners in smart grids using grey-box room thermal model. Applied Energy, 207, 324-335.

2018 **Hu, M.**, & Xiao, F. (2018). Price-responsive model-based optimal demand response control of inverter air conditioners using genetic algorithm. Applied Energy, 219, 151-164.

2019 **Hu, M.**, Xiao, F., Jørgensen, J.B., & Wang S. (2019). Frequency control of air conditioners in response to real-time dynamic electricity prices in smart grids. Applied Energy, 242, 92-106.

2019 **Hu, M.**, Xiao, F., Jørgensen, J. B., & Li, R. (2019). Price-responsive model predictive control of floor heating systems for demand response using building thermal mass. Applied Thermal Engineering, 153, 316-329.

2019 Shan, K., Wang, J., **Hu, M.**, & Gao, D.-c. (2019). A model-based control strategy to recover cooling energy from thermal mass in commercial buildings. Energy, 172, 958-967.

2019 **Hu, M.**, & Xiao, F. (2019). A simplified energy performance model of residential variable-speed air conditioners for building energy analysis. Science and Technology for the Built Environment. (Under review).

Conference Papers

2016 **Hu, M.**, & Xiao, F. (2016). Investigation of the Demand Response Potentials of Residential Air Conditioners Using Grey-box Room Thermal Model. 8th International Conference on Applied Energy, 8-11 October 2016, Beijing, China.

2017 **Hu, M.**, & Xiao, F. (2017). Model-based optimal load control of inverter-driven air conditioners responding to dynamic electricity pricing. 9th International Conference on Applied Energy, 21-24 August 2017, Cardiff, UK.

2018 **Hu, M.**, & Xiao, F. (2018). Model Predictive Control of Inverter Air Conditioners Responding to Real-Time Electricity Prices in Smart Grids. 5th International High Performance Buildings Conference, 9-12 July 2018, West Lafayette, IN, USA. **(1st place of the Best Student Paper Award)**

2018 Wang, L., Xiao, F., **Hu, M.**, Lu, T. (2018). Performance Analysis of a Novel Hybrid Energy Storage System for Distributed Energy Systems. International Conference on Cryogenics and Refrigeration, 12-14 April 2018, Shanghai, China.

2018 Wang, L., Xiao, F., Cui B., **Hu, M.**, Lu, T. (2018). Performance Analysis of Absorption Thermal Energy Storage for Distributed Energy Systems. 10th International Conference on Applied Energy, 22-25 August 2018, Hong Kong.

ACKOWLEDGEMENTS

I would like to express my sincerest gratitude to my supervisor Dr. Linda Fu Xiao for her readily available supervision, valuable suggestions, patient encouragement and continuous support during the course of this research. Also, I would like to thank Professor Shengwei Wang for his suggestions and support to me over the entire process of my Ph.D. study.

My sincere gratitude also goes to my fellow colleagues and friends. Their kind help and support motivated me to accomplish the study. I will always cherish the companionship developed through these memorable years.

Finally, I am truly grateful for the unconditional love and support from my beloved family: my parents and my sister. I am blessed and proud to have them in my life. Without the care and encouragement from them, I would not be able to commence and complete this journey. This thesis is dedicated to them.

TABLE OF CONTENTS

LIST OF FIGURES

LIST OF TABLES

NOMENCLATURE

A	area, m^2
A	system matrix in state-space model
AC	air conditioner
B	input matrix in state-space model
BAS	building automation system
C	electricity price
C	equivalent overall thermal capacitance, J/K
C	orifice coefficient
c	specific heat, J/K
C	output matrix in state-space model
CAV	constant air volume
CPP	critical peak pricing
DAP	day-ahead electricity pricing
DR	demand response

DSP	Duct static pressure
E	energy consumption during a period
E	disturbance matrix in state-space model
e	slack variable
EEV	electronic expansion valve
ERCOT	Electric Reliability Council of Texas
ETP	equivalent thermal parameter
FLC	fuzzy logic control
GA	genetic algorithm
h	specific enthalpy, J/kg
HEMS	home energy management system
HTC	heat transfer coefficient
HVAC	heating, ventilation and air conditioning
ISO	independent system operator
J	cost function
K	coefficients of PID controller

MAE	mean absolute error
MAPE	mean absolute percentage errors
MIMO	multiple-input multiple-output
MPC	model predictive control
N	operating frequency of compressor motor, Hz
NN	neural network
NTU	number of transfer unit
ODE	ordinary differential equation
P	power consumption, W
P	pressure, Pa
P	covariance matrix of state estimate error
PEV	plug-in electric vehicle
PID	proportional–integral–derivative control
PSO	particle swarm optimization
Q	cooling capacity of AC, W
Q	heat gains, W

Q	covariance matrix of process noise
R	equivalent overall thermal resistance, K/W
R	covariance matrix of measurement noise
RC	resistance-capacitance room thermal model
RMSE	root mean square error
RTO	regional transmission organization
RTP	real-time electricity pricing
SC	sub-cooling
SH	superheat
SHGC	solar heat gain coefficient
SVM	support vector machine
T	temperature, ℃
TMY	typical meteorological year
TOU	time-of-use pricing
TRA	trust region algorithm
V	effective displacement volume of compressor

v	measurement noise
VAV	variable air volume
VCC	vapor compression cycle
VFD	variable frequency drive
w	process noise
WWR	window-wall-ratio
$\dot{m}$	mass flow rate, kg/s

Greek symbols

α	heat transfer coefficient
α	weighting of thermal comfort
β	weighting of peak power
ε	heat transfer effectiveness
η	compressor efficiency
ρ	refrigerant density
ρ	penalty

Subscripts

c	condenser
comp	compressor
d	discrete-time
e	evaporator
ex	heat exchanger
ext	external surface of wall
i	inlet
in	indoor air
int	internal surface of wall
inter	internal heat gains
is	isentropic process
k	sampling time step
lb	lower bound
m	internal thermal mass
max	maximum
norm	nominal performance data

o	outdoor air/outlet
p	constant-pressure process
r	pressure ratio
real	real performance data
ref	refrigerant
set	set-point
solar	heat gain from solar radiation
sur	surface
thsh	threshold
TRN	TRNSYS
ty	typical
ub	upper bound
v	constant-volume process
w	wall
win	window

CHAPTER 1 INTRODUCTION

1.1 Background and Motivations

The power imbalance between the supply and demand sides is a critical issue faced by current electrical grids. The increasing penetrations of intermittent renewable energy resources, such as wind and solar energy, cause the deterioration of the imbalance situation. The smart grid has been gradually replacing the traditional electrical grid, which uses two-way information and communication technologies and computational intelligence to achieve a clean, secure, reliable, resilient, efficient and sustainable power system (Fang et al., 2012; Güngör et al., 2011; Ipakchi & Albuyeh, 2009). With the assistance of smart grid technologies, such as smart meters and smart home energy manage systems (HEMSs) (B. Zhou et al., 2016), the end-use customers are able to change their normal consumption patterns in response to changes in the price of electricity over time, or to the incentive payments at times of high wholesale market prices or when system reliability is jeopardized (U.S. Department of Energy, 2006). The actions made by the customers in response to the signals from utilities during peak demand periods is called demand response (DR). DR has short-term impacts on the electricity markets, resulting in economic benefits for both the customers and the grid operators. Moreover, in the long term, lowering the peak demand and improving the reliability of the power system can avoid additional capacity investments.

Buildings are responsible for around 40% of the total energy consumptions worldwide, and consume over 70% of the total electrical energy in the USA (Somasundaram et al., 2014) and over 90% of the total electricity in Hong Kong (Electrical and

Mechanical Services Department, 2017). As the major end-user of electricity, buildings have great responsibilities and potentials to provide peak power reductions during on-peak hours. Building owners should look beyond the buildings themselves and consider the impacts of buildings on power grids for the benefits of both power grids and building owners. For modern buildings, they need to be not only energy-efficient, green, sustainable, or intelligent but also grid-friendly and gird-responsive (S. Wang, 2016; S. Wang et al., 2014).

Centralized heating ventilation and air conditioning (HVAC) systems in commercial and industrial buildings and decentralized HVAC equipment in residential buildings, such as air conditioners (ACs) and heap pumps, account for a large proportion of the total building electricity use. Their power consumptions have direct impacts on power grids (Electrical and Mechanical Services Department, 2017). According to California energy demand report, HVAC systems are the major contributors to most of the peak power demands in summer in California (California Energy Commission, 2000). DR control of building HVAC systems and equipment is considered as one of the most promising solutions to grid power imbalance issue.

In commercial buildings, DR technologies such as the use of building thermal mass (P. Xu & Haves, 2006; Yin et al., 2010) and thermal energy storage systems (Cui et al., 2015; Patteeuw et al., 2015; Ruan et al., 2016) have been adopted to reduce and shift power consumptions of large centralized HVAC systems. Centralized HVAC systems are normally managed by advanced building automation systems (BAS) and professional engineers, which enable them to fulfill automatic DR control. Residential

HVAC equipment, is still facing challenges to make automatic DR during peak demand periods.

Single-speed ACs with on-off control are the first generation of ACs and widely used in residential buildings. The indoor air temperature is controlled by switching on and off the compressor. However, the state transitions have a big disadvantage of undesired current peaks (Aswani et al., 2012). For this reason, residential ACs have been improved from the single-speed to variable-speed ACs, which have gained an increasing market share in recent years due to its higher efficiency under part-load conditions (Qureshi & Tassou, 1996). DR control strategies of residential single-speed ACs have been extensively studied in the literature, however, few studies have been carried out on variable-speed ACs. Thus, the present thesis aims at developing automatic DR control strategies/methods for residential variable-speed ACs in response to dynamic electricity pricings.

Energy-efficiency is the major consideration in the developments of residential variable-speed ACs in recent decades. Various control methods have been developed to improve the energy efficiency of variable-speed ACs, such as proportional-integral-derivative (PID) control, fuzzy logic control and artificial neural networks (ANNs) (Asakawa & Takagi, 1994; Chiou et al., 2009; Ekren et al., 2010; Soyguder et al., 2009; J. Wang et al., 2006). In the context of smart grids, the new control method for variable-speed ACs needs to be able to respond to dynamic pricing or other incentive signals from grid operators with the assistance of advanced information and communication technologies and intelligent control and automation techniques. As a result, the ACs can help to reduce the power consumptions during on-peak periods

and save electricity bills for end-use customers. To conclude, being gird-friendly, grid-responsive and DR-enabled is the new important feature for the next generation of residential ACs.

The residential ACs still need to satisfy the thermal comfort of occupants while making demand response. The simplest way of achieving DR from residential ACs is to directly limit the power consumption when the prices are high. However, this will, inevitably, result in the thermal discomfort. Precooling the building using the building thermal mass is a promising solution to address this issue (Sun et al., 2012; Turner et al., 2015; P. Xu et al., 2004; Yin et al., 2010). For example, residential ACs can start up in advance before the room is occupied to precool the room when the prices are low. When the prices are high, the residential ACs can turn off or run at a low operating frequency to reduce the power consumption. In this way, the thermal comfort could be guaranteed by using the stored cooling in the building.

However, the determination of the start-up time and duration of the precooling is a great challenge. The start-up time and duration of the precooling should be different for rooms with different thermal masses, which are also influenced by the dynamic weather conditions and occupancy profiles on different days. To simultaneously consider the thermal characteristics of the room and all the influential variables including weather conditions, occupancy profile and dynamic electricity pricing, advanced model-based optimal control strategies/methods are needed to automatically determine the optimal precooling start-up time and duration under various operating conditions.

Two types of dynamic electricity pricings are widely used by most utilities in the United States, i.e., day-ahead pricing (DAP) and real-time pricing (RTP) (Federal Energy Regulatory Commission, 2014). For DAP, the prices at hourly intervals are announced to the end-consumers one day ahead. For RTP, the electricity prices are offered every 5 minutes based on the current electricity supply and demand of grid nodes. To respond to hourly DAP, the indirect model-based control method is competent, which usually adopts a two-level hierarchy structure. The high-level controller, i.e., the supervisory controller, is used to set the optimal set points for the low-level local controllers. The local controllers, e.g., the on-off controller and PID controller, are used to track the set points and output the command signals for actuators such as rotational speed of compressor and opening degree of valve.

However, the indirect model-based control method is incompetent for variable-speed ACs to respond to 5-minute RTP. There are two major reasons: 1) Due to the thermal mass, the change in the indoor air temperature is much slower than the response speed of a controller. That means if we adjust the temperature set-points every 5 minutes to respond to real-time pricing, the indoor air temperature could not track the frequently changed set-points well. 2) Direct control of the compressor frequency is closely relates to the power consumption, which is more effective in shifting power consumption than adjusting the temperature set-points of a local controller every 5 minutes. Thus, there is a lack of frequency-based optimal DR control method for variable-speed ACs in response to RTP.

Model predictive control (MPC) is a promising method for frequency-based DR control of residential variable-speed ACs, which has been shown the superiority in

energy-efficient/cost-effective based optimal control of building energy systems. The major advantage of MPC is that it can simultaneously take account of all the influential variables at the controller design stage while satisfying the system operating constraints. In this study, we make the first attempt to apply MPC method to directly control the operating frequency of variable-speed ACs in response to RTP.

1.2 Aim and Objectives

The aim of the present study is to develop two types of model-based optimal DR control methods for residential variable-speed ACs in response to two types of dynamic electricity pricings, respectively: 1) Indirect model-based optimal control method in response to hourly day-ahead pricing by optimal scheduling of temperature set-point; 2) Direct model predictive control method in response to 5-minute real-time pricing by direct control of operating frequency of AC.

To achieve the aim, the following objectives are set and attained in this study:

(1) To develop and validate a semi-physical (grey-box) room thermal model for predicting the indoor air temperature under dynamic operating conditions. The model parameters can be learnt by making effective use of the data available in the today's smart in-home sensors. Due to the simple structure and moderate computation load, the developed room thermal model is suitable for the applications in the HEMSs, such as model-based optimal control of residential ACs in response to dynamic DR signals.

(2) To develop a methodology to transform the model in the form of ordinary differential equations (ODE) to stochastic discrete-time state space model. In

order to make the model more realistic, random white Gaussian noises are added into the system model. The state space model explicitly expresses the relationships between the outputs and inputs. Moreover, it can be used to formulate convex optimization problems which in general can be conveniently solved by using state-of-the-art optimization techniques.

(3) To develop and validate a simplified energy performance model of variable-speed ACs to characterize the AC performances under various operating frequencies and environmental conditions. The proposed simply structured energy performance model of variable-speed ACs can be readily used by electrical researchers and engineers for either model-based DR control in smart HEMSs or DR potential estimation of a single variable-speed AC or a large population of variable-speed ACs.

(4) To develop and validate a model-based optimal control method for variable-speed ACs in response to hourly DAP. The proposed model-based optimal control method is intended to be implemented in the smart HEMSs and enable the residential variable-speed ACs to achieve the optimal trade-offs among electricity costs, occupant comfort and peak power reductions during DR hours.

(5) To develop and validate a frequency-based model predictive control method for variable-speed ACs in response to 5-minute RTP. The advanced MPC method is intended to directly control the operating frequency of variable-speed AC while considering all the influential variables including weather conditions, occupancy and RTP.

(6) To develop a TRNSYS-MATLB co-simulation testbed to test the performances of various control methods using the integrated building energy

system. Instead of using the typical meteorological year (TMY) weather data at hourly intervals, historical weather data from local observatory are used for the tests.

1.3 Organization of the Thesis

The whole thesis is divided into 9 chapters. Figure 1.1 shows the outline of the present study.

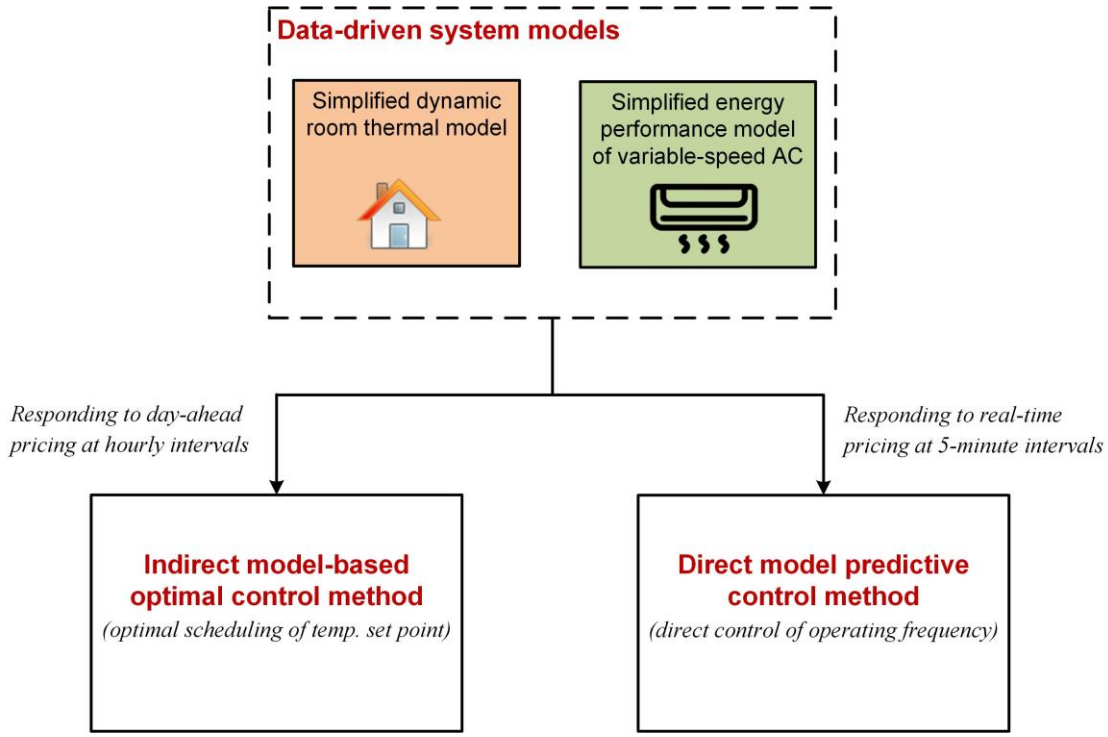

Figure 1.1 Outline of the present study.

The main content of each chapter is presented as follows.

Chapter 1: The background and motivation of the present study is outlined, which is to develop model-based control strategies/methods for residential variable-speed ACs in response to two widely-used electricity pricings, i.e., DAP and RTP, with the

assistance of advanced information and communication technologies and computational intelligence techniques in smart grids. The aim/objectives and thesis organization are presented.

Chapter 2: Literature survey is conducted in terms of DR in smart grids, DR control strategies for buildings, dynamic room thermal model and performance model of ACs. Research gaps are then summarized.

Chapter 3: This chapter introduces the frameworks of two types of DR control methods for variable-speed ACs: (1) Indirect model-based optimal control method in response to hourly day-ahead pricing; (2) Direct model predictive control method in response to 5-minute real-time pricing. The reason why the direct MPC controller is needed is explained. The detailed differences between the two types of DR control methods are compared. Both of the two DR control methods need to use the system model to predict the future evolutions of the system. Simplified models for both room thermal dynamics and energy performances of AC are needed. The procedure of developing the simplified models is introduced.

Chapter 4: This chapter introduces the development of simplified dynamic room thermal model for model-based online control. We propose an accurate semi-physical (grey-box) room thermal model for predicting the indoor air temperature under dynamic operating conditions. To improve the computational efficiency of both offline parameter identification and online model predictive control, the ODE model is transformed to the stochastic discrete-time state space model. Pre-estimation and scaling approaches are proposed to pre-process the model parameters, which help to improve the accuracy and computational efficiency of the parameter identification

process. Three popular optimization techniques including trust region algorithm (TRA), genetic algorithm (GA) and particle swam optimization (PSO) are used for parameter identification. Case studies are carried out to validate the simplified room thermal model using field test data and simulation data.

Chapter 5: This chapter aims to develop a simplified energy performance model of variable-speed ACs and apply the model to model-based DR control. A simplified energy performance model structure of variable-speed ACs is proposed in the form of piecewise polynomial functions to characterize the performances of variable-speed ACs under various operating frequencies and environmental conditions. However, the AC manufacturers seldom provide enough data for coefficient identification. Thus, a steady-state physical model of variable-speed ACs is developed to generate enough performance data to identify the simplified AC model.

Chapter 6: This chapter presents a novel model-based DR control method for residential variable-speed ACs to automatically and optimally respond to day-ahead electricity prices. The proposed control-oriented room thermal model and steady-state energy performance model of variable-speed ACs in last two chapters are integrated to predict the coupled thermal response of the room and AC for the purpose of model-based control. Optimal scheduling of indoor air temperature set-points is formulated as a nonlinear programming problem which seeks the preferred trade-offs among electricity costs, thermal comfort and peak power reductions. Genetic algorithm (GA) is used to search the optimal solution of the nonlinear programming problem.

Chapter 7: Prior to applying MPC to the control of variable-speed ACs, the fundamentals behind the MPC method is first introduced including the general control

procedure of MPC and the features of critical components in MPC, such as cost function, dynamics, constraints and current state. The existing applications of MPC in the area of built environment control are then presented.

Chapter 8: In this chapter, we make the first attempt to use the advanced MPC method to directly control the operating frequency of variable-speed AC while considering all the influential variables including weather conditions, occupancy and RTP. The stochastic state-space room thermal model and the simplified energy performance model of variable-speed ACs are used for online predicting the future evolutions of the system. Based on the integrated thermal response model, we proposed two types of MPC controllers: an MPC controller without DR function and a DR-enabled MPC controller. A TRNSYS-MATLB co-simulation testbed is developed to test the performances of various control methods using the integrated building energy system.

Chapter 9: Main conclusions and contributions are summarized. Recommendations for the future study are presented.

CHAPTER 2 LITERATURE REVIEW

Since this study attempts to develop model-based DR control methods for variable-speed air conditioners in response to dynamic electricity pricings in smart grids, previous research efforts on DR measures and programs, dynamic pricings, DR control strategies for buildings, building thermal model and AC model are reviewed.

Section 2.1 presents an overview of DR and smart grid, typical DR measures and programs and potential benefits of DR. Section 2.2 presents the existing studies on DR control strategies for both commercial and residential buildings. Section 2.3 and Section 2.4 present the existing models for room thermal dynamics and AC energy performance, respectively.

2.1 Demand Response in Smart Grids

DR is the background of our research. Thus, in this section we presents the critical points of DR including the definition, the relationship with smart grids, the typical programs, the potential benefits and the enabling technologies.

2.1.1 Overview of DR and Smart Grids

DR refers to changes in electric usage by end-use customers from their normal consumption patterns in response to changes in the electricity prices over time, or to incentive payments designed to induce lower electricity use when wholesale market prices are high or when system reliability is jeopardized (Federal Energy Regulatory Commission, 2010; U.S. Department of Energy, 2006). The responses made by the customers during peak demand periods have short-term impacts on the electricity

markets, resulting in economic benefits for both the customers and the grid operators. Moreover, in the long term, lowering the peak demand and improving the reliability of the power system can avoid additional capacity investments.

Smart grid and DR are intrinsically linked in many areas of application (Federal Energy Regulatory Commission, 2010). The advancements of smart grid can apply digital technologies to the conventional grid and enable real-time communication and coordination of information among supply resources, demand resources and distributed energy resources (DER), which brings about high operating efficiency for grid operators(Güngör et al., 2011; Messner & Nadel, 2011). Smart grid technologies, such as smart meters, help to achieve the DR potential (Camyab, 2015). In turn, some benefits related to investment in the smart grid, such as change in electricity usage of customers in response to prices or signals from grid operators, are essentially DR actions.

2.1.2 Typical DR Measures and DR Programs

Classifications of DR measures

In general, DR participants can change their electricity usage in three possible ways (Siano, 2014):

1) **Demand shaving**. The customers can reduce their energy consumption using load curtailment strategies.
2) **Demand shifting**. The customers can move the energy consumption to a different time period, e.g., from high-price to low-price period.

3) **Onsite generation**. The customers can limit their dependence on the electric grid by using onsite standby distributed energy resources, such as wind and solar energy.

Customers can participate in DR programs directly with the utility or through an intermediary. In the electricity markets, the end-use customers are usually aggregated by intermediaries, normally called as aggregators, services providers or DR providers. According to the amount of the consumption within their facilities, customers can be divided into the following classes (Siano, 2014): 1) large commercial and industrial customer; 2) small commercial and industrial customer; 3) residential customer; 4) individual plug-in electric vehicle (PEV); and 5) fleet of PEVs.

Classifications of DR programs

In general, DR is divided into two basic categories, namely price-based programs, and incentive or event-based programs (Mohamed H Albadi & El-Saadany, 2007; M. H. Albadi & El-Saadany, 2008).

In price-based programs, the electricity price changes in different periods according to the electricity supply cost, including high price for peak period, medium price for off-peak and low-price for low-load period, and there is no incentive nor penalty for these programs. The types of price-based DR programs are as follows.

- **Time-of-use pricing (TOU):** the electricity prices are set for the specific time periods (e.g., on-peak period and off-peak period). These price settings aim to prompt end-users to shift their electricity usage from on-peak to off-peak

period for financial benefits, helping the grid improve load factor and reduce generation capacity(Torriti, 2012; Vanthournout et al., 2015).

- **Critical peak pricing (CPP):** it is a kind of TOU pricing in fact but with special prices for the peak demand days or hours when the prices can be several times higher than usual prices. When utilities observe or anticipate high wholesale market prices or power system emergency conditions, they may call critical events during a specified time period and the price for electricity during these time periods is substantially raised (Herter et al., 2007; Herter & Wayland, 2010).
- **Real-time pricing (RTP):** it is also called dynamic pricing, is that the electricity prices may change as often as hourly or even more quickly (e.g., 5 minutes). The real time prices are usually announced a day ahead or a few hours ahead(Avci et al., 2013; Chassin et al., 2015; S. Li & Zhang, 2014; Lujano-Rojas et al., 2012; Vrettos et al., 2013).

Incentive-based DR programs represent contractual arrangements designed by load-serving entities, policymakers, and grid operators for demand reductions from end-use customers at critical times called program events. These programs provide DR participants with monetary incentives to reduce load that are separate from, or additional to, those customers' retail electricity price. The forms of the incentives may be explicit bill credits or payments for load reductions (pre-contracted or measured). To determine the amount of the demand reductions for program participants, a method is usually specified to establish the baseline energy consumption which will be used for the calculation of demand reduction. The types of incentive-based DR programs are as follows.

- **Direct load control:** the electricity utilities have the access to directly control, such as turn off, the specific devices/systems of end-users by offering a certain payment based on the previous signed agreements. Direct load control is usually conducted during peak demand periods or emergency situations of the grid (Bargiotas & Birdwell, 1988; S. Wang & Tang, 2016; F. Zhang & de Dear, 2015; F. Zhang et al., 2016).
- **Interruptible/curtailable service:** customers on interruptible/curtailable service rates/tariffs receive a discount or bill credit in exchange for agreeing to reduce load during system contingencies. This program is mandatory for end-users and if they do not accomplish the load reduction signed ahead, they would be subject to penalties. The tariffs used for this program are always offered by an electric utility or load-serving entity that has the right to implement the program when necessary, which is the main difference with that for emergency DR and capacity-program alternatives (H. A. Aalami et al., 2010; Mohamed H Albadi & El-Saadany, 2007).
- **Demand bidding program:** this is a competitive and negotiated program. End-use customers offer their expected cost benefits and availabilities in power reduction in advance. After the market receives and accepts the offer, the end-use customers are expected to reduce the pre-determined load and will receive their stated payments. Otherwise, the end-users will be subject to penalties if they cannot finish the declared load reduction. The main difference between the demand side bidding and other demand side management methods is that demand side bidding involves the short-term discrete changes into individual load profiles of end-users while other demand side managements

involve sustainable and permanent changes into the load profiles (Bode et al., 2013; Cappers et al., 2013).

- **Emergency demand response program:** this DR programs provide incentives for end-users to reduce their power loads during grid reliability-triggered events, but load reduction is voluntary. Customers can decide/choose whether receive the payment and accomplish the load reduction when notified. If customers do not reduce their power use, they will not be penalized (H. Aalami et al., 2008).
- **Capacity-market programs:** as for this DR program, customers should achieve pre-signed load reductions with utility companies when facing the power grids contingencies. This program is mandatory and end-uses will be penalized if they do not reduce the power use when notified. Capacity market programs can be also viewed as a form of insurance. In exchange for being obligated to reduce power use when notified, participants can receive guaranteed payments (i.e., insurance premiums). Just like insurance, in some years power reductions for smart grids will not be required, even though participants are paid to be on call. Capacity market programs are typically offered by regional transmission organizations (RTOs) or independent system operators (ISOs) (H. A. Aalami et al., 2010; Cappers et al., 2010).
- **Ancillary services market programs:** this program allows end-users to bid load curtailments in wholesale market providers, ISO/RTO markets, as operating reserves. After their bids are accepted, the market price is paid to them for the commitment of being on standby. For end-users, being able to quickly reduce the consumption when a reliability event occurs is the key

requirement for ancillary-service markets. (Bode et al., 2013; Cappers et al., 2013).

2.1.3 Potential Benefits of DR

Financial and reliability benefits are the major two potential benefits of DR.

- **Financial benefits.** Customers can obtain monetary benefits including: (1) cost savings on customers' electric bills from shaving or shifting power consumptions during on-peak periods; (2) some explicit financial payments the customer receives for curtailing usage in a DR program. The benefits of DR programs are market-wide, and not only for program participants. An overall electricity price reduction is expected eventually because of a more efficient utilization of the available infrastructure. DR programs also result in an avoided or deferred capacity costs. The cascaded impact of DR programs includes avoided or deferred need for distribution and transmission infrastructure enforcements and upgrades. All of the avoided or deferred costs will be reflected in the price of electricity for all electricity consumers (Strbac, 2008).
- **Reliability benefits.** Reliability benefits refer to the reduced chance of losing services in blackouts. This benefit may be associated with an internalized benefit, in cases where the customer perceives (and monetized) benefits from the reduced likelihood of being involuntarily curtailed and incurring even higher costs, or societal, in which the customer derives satisfaction from helping to avoid widespread contingencies (Dodrill, 2011).

2.2 Demand Response from Buildings

2.2.1 Why Buildings and HVAC Systems Need to Be Grid-responsive?

Buildings are responsible for around 40% of the total energy consumptions worldwide, and consume over 70% of the total electrical energy in the USA (Somasundaram et al., 2014) and over 90% of the total electricity in Hong Kong (Electrical and Mechanical Services Department, 2017). As the major end-user of electricity, buildings have great responsibilities and potentials to provide peak power reductions during on-peak hours. Building owners should look beyond the buildings themselves and consider the impacts of buildings on power grids for the benefits of both power grids and building owners. For modern buildings, they need to be not only energy-efficient, green, sustainable, or intelligent but also grid-friendly and gird-responsive (S. Wang, 2016).

Heating, ventilation and air conditioning (HVAC) systems account for a large proportion of the total building electricity use. Their power consumptions have direct impacts on power grids (Electrical and Mechanical Services Department, 2017). According to California energy demand report, HVAC systems are the major contributors to most of the peak power demands in summer in California (California Energy Commission, 2000). DR management of building HVAC systems is considered as one of the most promising solutions to grid power imbalance issue. The development of smart grids imposes a new feature for HVAC systems and equipment, i.e., being grid-responsive.

2.2.2 DR Control Strategies for Commercial Buildings

Central HVAC systems are normally managed by advanced building automation systems (BAS) and professional engineers, which enable them to fulfill automatic DR control. This section describes the existing DR control strategies for air-conditioning system. Two main categories of DR strategies for HVAC systems were summarized by Watson et al. (Watson et al., 2006): (1) global temperature adjustment, and (2) air distribution and cooling system adjustment. Global temperature adjustment is carried out by increasing building zone temperature set-points during DR events. Air distribution and cooling system adjustment includes duct static pressure set-point reduction, fan speed limit, chiller demand limit, etc.

- **Global temperature adjustment**: this strategy allows commercial building operators to easily adjust the space temperature set-points for an entire facility by one command from one location. Typically, this is done from a screen on the human machine interface. In field tests, global temperature adjustment is shown to be an effective and least objectionable strategy of the HVAC DR strategies tested (Piette et al., 2004; Piette et al., 2006). It is most effective because it reduces the loads of all associated air handling and cooling equipment. This control strategy achieves even reduction of service level among all zones and can be activated automatically by remote signals or manually by building operators.

- **Passive thermal mass storage**: this method takes advantages of thermal mass of a building to reduce the peak load. In summer, the cooling can be charged in the building thermal mass during non-peak hours and discharged to reduce the cooling demand during peak period. As a result, the cooling demand load is shifted from

off-peak period to on-peak period. The building thermal mass is always cooled during unoccupied period when the comfort constraints are relatively relaxed. For example, precooling is always conducted in the morning. When the precooling is sufficient and the daytime cooling demand is low, the indoor air temperature may be possible to be ensured within the acceptable range during the peak period without any mechanical cooling (X. Li & Malkawi, 2016; P. Xu & Haves, 2006; P. Xu et al., 2004; Yin et al., 2010).

- **Duct static pressure (DSP) adjustment**: for variable air volume (VAV) systems, the DSP set-points should be high enough in order to provide enough pressure for each terminal (i.e., VAV box) to work properly. The measured point of DSP is always located about two-thirds of the way down the duct system. In the conditions of less demand, energy waste may occur. This is because the DSP set-points are higher than the need to meet demands and the openings of VAV boxes are nearly to be closed. During DR events, there is no doubt that reducing the DSP set-points can achieve some shed savings without any reduction in thermal comfort to the occupants. But additional shed savings would result in some VAV terminal boxes fully open because of the very low DSP set-points (Goddard et al., 2014).

- **Fan speed limit**: Like duct static pressure set point reduction mentioned above, this DR strategy is relevant to fans with variable frequency drives (VFD). During the DR event, the speed of the VFD is limited to a fixed value. To be effective, the fixed value must be lower than that under normal closed loop conditions. Fan speed limiting saves energy for the same reasons as duct static pressure set point reduction. Its effect on the air distribution systems and associated occupied zones

is somewhat less predictable because of the open-loop nature of the control. Fan speed limits may be useful as part of other DR strategies such as cooling system adjustments described below. This strategy may also be used on fans with inlet guide vanes (Lin et al., 2015).

- **Supply air temperature adjustment**: this method differs from constant air volume (CAV) and VAV systems. In a CAV system, the power demand can be reduced by increasing its supply air temperature set-point. In packaged direct expansion units and heat pumps, the savings will be achieved at each unit by reducing compressor load. For air handlers with cooling coils, the savings will occur at the central cooling plant. While, in a VAV system, this method causes the cooling supply to zones insufficient and each damper of VAV box will be fully opened to maintain its corresponding indoor air temperature set-point. The air delivery fan will be over-speeding because of the fully open dampers. If this method is implemented in such VAV system, the fan' speed of inlet guide vane would be fixed to avoid the over-speeding of fans to reduce the effectiveness of DR controls (Motegi et al., 2007).

- **Chilled water temperature adjustment**: the efficiency of chiller can be improved by increasing chilled water supply temperature. But this leads to the increase on chilled water flow and increase the power demand of variable speeds of chilled water pumps unless the speed of variable volume devices is limited. Therefore, the power reduction will be based on the trade-off between the reduced chiller power demand from increased efficiency and the increased distribution devices (e.g., pumps) (Su & Norford, 2015).

- **Chiller demand limit**: this strategy saves cooling demand by directly controlling the chiller compressor. If the chillers operate at nearly full load, this strategy is beneficial just by limiting the demand at the most efficient part - load operation. The chiller compressor adjusts its capacity based on the supply chilled water temperature. For a constant volume chilled water system, the pump power will not increase by limiting its demand capacity. For a variable volume system, the chilled water pumps speed up to increase chilled water flow to maintain the supply air temperature. When this strategy is employed, the chiller cannot provide more cooling than the demand limit allows. Therefore, the pump speed should be locked at the state prior to DR. Similarly, locking fan VFD or inlet guide vanes at the position prior to the DR operation is required to achieve demand savings (Tang et al., 2016).

2.2.3 DR Control Strategies for Residential Buildings

To fully exploit the DR potentials of residential electrical appliances, advanced metering infrastructure such as smart meters (Federal Energy Regulatory Commission, 2014) and HEMSs (B. Zhou et al., 2016) have been developed and implemented in many residential buildings, which provide great opportunities for residential ACs to achieve automatic DR.

Smart meter is an advanced meter that measures the electricity consumption hourly or more frequently, and provides bidirectional communications between residential end-users and electric utilities/third-party load aggregators (Depuru et al., 2011; Federal Energy Regulatory Commission, 2018). The major signals sent from utilities toward residential DR participants are dynamic electricity prices (Faruqui et al., 2010).

Residential DR participants can reduce the electricity use during high-price periods and shift the electricity use to low-price periods. Automatic DR control strategies are essential for residential electrical appliances to respond to dynamic pricing. Smart HEMSs facilitate the implementation of automatic DR control methods and strategies for residential appliances including ACs.

Many studies have been conducted on DR control of residential electric appliances in the dynamic pricing environment. The commonly used DR control method for residential ACs is indoor air temperature set-point reset based on the dynamic electricity prices. Chen et al. (Z. Chen et al., 2012) used stochastic optimization and robust optimization approaches to optimize the operation scheduling of six typical residential appliances based on real-time electricity prices. The objective was to minimize the whole-day electricity payment without largely sacrificing thermal comfort. A mixed-integer linear programming problem was formulated and solved by Hubert et al. (Hubert & Grijalva, 2012) to minimize electricity costs. Their study showed that advanced scheduling controllers implemented in HEMS were valuable to fully achieve the DR benefits. Li et al. (S. Li et al., 2014) investigated and compared different DR strategies for residential ACs under different dynamic electricity pricings and environmental conditions based on eQUEST simulations. Lujano-Rojas et al. (Lujano-Rojas et al., 2012) proposed an optimal energy management strategy for residential energy system consisting of renewable power generations and electrical vehicles based on real-time electricity prices. The optimized operation scheduling for household appliances and electrical vehicles reduced the electricity bills by 8% to 22% on typical summer days. Thomas et al. (Thomas et al., 2012) developed an intelligent AC controller which can provide the optimal comfort and cost trade-offs for the

residents by scheduling the AC on/off status. Yoon et al. (Yoon et al., 2014) proposed a price-responsive controller for residential HVAC system which enables to reset temperature set-point when the retail price is higher than the preset price. Simulation results showed that the DR controller can provide up to 10.8% energy cost savings and 24.7% peak power reductions. Hu and Xiao (Hu & Xiao, 2018) made the first attempt at automatic DR control of variable-speed ACs in response to day-ahead dynamic prices. The optimal set points for the next-day indoor air temperature were obtained by solving a compound objective function of electricity costs, peak power reduction, and thermal comfort using a genetic algorithm.

2.2.4 Conclusive Remarks

Although DR control methods of residential AC have been extensively studied, the ACs considered in previous studies were all single-speed ACs which only allowed on-off control. The on-off controlled ACs have a big disadvantage of undesired current peaks during state transitions (Aswani et al., 2012). The single-speed ACs are also gradually replaced by variable-speed ACs which have gained an increasing market share in recent years due to its higher efficiency under part-load conditions (Qureshi & Tassou, 1996). A major difference between single-speed and variable-speed ACs is the performances of the latter depend on not only the indoor and outdoor environmental conditions, but also the operating frequencies of the compressor motor. Therefore, the energy performance models of AC in previous residential DR research are not applicable for DR study of variable-speed AC.

In addition, conventional local control methods for variable-speed AC such as PID control, fuzzy logic control and artificial neural network, are incompetent to address

the DR optimization problems involving multiple objectives and multiple variables such as weather conditions, occupancy and dynamic electricity pricing (Henze et al., 2004; Y. Ma, A. Kelman, et al., 2012). Model-based optimal control method, as an advanced control approach, can simultaneously take account of all influential variables in a real process using model-based prediction techniques and optimally control the dynamic system by solving optimization problems.

2.3 Dynamic Room Thermal Model

Both electric utilities and smart HEMSs require the predictions of power reductions of residential ACs to implement DR strategies. For the former, many influential decisions on grid operations are made based on the predicted power reduction, such as generation and reserve planning, dynamic electricity prices and payments to homes joining DR program (Amini et al., 2013; Kamyab et al., 2016). For the latter, the widely adopted optimal load scheduling methods for DR in the presence of dynamic electricity pricings are also developed based on the predication of AC power consumption. Dynamic room thermal models are necessary to make prediction of the power consumption and power reduction of residential ACs.

2.3.1 Typical Room Thermal Models

There are a variety of available modeling methods for the analysis of energy use in buildings. They can be divided into three categories (Foucquier et al., 2013): white box method, black box method and grey-box method. Generally speaking, the white-box model can be used to solve the forward problems and the black box and grey box model can be used to solve the inverse problems (Rabl, 1988). It is hard to determine

which method is absolutely the best. To a large extent, the choice usually depends on the given information and the output requirements.

White box model

White box or physical techniques are based on the solving of equations describing the physical behavior of heat transfer in detail. Therefore, its solution heavily depends on the detailed description of model. The sophisticated simulation software packages, such as DOE-2 (Winkelmann et al., 1993), EnergyPlus (Crawley et al., 2000), and TRNSYS (S. A. Klein, 1979), are all used the white box method. But they require a large amount of detailed characteristics data as inputs and significant amount of CPU time, so simplified white box methods are used based on some assumptions. Unfortunately, due to the assumptions and the uncertainties induced by geometric and thermal parameters, even for the newly designed buildings, it is still hard to evaluate the accuracy degree of models.

Li et al. (S. Li et al., 2014) used the building model in eQUEST to investigate and compare different DR strategies for residential ACs under different dynamic electricity pricings and environmental conditions. Yoon et al. (Yoon et al., 2014) used the building model in EnergyPlus to test the proposed price-responsive control strategy for residential HVAC systems.

Black box model

In contrast to the white box models, black box models mainly use statistical tools and machine learning techniques to analyze a large amount of data, but don't require any physical building information. Thus, these models are well suitable when the building

physical characteristics are extremely poor or even not known. However, the black box model may not always reflect the actual physical behavior. In other words, the modelling results sometimes are difficult to interpret from the physical perspective and usually specific to the modelled case, not valid for others. Besides, it is both expensive and time-consuming to measure and collect a large amount of data when the black box methods are used.

Neural-network (NN) -based model is the most common back box model for the prediction of room thermal dynamics (Afram et al., 2017; J. Chen et al., 2018; Ferreira et al., 2012; Reynolds et al., 2018). Ferreira et al. (Ferreira et al., 2012) used radial basis function NNs to predict the room thermal comfort, which was assessed by predicted mean vote (PMV) index. The parameters in the NNs were identified using the multi-objective genetic algorithm. Reynolds et al. (Reynolds et al., 2018) developed zone-level artificial NNs to predict the energy consumption and indoor air temperature, which took weather, occupancy, set point schedule, and previous indoor air temperature as inputs. The NN model was trained using the simulation data from EnergyPlus.

In addition to NNs, support vector machines (SVMs) were applied to predict the cooling loads (Q. Li et al., 2009a, 2009b; Xuemei et al., 2010), energy consumptions (Che et al., 2012; Dong et al., 2005; Kavaklioglu, 2011), daily maximum temperature (Paniagua-Tineo et al., 2011) and short-term wind speed (K. Chen & Yu, 2014), respectively. Smarra et al. (Smarra et al., 2018) developed regression trees and random forests based on historical building data for data-driven predictive control.

Grey box model

Grey-box model, a hybrid of white box model and black box model, combines the basic prior knowledge of room thermal features with a reasonable amount of measured data to describe the building thermal performance. It bridges the gap between limited physical knowledge and limited sampled data. Moreover, in recent years the rapid developments of smart household monitoring, communication and automated control technologies and products, e.g., smart meters, and HEMSs, have facilitated the use of the grey-box techniques. The grey-box models can conduct the self-learning procedure by getting access to and making use of the real-time performance data from in-home smart meter readings. Then the identified models can be used for different purposes, e.g., forecasting and optimal supervisory control of energy consumption.

One of the most popular grey-box methods for modelling the building energy consumption is RC (resistance and capacity) thermal network model. Braun and Chaturvedi (Braun & Chaturvedi, 2002) proposed a thermal network model and trained it using one to two weeks of data to accurately predict transient building load. Wang and Xu (S. Wang & Xu, 2006; X. Xu & Wang, 2007) developed a genetic algorithm to estimate the lumped thermal parameters of building using a thermal network structure and operation data from site monitoring. Bacher and Madsen (Bacher & Madsen, 2011) used prior physical knowledge and a forward selection strategy to formulate a series of RC network models with different complexity. Then likelihood ratio tests were used to determine the performance of each model.

A widely used grey-box model for residential DR purpose is equivalent thermal parameter (ETP) model, which simplifies the room thermal dynamics as a second-order electric circuit analog. Lu (Katipamula & Lu, 2006; Lu, 2012) used the ETP

model to study the impacts of various residential HVAC control strategies on electric distribution feeder load profile during DR periods for both a single residence and a population of residences. Thomas et al. (Thomas et al., 2012) proposed an intelligent residential AC system controller which can provide optimal comfort and cost trade-offs for the resident using the ETP model. Zhang et al.(W. Zhang et al., 2013) adopted the ETP model to describe the thermal dynamics of each individual load and deal with a population of heterogeneous loads. Besides, GridLAB-D, an open-source power systems modeling and simulation environment, also use the ETP method to model the AC energy consumption (Pacific Northwest National Laboratory).

However, there are two main critical issues about the ETP model. First, the model is too simplified to consider the impacts of specific building features such as wall material, window arrangement, and internal thermal mass. The network structure of the required model should be more detailed and include more physical descriptions, and a moderate amount of data arising from smart in-home sensors should also be needed to train the model. Second, the values of the ETP model parameters were determined according to the room geometry and thermal parameters in a database developed over 20 years ago (Pratt et al., 1991). The room thermal parameters are only applicable to the residential buildings in the US. The architecture design and envelop thermal properties are very different from the high-rise residential buildings in modern cities like Hong Kong and Shanghai. The uncertainties of the parameters have significant impacts on the accuracy of the modelling results.

2.3.2 Conclusive Remarks

To conclude, considering the computational efficiency for online applications, grey-box room thermal model is a better choice for predicting the future thermal response of the room and the energy consumption of the HVAC system. It needs to capture adequate thermal behaviors of the system to keep its robustness under different operating conditions. It should also not be too complicated for online applications. It can make full use of the indoor air temperature data from smart in-home sensors to identify the unknown model parameters with the assistance of data-driven optimization techniques.

2.4 Performance Models of Air Conditioners

The thermal dynamic characteristics of AC are mainly determined by the components, which accomplish the vapor compression cycle (VCC). A cycling refrigerant serves as a medium to move energy in AC. The generic VCC consists of four major components: an evaporator, a compressor, a condenser, and an expansion device. For simplification purpose, additional components such as accumulators and receivers are usually not considered. Both evaporator and condenser are heat exchangers, transferring heat between two mediums without allowing them to directly contact. The refrigerant flow in each heat exchanger is said to be on the “refrigerant side”. The other medium with which the component exchanges energy, often air or a single-phase fluid, is said to be on the “secondary side”.

In a refrigerant-to-air system, up to four actuator inputs are used to control the operation of the VCC. They are the speed of the fan blowing air across the external

surfaces of the evaporator, the rotational speed of the compressor motor, the speed of the fan blowing air across the external surfaces of the condenser, and the opening degree of the expansion device. The fan speeds are fixed in some systems, leaving only two actuator inputs. The heat exchanger fans and compressor all consume electrical power in driving these actuators. Expansion devices may or may not consume electrical power as well depending on the type.

Figure 2.1 shows a schematic and typical Pressure-Enthalpy (P-h) diagram of a basic VCC. Refrigerant flows through the evaporator at low pressure side and absorbs energy from the secondary side of the evaporator, typically undergoing a phase change from two-phase to superheated vapor in the process. The refrigerant then flows into the compressor, where it is pressurized to a high-temperature superheated vapor. Next, the refrigerant enters the condenser, where it rejects energy to the condenser secondary side, typically changing to a subcooled liquid phase in the process. After exiting the condenser, the refrigerant flows through the expansion device. In the expansion device, its temperature and pressure are reduced, causing a phase change to a two-phase liquid before the refrigerant again enters the evaporator. In this way, the refrigerant is used as a means to “pump” energy from the evaporator secondary side to the condenser secondary side.

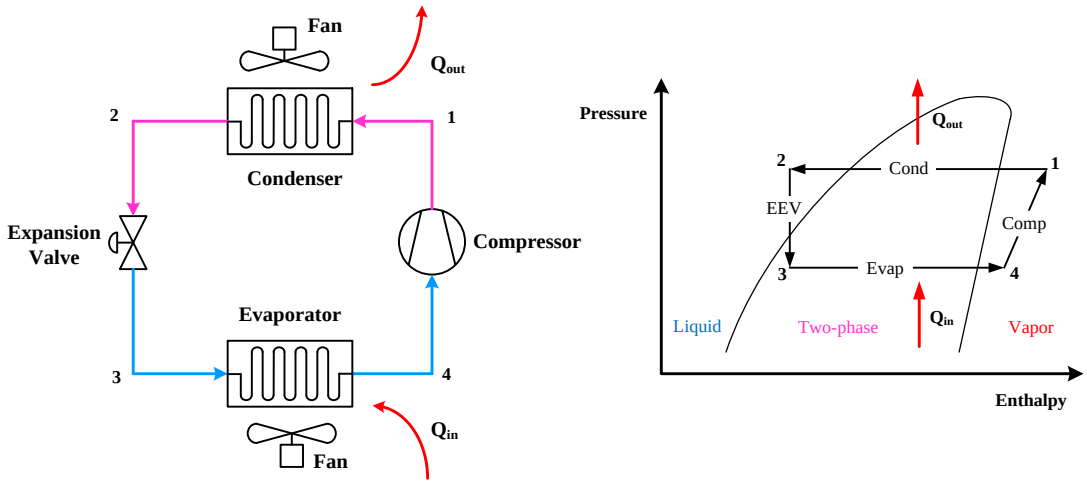

Figure 2.1 Schematic of VCC (left) and P-h diagram (right).

The typical phases at the entrance and exit of each heat exchanger during nominal operation are shown in Figure 2.1. However, this is not the case at all times. Startup or shutdown conditions, large disturbances on the secondary-side, or faults in control can all result in off-nominal phase flow combinations in the heat exchangers.

In general, the basic methods for modeling the VCC can be divided into two categories: empirical modeling and numerical modeling. According to scales of system time-regimes, both the empirical and numerical modeling can be further divided into transient and steady state modeling again. Typically, the transient state is the case when the system is started-up and is approaching steady state, or when it is shutdown from a steady state, or when it is disturbed from its steady state. Noted that the steady state of VCC in practice usually does not maintain for a long period, therefore a third time-regime in between the true steady state and non-steady state, termed the ‘quasi- steady state’, occurs more often. In that case, the VCC transient responses are much faster than the transients of the inputs. This means the refrigeration system switches the

operation conditions in a sequence of steady states. For such cases, steady-state modeling could be used to study dynamic behavior.

2.4.1 Empirical Models of ACs

Empirical steady-state model

The DOE-2, a widely used and accepted building energy analysis program, provides characteristic curves for cooling capacity and energy input ratio (EIR, the inverse of COP) of room air conditioners (York & Tucker, 1980). Dimensionless factors for cooling capacity and EIR are functions of the wet-bulb temperature of the outdoor air and dry-bulb temperature of the indoor air, and are mathematically express as a bi-quadratic equation. The characteristic curves have been widely used in the simulation of AC energy consumption (Pacific Northwest National Laboratory; Thomas et al., 2012). Meissner et al. (Meissner et al., 2014) trained this mathematical AC model by doing experimental tests on climatic chambers under a set of environmental conditions, then integrated the model into a building energy program. Cherem-Pereira and Mendes (Cherem-Pereira & Mendes, 2012) empirically modeled the total cooling capacity, the sensible cooling capacity and the Energy Efficiency Ratio of four room air conditioners in various environment psychrometric conditions. The obtained mathematical correlations were the functions of room air wet-bulb temperature and outdoor-side dry-bulb temperature.

Empirical transient model

Mulroy and Didion (Mulroy & Didion, 1985) experimentally studied refrigerant migration with time by installing pneumatic valves in the system. They showed that

during start-up more charge was in the evaporator but during steady-state operation it migrated to the condenser. Regression analysis was carried out on the experimental data to obtain the equation for instantaneous refrigeration capacity as a function of time, accounting for the transient loss due to both the thermal mass of heat exchangers and the refrigerant migration. Tree and Weiss (Tree & Weiss, 1986) developed a two time constant modeling approach for residential heat pump. The results showed that the two time constant approach can be used to model the change in air temperature as it flows over the indoor coil of a heat pump both in in the heating and cooling modes. Kim and Bullard (Kim & Bullard, 2001) tested the shutdown and startup characteristics of a residential R-410A air conditioner with a capillary tube. The test results showed that the cooling capacity and the coefficient of performance after startup can be expressed as the combination of two exponential functions of time, approaching the cooling capacity of steady-state. The cooling capacity and coefficient of performance (COP) were found to increase gradually and reach the steady-state values in about 15 min.

2.4.2 Numerical Models of ACs

Numerical steady-state model

Richardson et al. (D. Richardson et al., 2002; D. H. Richardson, 2006) developed the simulation tool “VapCyc” for the steady-state analysis of vapor compression cycles that allows the optimization of refrigerant charge and design for different components configurations. A correlation is used to capture the pressure drop in the heat exchangers, therefore the momentum balance equation is not included. Zhou and Zhang et al. (R. Zhou et al., 2010) developed the steady-state model of VCC and used

it to optimize the refrigeration system for high heat flux removal. A parametric study was performed to study the effect of various external inputs on the system performance using the developed steady-state model.

Numerical transient model

Transient modeling is the predictive analysis of the system' operation when disturbances come, and aims to improve the performance efficiency at local control levels. Therefore, the components in VCC usually need to be detailed and specific. For example, assuming the whole refrigeration system is at one steady-state operating point, due to the cooling demand of the air-conditioned room increases, the compressor motor will speed up to meet the sudden change of cooling capacity. However, the acceleration of compressor speed may increase the superheat in the evaporator, lowering the performance efficiency. Then, the expansion devices, like capillary tube, TEV and electronic expansion valve (EEV), will expand the opening degree to increase the mass flow rate. In this way, the refrigeration COP will be compensated to some extent. It normally takes around 100 seconds for the VCC system to arrive at another steady-state point.

Numerous studies in the literature have been dedicated to modeling VCC with various levels of details and emphasis on different parts of the system behavior. In this subsection, we introduce a few of them, which have inspired the present study in particular. Wedekind et al. (Wedekind et al., 1978) were among the first to study transient modeling of the two-phase flow dynamics in heat exchangers. To simplify the representation of two-phase flow, volumetric mean void fraction over the two-phase region was assumed. The mean void fraction assumption was applied almost

universally by other researchers developing moving boundary models, allowing the two-phase region to be modeled in lumped form. Chi and Didion's (Chi & Didion, 1982) model was among the few that works with the transient form of the momentum equation. A moving boundary lumped parameter formulation was used to model an air-to-air heat pump system. The dynamics of all components were considered, including the momentum of air flowing across the heat exchangers. Murphy and Goldschmidt (Murphy & Goldschmidt, 1985) developed simplified system models to study start-up and shutdown transients of an air-to-air system. In the start-up model, the target dynamics were those in the capillary tube and the phenomenon of liquid flowing back into the condenser during start-up. The compressor was modeled from steady-state measurements and actual measurements of evaporator performance were used in place of an evaporator model. The condenser dynamics modeled were those of the refrigerant pressure response and the tube material. In the shutdown study, both the heat exchangers were modeled as tanks containing two-phase refrigerant at different pressures to begin with, with air as the secondary fluid cooling or heating the coils by natural convection. MacArthur and Grald (MacArthur & Grald, 1989) presented one of the first fully distributed models, which adopted an unsteady compressible two-phase flow model to predict heat pump performance. This kind of model is known to be able to predict with a good accuracy dynamic evolutions of characteristics as superheat, spatial distributions of pressure and enthalpy, but the simulation time is not adapted to process control and optimization purposes.

2.4.3 Conclusive Remarks

Although DR of residential ACs has been extensively studied, the residential ACs in the literature were single-speed ACs with on-off control method. The on-off control has a big disadvantage of undesired current peaks during state transitions (Aswani et al., 2012). The single-speed ACs are also gradually replaced by the variable-speed ACs which have gained an increasing market share in recent years due to its improved efficiency at part-load conditions (Qureshi & Tassou, 1996). Hence further studies should be conducted to explore the DR potential and control methods of variable-speed ACs. One of the major challenges is the lack of a simple yet accurate variable-speed AC model. A major difference between single-speed ACs and variable-speed ACs is that the performances of variable-speed ACs are influenced by not only the indoor and outdoor environmental conditions, but also the operating compressor frequencies. Thus, the previous steady-state models are not applicable to variable-speed ACs.

As shown in the literature survey, AC models can be generally classified into transient models and steady-state models. The refrigerant dynamics in residential ACs are much quicker than the thermal dynamics of the room. The refrigerant re-distributions in different AC components normally accomplish in a short period, around 100 seconds (He et al., 1997; B. P. Rasmussen, 2005). Therefore, a steady-state AC model is sufficient to predict the coupled dynamic behaviors of the room and the AC under time-varying internal and external conditions.

2.5 Summary

This chapter presents a review on the DR in smart grids, DR control strategies for both commercial and residential buildings, dynamic room thermal model and performance model of ACs. From the above review, the following research gaps are identified:

i. Research on DR potential and DR control methods for residential variable-speed ACs are seriously insufficient and needs more efforts.

ii. Conventional local control methods for variable-speed ACs, such as PID control and fuzzy logic control, are incompetent to address the complicated problems, which are subject to multiple constraints (e.g., occupant's thermal comfort and system dynamics) and involve multiple variables (e.g., weather conditions, occupancy and dynamic electricity pricing) and multiple objectives (e.g., maximization of power reduction and minimization of operation cost). Model-based optimal control methods are competent, which can simultaneously take account of all influential variables in a real process using model-based prediction techniques and optimally control the dynamic system using optimization techniques.

iii. Unlike the day-ahead pricing (DAP) at hourly intervals, the real-time pricing (RTP) is provided every 5 minutes based on the current electricity supply and demand of grid nodes. Previous studies of DR control of residential appliances mainly targeted at DAP. There is a lack of DR control methods for responding to RTP. The widely used DR control strategy for ACs, i.e., optimal temperature set point reset, is incompetent for DR control of variable-speed ACs in response to RTP. Due to the thermal mass, the change in the indoor air

temperature is much slower than the response speed of an AC controller. If the temperature set points are adjusted every 5 minutes in response to RTP, the indoor air temperature could not track the frequently changed set points well. In order to respond to RTP every 5 minutes, direct control of the compressor frequency, which largely determines the AC power consumption, is more effective in regulating power consumption and hence more grid-friendly. New DR control methods are needed for achieving automatic DR from residential variable-speed ACs in response to RTP at 5-minute intervals.

iv. Considering the computational efficiency of online control, a simplified dynamic room thermal model is needed which can predict the thermal dynamics of the room under the future weather disturbances and occupancy.

v. For online applications, a simplified energy performance model of variable-speed ACs is needed to characterize the performances under various operating frequencies and environmental conditions. Due to its structural simplicity, it can be used by electrical researchers and engineers for either model-based DR control in smart HEMSs or DR potential estimation of a single or a large population of variable-speed ACs.

CHAPTER 3 FRAMEWORKS OF THE PROPOSED MODEL-BASED DEMAND RESPONSE CONTROL METHODS FOR VARIABLE-SPEED AIR CONDITIONERS

In order to automatically respond to dynamic electricity pricings, including hourly day-ahead pricing and 5-minute real-time pricing, two types of model-based DR control methods are developed in the present study:

- Indirect model-based optimal control method in response to hourly day-ahead pricing via temperature set-point reset;
- Direct model predictive control method in response to 5-minute real-time pricing via operating frequency adjustment.

This chapter presents the frameworks of the proposed two types of DR control methods for variable-speed ACs. Section 3.1 introduces the outlines of the online control parts and compares the differences between them in terms of input, output and optimization scheme. Section 3.2 introduces the procedure of developing the simplified models using data-driven techniques. The simplified system models are used in both model-based control methods.

3.1 Overview of the Two Control Methods in Response to Different Dynamic Pricings

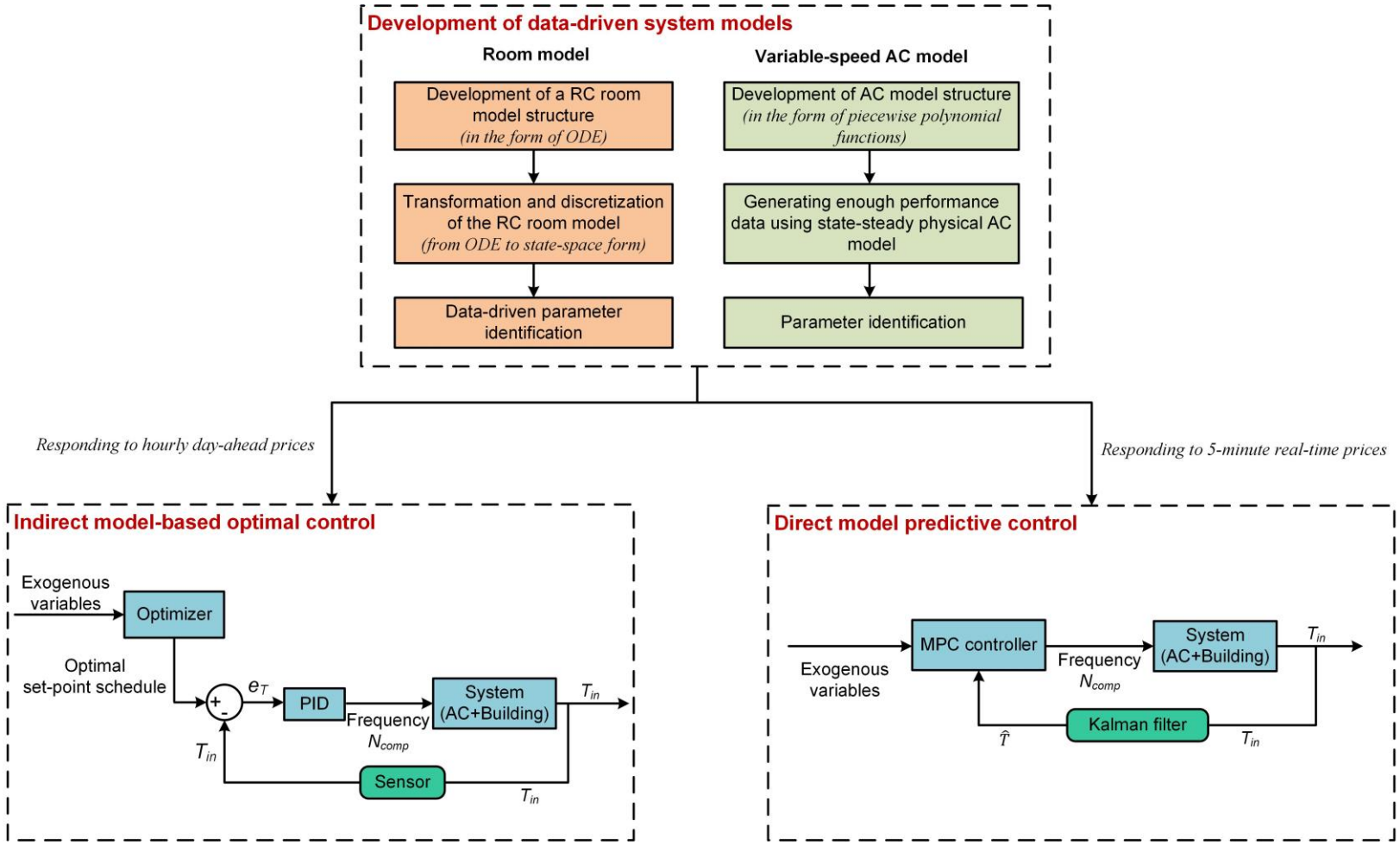

Figure 3.1 Block diagram of data-driven system modeling (top), indirect model-based optimal control method (bottom left) and direct MPC method (bottom right) for variable-speed ACs.

3.1.1 Indirect Model-based Optimal Control in Response to Hourly Day-ahead Pricing

Model-based optimal control, also known as supervisory control, has been used in the control of HVAC systems, which normally aims at minimizing the energy consumption or operating cost while satisfying thermal comfort when subject to the changing indoor and outdoor conditions as well as the characteristics of building and HVAC systems (S. Wang & Ma, 2008). The model-based optimal control in the literature usually adopted a two-level hierarchy structure in which the command signals for actuators such as rotational speed of compressor and opening degree of valve were sent by local controllers, e.g., the on-off controller and PID controller. The high-level controller, i.e., the supervisory controller, was used to set the optimal set points for the low-level local controllers.

This local-controller-based supervisory control is also adopted for the control of variable-speed air conditioners in response to hourly day-ahead pricing. The block diagram of indirect model-based optimal control method for variable-speed ACs is shown in the bottom left corner of Figure 3.1.

3.1.2 Direct Model Predictive Control in Response to 5-minute Real-time Pricing

In this study we also apply model predictive control method for directly regulating the operating frequencies of the compressors in variable-speed ACs to minimize the operating cost in the presence of real-time pricing. The major reasons for adopting the direct model predictive control method are given as follows:

1) Due to the thermal mass, the change in the indoor air temperature is much slower than the response speed of a controller. That means if we adjust the temperature set-points every 5 minutes to respond to real-time pricing, the indoor air temperature could not track the frequently changed set-points well.

2) Direct control of the compressor frequency is closely related to the power consumption, which is more effective in shifting power consumption than adjusting the temperature set-points of a local controller every 5 minutes.

The bottom right corner of Figure 3.1 shows the block diagram of direct model predictive control method for variable-speed ACs. The state-space room thermal model and performance maps of variable-speed AC are adopted in the MPC controller for online prediction of the system evolutions under the influence of predicted future exogenous variables such as weather conditions, occupancy and real-time pricing.

3.1.3 Comparison of the Two Control Methods

The differences in control logic between indirect model-based optimal control and direct model predictive control are shown in Figure 3.2. The detailed differences, including of input, output and optimization scheme, are listed in Table 3.1.

- **Input.** For both demand response control methods for variable-speed ACs, predictions of exogenous input variables, including weather conditions, occupancy, and dynamic electricity pricings are needed. The differences lie in the intervals of the price signal. The day-ahead pricing is at hourly intervals and the real-time pricing is at 5-minute intervals. Besides, the day-ahead pricing for the following day is fixed once it is determined at the midnight.

However, the real-time pricing is updated every 5 minutes based on the current electricity supply and demand of grid nodes.

- **Output.** The output of the model-based optimal control method is the scheduling of the temperature set-points for the local controller, such as PID controller or fuzzy logic controller. The local controller is responsible for tracking the dynamic set-points. However, the MPC controller is used to directly output the operating frequency of the compressor. Based on the differences in output signals, ‘direct’ and ‘indirect’ are used in the thesis to distinguish the two control strategies in a clearer way.

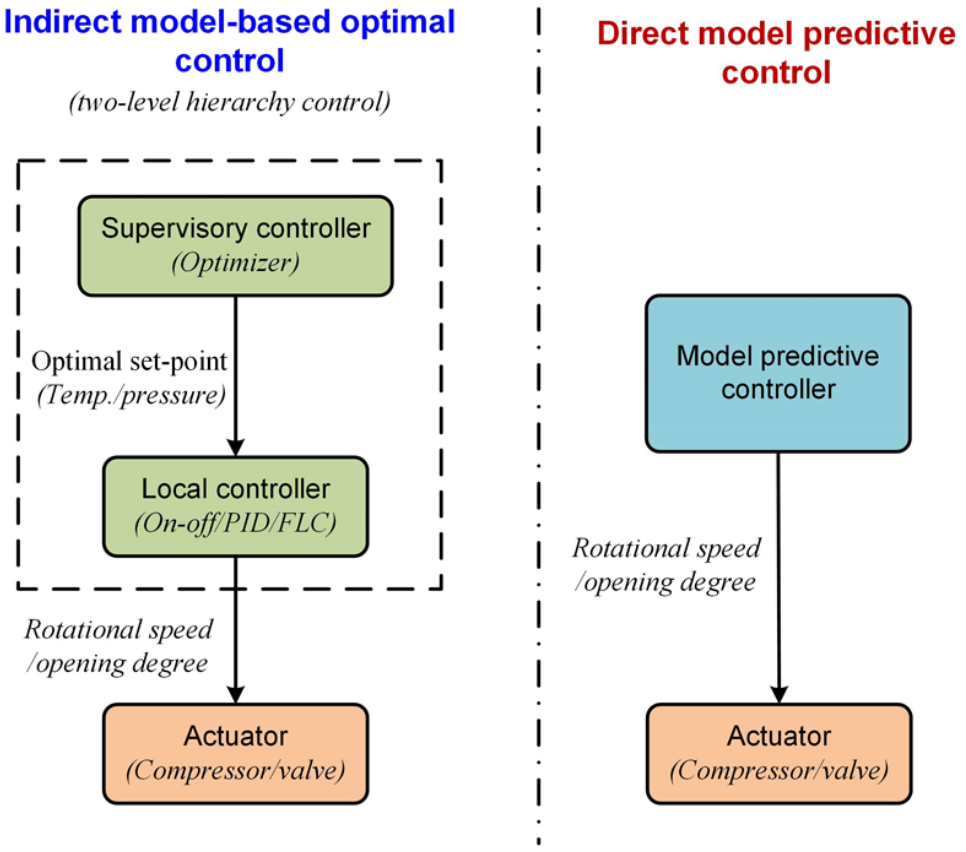

Figure 3.2 Comparison between indirect model-based optimal control and direct model predictive control for HVAC systems.

Table 3.1 Comparison between indirect model-based optimal control and direct model predictive control in terms of input, output, optimization times and allowed runtime.

DR control method	**Input** *(price signal)*	**Output**	**Number of optimization runs**	**Allowed optimization runtime**
Indirect model-based optimal control	Day-ahead pricing (hourly)	Optimal set-point for local controller	One-shot optimization	No strict requirement
Direct model predictive control	Real-time pricing (5-minute)	Optimal operating frequency for compressor	Receding horizon optimization	Less than prediction interval (5 minute)

- **Number of optimization runs.** Because the day-ahead pricing for the following day is fixed and will not be changed once it is determined at the midnight, the optimization in model-based optimal control is implemented only once, i.e., one-shot. However, the prediction of the real-time pricing is updated and announced every 5 minutes based on the supply and demand conditions. The optimization problem needs to be solved every 5 minutes based on the updated real-time prices. The essence of model predictive control is receding horizon control.

- **Allowed optimization runtime.** For the day-ahead pricing, the DR participants normally have access to the pricing signals at the midnight. The optimization solver has plenty of time to make the optimal decisions for the next day. However, in order to respond the 5-minute real-time pricing, the

optimal decision-making must be finished in 5 minutes, which proposes a high requirement for the formulation and solving of the optimization problem.

- **Practical implementation.** In practice, the two control strategies work independently, as the control output signals are different. For the indirect model-based optimal controller, the output signal is the set-point schedule, which is delivered to the programmable thermostat in AC. The whole optimization process could be implemented in external home energy management system. For the direct model predictive controller, the output signal is the operating frequency of variable-speed compressor. A dedicated controller needs to be embedded in AC to replace the conventional controller such as PID controller.

3.2 Development of Data-driven System Models

For both indirect model-based optimal control and direct model predictive control, simplified model of to-be-controlled system is needed for on-line applications. The target system in this study is an integrated system consisting of an air-conditioned room and a variable-speed AC. The AC delivers the cooling into the room to remove the accumulated heat and to maintain the temperature at the set-points or between the temperature ranges. Considering computational efficiency, both simplified dynamic room thermal model and energy performance model of variable-speed ACs are needed for online predictions.

For the dynamic room thermal model, it needs to be neither too simple nor too complex. It should be able to capture adequate thermal behaviors of the system to keep its

robustness under different operating conditions. Considering the computational efficiency, it should not be too complicated. To meet the aforementioned requirements, a semi-empirical (grey-box) resistance-capacitance (RC) dynamic room thermal model is first developed in the form of ordinary differential equations (ODE). To formulate convex optimization problems and to be conveniently solved using state-of-the-art optimization techniques, the model in the ODE form is then transformed and discretized to a state-space model. Before being used for online prediction, the unknown parameters in the grey-box room thermal model need to be identified using data-driven techniques.

AC models can be generally classified into transient models and steady-state models. The refrigerant dynamics in residential ACs are much quicker than the thermal dynamics of the room. The refrigerant re-distributions in different AC components normally accomplish in a short period, around 100 seconds (He et al., 1997; B. P. Rasmussen, 2005). Therefore, a steady-state AC model is competent to predict the coupled dynamic behaviors of the room and the AC under time-varying internal and external conditions. In view of this, we first develop a steady state physical model of variable-speed ACs. Performance maps of a variable-speed AC under typical operating conditions are then generated using the steady-state physical model.

3.3 Summary

In this chapter, we introduce the frameworks of two types of DR control methods for variable-speed ACs: (1) Indirect model-based optimal control in response to hourly day-ahead pricing; (2) Direct model predictive control in response to 5-minute real-

time pricing. In the former one, the outputs of the optimizer are the optimal scheduling of temperature set-points. The local controller, i.e., PID controller, is used to track the temperature set-points. In the latter one, the outputs of the MPC controller are the operating frequency of the compressor. The reason why the direct MPC controller is needed is explained. The detailed differences between the two types of DR control methods are compared.

Both of the two DR control methods need to use the system model to predict the future evolutions of the system. The target system in the present study is an integrated system consisting of an air-conditioned room and a variable-speed AC. Thus, simplified models for both room thermal dynamics and energy performances of AC are needed. The procedure of developing the simplified models is introduced.

CHAPTER 4 DEVELOPMENT OF A SIMPLIFIED DYNAMIC ROOM THERMAL MODEL FOR ONLINE APPLICATIONS

For both indirect model-based optimal control method and direct model predictive control method, a simplified model of room thermal dynamics is needed for on-line predicting the thermal evolutions of the target room. The room thermal model needs to be neither too simple nor too complex. It should be able to capture adequate thermal behaviors of the system to keep its robustness under different operating conditions. Considering the computational efficiency, it should not be too complicated. In this chapter, we aim at developing and validating a simplified room thermal model for online applications. Figure 4.1 shows the flow chart of the development of the simplified dynamic room thermal model.

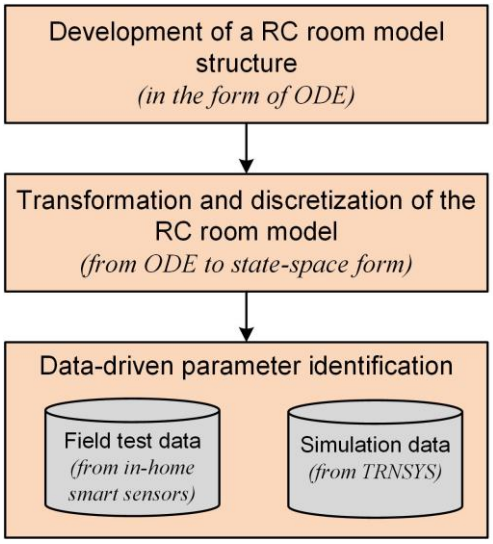

Figure 4.1 Flow chart of the development of the simplified dynamic room thermal model.

The whole chapter is organized as follows. Section 4.1 introduces the requirements for the dynamic room thermal model, which needs to be used for online predictions. Section 4.2 presents the structure of a semi-physical (grey-box) dynamic room thermal model in the form of ODE. In section 4.3, we transform the model from ODE form to stochastic discrete-time state space form so as to formulate convex optimization problems which can be conveniently solved using state-of-the-art optimization techniques. In Section 4.4, we propose the pre-estimation and scaling approaches to pre-process the model parameters, which help to improve the accuracy and computational efficiency of the parameter identification process. In Section 4.5, the proposed dynamic room thermal model is validated using both field test and simulation data.

4.1 Requirements for Online Applications

Building models used in popular building simulation tools such as TRNSYS (S. Klein et al., 2017), EnergyPlus (Crawley et al., 2000) and eQUEST(Hirsch, 2010) are not suitable for the development of model-based control methods since the complex building models are usually time-consuming. Besides, a large amount of building parameters are required as inputs in the simulation software, which is difficult even for the newly designed buildings.

A widely-used room thermal model for DR analysis is the equivalent thermal parameter (ETP) model, which simplifies the room thermal dynamics as a second-order electric circuit analog (Katipamula & Lu, 2006; Lu, 2012; Thomas et al., 2012; W. Zhang et al., 2013). However, the model is too simplified to consider the impacts

of specific building features such as wall material, window arrangement, and internal thermal mass. Moreover, the values of the ETP model parameters were determined according to the room geometry and thermal parameters in a database developed over 20 years ago (Pratt et al., 1991). The room thermal parameters are only applicable to the residential buildings in the US. The architecture design and envelop thermal properties are very different from the high-rise residential buildings in modern cities like Hong Kong and Shanghai. The uncertainties of the parameters have significant impacts on the accuracy of the modelling results.

In general, a simplified dynamic room thermal model is needed for online applications, which needs to be neither too simple nor too complex. It needs to capture adequate thermal behaviors of the system to keep its robustness under different operating conditions. Considering the computational efficiency, it should not be too complicated. To meet the aforementioned requirements, a control-oriented semi-physical (grey-box) dynamic room thermal model is developed in this study.

4.2 A Semi-physical Dynamic Room Thermal Model

In general, the room thermal dynamics can be expressed as a set of first-order ordinary differential equations containing several uncertain parameters to be identified. Figure 4.2 illustrates the components included in the model and the heat fluxes exchanged between them. The model mainly contains four parts, i.e., outdoor environment, building envelope, indoor air, and internal thermal mass.

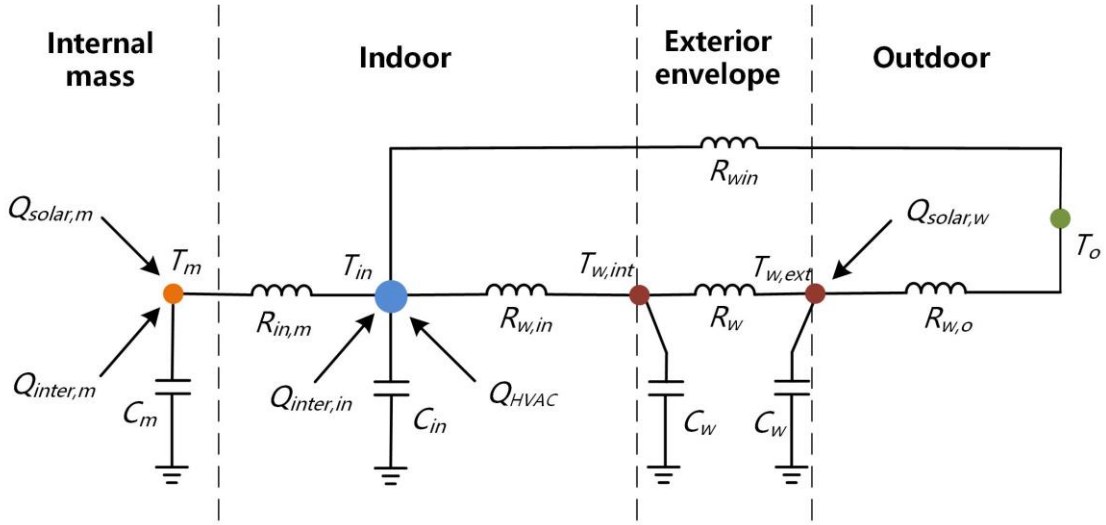

Figure 4.2 Schematic of the grey-box thermal model of residential buildings (5R4C).

The exterior building envelop consists of opaque walls and transparent windows. Considering the climate in Hong Kong, most residential buildings are constructed with light-weight wall and without thermal insulation. Therefore, it is reasonable to consider the external wall as one thermal resistance and two equal thermal capacitances (Seem, 1987). Two types of heat transfer on the external wall surface are considered, i.e., convective heat transfer with the outdoor air and radiative heat transfer with the sky. Heat flows through the windows consist of 1) conductive and convective heat transfer caused by the temperature difference between outdoor and indoor air, 2) solar radiation incident on the windows, either directly from the sun or reflected from the ground or adjacent buildings. The solar radiation through the window is first absorbed by the internal thermal mass constituted by floor, ceiling, partitions and furniture. Besides the solar radiation through the windows, the bulk of internal mass absorbs the heat from indoor heat sources as well. It then gradually transfers the heat into the space by heat convection. The air in the interior zone, which

exchanges heats with the internal thermal mass, internal wall surface and outdoor air through windows, is represented by a lumped node. Besides, the energy from the solar radiation, HVAC system, and internal heat sources (e.g., occupants, lights, and equipment) is assumed to be immediately absorbed by the indoor air.

The energy balances for the external and internal wall surfaces, the indoor air, and the internal thermal mass are given by Equations (4.1) – (4.4).

$$C_w \frac{dT_{w,ext}}{dt} = \frac{T_o - T_{w,ext}}{R_{w,o}} + \frac{T_{w,int} - T_{w,ext}}{R_w} + f_{solar,w} A_w I_{solar} \tag{4.1}$$

$$C_w \frac{dT_{w,int}}{dt} = \frac{T_{w,ext} - T_{w,int}}{R_w} + \frac{T_{in} - T_{w,int}}{R_{w,in}} \tag{4.2}$$

$$C_{in} \frac{dT_{in}}{dt} = \frac{T_m - T_{in}}{R_{in,m}} + \frac{T_{w,int} - T_{in}}{R_{w,in}} + \frac{T_o - T_{in}}{R_{win}} + f_{inter,in} Q_{inter} + Q_{HVAC} \tag{4.3}$$

$$C_m \frac{dT_m}{dt} = \frac{T_{in} - T_m}{R_{in,m}} + f_{solar,m} A_{win} I_{solar} + f_{inter,m} Q_{inter} \tag{4.4}$$

where R and C represent the overall heat resistance and capacitance; T denotes temperature; subscripts *in*, *o*, *w*, *int*, *ext*, *win* and *m* indicate indoor air, outdoor air, exterior wall, internal wall surface, external wall surface, window and internal mass, respectively; Q_{inter} denotes the internal heat gain; I_{solar} denotes the global solar radiation; A denotes the geometric area; f denotes the conversion coefficients for the heat gains, which are also identified together with R and C.

In the grey-box model, R, C and f are free parameters which need to be identified based on historical data. There are two points that should be noticed. 1) The free parameters for a time-invariant model are not functions of time, although the values of the

parameters actually change with time or under different weather conditions. For instance, when the outdoor wind speed increases, the convective heat transfer coefficient between the external wall surface and the outdoor air increases as well. The changes of these free parameters are so small that they are assumed to be fixed instead of being function of time. 2) *R* and *C* characterize the building inherent thermal features. It will make no difference to the identification results whether or not the heat gains from internal sources or HVAC are considered.

4.3 Stochastic Discrete-time State-Space Model Considering the Uncertainties

The dynamic room thermal model as described by the differential equations (4.1) – (4.4) is a multiple-input multiple-output (MIMO) system. State space models are commonly used for modeling MIMO systems because of their advantage in explicitly expressing the relationships between the outputs and inputs. In addition, they can be used to formulate convex optimization problems which in general can be conveniently solved by using state-of-the-art optimization techniques. In order to make the model more realistic, white Gaussian noise is added into the system model. Equations (4.1) – (4.4) can be converted into a continuous-time state-space model with unknown stochastic noise, as shown in Equations (4.5).

$$dT = (AT + Bu + Ed)dt + dw(t) \tag{4.5}$$

Where the system state $T = [T_{w,ext} \quad T_{w,int} \quad T_{in} \quad T_m]^T$;

the input vector $u = Q_{HVAC}$;

the disturbance vector $d = [T_o \quad I_{solar} \quad Q_{inter}]^T$;

the system matrix

$$A = \begin{pmatrix} \frac{-1}{C_w R_{w,o}} + \frac{-1}{C_w R_w} & \frac{1}{C_w R_w} & 0 & 0 \\ \frac{1}{C_w R_w} & \frac{-1}{C_w R_w} + \frac{-1}{C_w R_{w,in}} & \frac{1}{C_w R_{w,in}} & 0 \\ 0 & \frac{1}{C_{in} R_{w,in}} & \frac{-1}{C_{in} R_{w,in}} + \frac{-1}{C_{in} R_{in,m}} + \frac{-1}{C_{in} R_{win}} & \frac{1}{C_{in} R_{in,m}} \\ 0 & 0 & \frac{1}{C_m R_{in,m}} & \frac{-1}{C_m R_{in,m}} \end{pmatrix}_{4\times 4};$$

the input matrix $B = (0 \quad 0 \quad 1/C_{in} \quad 0)^T$;

the disturbance matrix $E = \begin{pmatrix} \frac{1}{C_w R_{w,o}} & \frac{f_{solar,w} \times A_w}{C_w} & 0 \\ 0 & 0 & 0 \\ \frac{1}{C_{in} R_{win}} & 0 & \frac{f_{inter,in}}{C_{in}} \\ 0 & \frac{f_{solar,m} \times A_{win}}{C_m} & \frac{f_{inter,m}}{C_m} \end{pmatrix}_{4\times 3}$;

w(t) is a Wiener process, which is a stochastic process with independent normal distributed increments.

In practical applications, the stochastic continuous-time state-space model needs to be discretized, and the stochastic discrete-time state-space model is given by Equations (4.6) – (4.7).

$$T_{k+1} = A_d T_k + B_d u_k + E_d d_k + w_k \tag{4.6}$$

$$y_k = C_d T_k + v_k \tag{4.7}$$

where A_d, B_d and E_d are the corresponding matrices of the discrete-time state-space model which depend on the sampling time. The observed output vector $y_k = T_{in}$; the output matrix $C_d = (0 \quad 0 \quad 1 \quad 0)$; The random variables w_k and v_k represent the

process and measurement noises, respectively, which are assumed to be independent, white and with normal distribution probabilities, i.e., $w_k \sim N(0, Q)$ and $v_k \sim N(0, R)$; Q and R are covariance matrices of process noise and measurement noise, respectively. Equations (4.6) – (4.7) are used in the MPC controller to predict the system evolutions.

4.4 Parameter Identification Method

In order to improve the accuracy and computation efficiency of the optimizations, the parameter pre-processing and different optimization techniques are proposed in this study. The optimal parameters can be accurately and efficiently obtained by the systematic identification procedure which is shown in Figure 4.3.

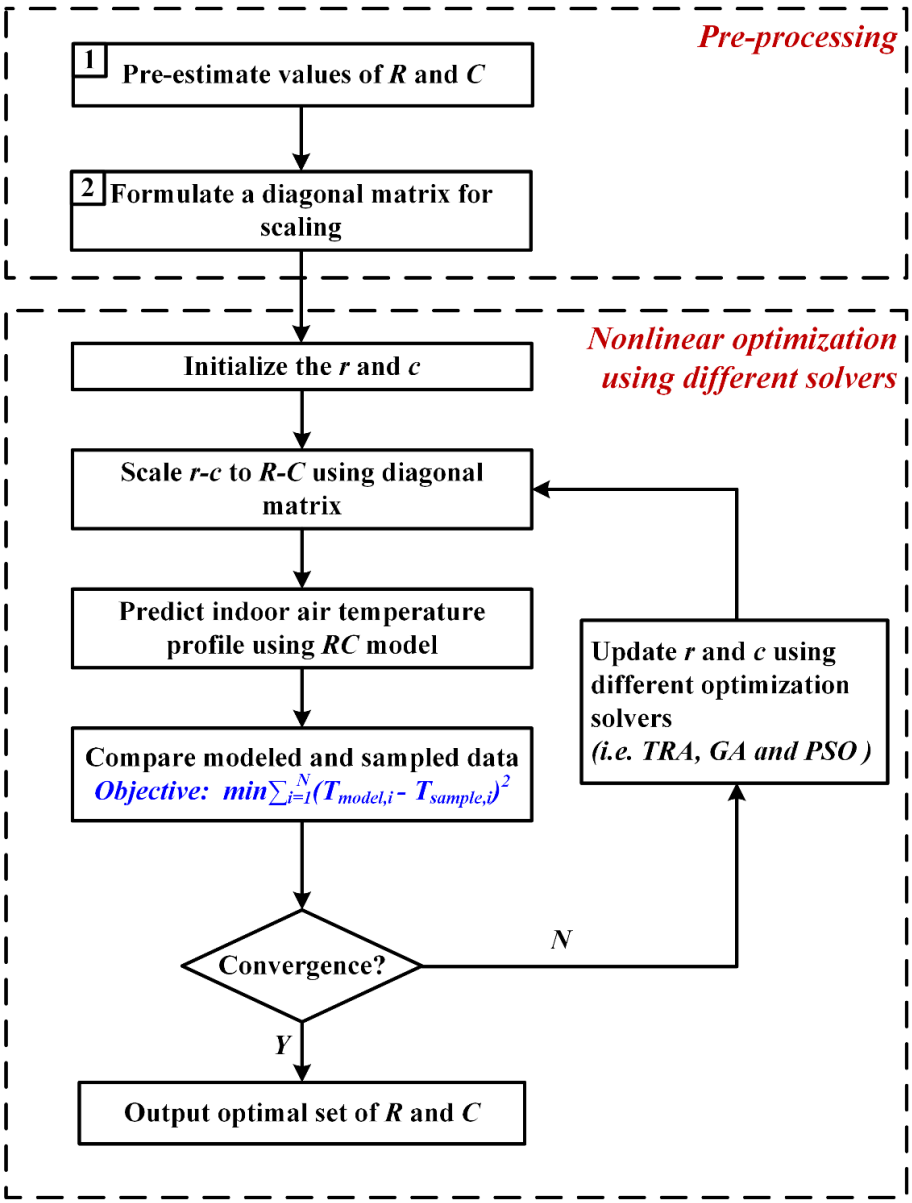

Figure 4.3 Flowchart of parameter identification for the grey-box model.

4.4.1 Parameter Pre-processing

The model robustness relies on not only the feasible physical structure but also the reasonable values of *R* and *C*. To make the identified *R* and *C* values physically reasonable, they are estimated based on the surveyed values of the thermal parameters of residential buildings in Hong Kong and the specific geometric size of the room.

With the pre-estimated values, the search ranges for the parameters can be narrowed down and thus the computation time for optimization can also be saved.

In Hong Kong, U-value of the exterior wall typically ranges from 2.2 to 2.9 W/(m^2·K), and average U-value of the single glazed window is 5.6 W/(m^2·K). Considering the average wind speed of 7.2 m/s during summer in Hong Kong, an average heat transfer resistance of the external wall surface is recommended as 0.036 (m^2·K)/W (Joseph C Lam et al., 2000; Joseph C. Lam et al., 2005). Typical range for the heat transfer resistance of the interior surface is from 0.12 to 0.2 (m^2·K)/W (ASHRAE, 2009). Thermal resistances, i.e., R_w, R_{win}, $R_{w,o}$, $R_{w,in}$, and $R_{in,m}$, are all overall thermal resistances, and can be calculated by Equation (4.8). Equivalent thermal capacitances including C_{in}, C_w, and C_m play functions of dampening the effects of heat transfer. Without them, instantaneous temperature changes in corresponding objects would occur. The building internal mass (e.g., partitions, furniture, carpet, etc.) can be summed to a lumped thermal mass C_m, ranging from 100 to 450 kJ/(K·m^2) (BRE, 2012; Domínguez-Muñoz et al., 2010). Thermal capacitance of half exterior wall can be calculated by Equation (4.9). With the estimated values of R and C, the search range of parameter then can be determined by adopting a search factor ζ ranging from 0 to 1. The upper and lower bounds of the search range can be calculated by Equations (4.10) - (4.11).

$$\mathrm{R} = \frac{1}{\mathrm{A} \times \mathrm{U}} \tag{4.8}$$

$$C_w = \frac{\sigma_w A_w \rho_w c_w}{2} \tag{4.9}$$

$$R_{ub} = (1 + \zeta) \times R_{est} \tag{4.10}$$

$$R_{lb} = (1 - \zeta) \times R_{est} \tag{4.11}$$

After pre-estimating the parameter values, we can easily find the orders of magnitudes (OM) of *R* and *C* vary a lot, namely the parametric model is poorly scaled. Poorly scaled problems usually arise in the simulation of physical and chemical systems where different processes take place at different rates (Nocedal & Wright, 2006). In the simulation of building thermal dynamics, the cost function is not the same sensitive to the changes of *R* and *C*. To solve this problem, a scaling method, i.e., diagonal scaling, is introduced to make the solution more balanced. As shown in Equation (4.12), the diagonal matrix can transform the poorly scaled variables to new variables within an order of magnitude of 1. The diagonal elements are orders of magnitudes of the estimated *R* and *C*.

$$\begin{pmatrix} C_w \\ C_{in} \\ C_m \\ R_{win} \\ R_w \\ R_{w,o} \\ R_{w,in} \\ R_{in,m} \end{pmatrix} = \begin{pmatrix} OM_1 & \cdots & 0 \\ \vdots & \ddots & \vdots \\ 0 & \cdots & OM_8 \end{pmatrix}_{8\times8} \begin{pmatrix} c_w \\ c_{in} \\ c_m \\ r_{win} \\ r_w \\ r_{w,o} \\ r_{w,in} \\ r_{in,m} \end{pmatrix} \tag{4.12}$$

4.4.2 Parameter Identification Using Optimization Techniques

In the present study, we formulate the system identification to a numerical optimization problem. Searching optimal values of the undetermined parameters in a grey-box model is a nonlinear optimization process. Given a set of *R* and *C*, the grey-box model can predict the indoor air temperature profile. An objective function can be used to evaluate the fitness between the predicted data and the measured data collected

from smart in-home sensors during the optimization process. The optimization objective is to minimize the integrated root-mean-square error, as defined in Equation (4.13).

$$J\left(C_w, C_{in}, C_m, R_{win}, R_w, R_{w,o}, R_{w,in}, R_{in,m}, f_{solar,w}, f_{solar,m}, f_{inter,in}, f_{inter,m}\right) = minimize \sqrt{\frac{1}{N}\sum_{i=1}^{N}(T_{model,i} - T_{sample,i})^2} \quad (4.13)$$

where $T_{model,in}$ is the predicted indoor air temperature and $T_{sample,in}$ is the actual measured indoor air temperature.

Optimization techniques are needed to find the optimal values of *R* and *C* which make the objective function reach the minimal value. Three types of optimization solvers including a mathematical solver i.e., trust region algorithm (TRA) , and two evolutionary solvers, i.e., genetic algorithm (GA) and particle swarm optimization (PSO) , are employed to identify the RC values in this study. Both GA (Molina et al., 2013; Tuhus-Dubrow & Krarti, 2010; S. Wang & Xu, 2006; Xuemei et al., 2010) and PSO (Kusiak et al., 2011) have been used to solve the optimization problems in the domain of HVAC. In this study, all optimizations are carried out in MATLAB, and performed on a desktop computer with Intel Core i7-4790 (3.60 GHz), 16 GB of memory, under Windows 10 64-bit operating system. Runtimes and optimization results of these three optimization strategies will be compared in the real cases.

It is worth mentioning that the identification method used in the present study is the classical least-squares based identification method with the assistance of GA or PSO. In the industrial control engineering, the commonly used method for MIMO model identification is the state-space identification method, such as subspace identification

method, due to simple parametrization and non-iterative numerical solution (Qin, 2006; Van Overschee & De Moor, 1994). However, since the subspace identification methods completely rely on historical data and statistical approaches, the identified parameters may not be physically reasonable (Lin et al., 2012; S. Prívara et al., 2010). In the future, we will attempt to use state-space based methods to identify the grey-box room thermal model.

4.5 Model Validation

4.5.1 Identification and Validation Using Field Test Data

One residential bedroom in Hong Kong was chosen to test the grey-box room thermal model. The geometric dimension of the room is 4.8m long, 3.6m wide, and 3m high. It has only one south-facing exterior wall (3.6m×3m) in which single glazed windows are embedded. The Window-Wall-Ratio (*WWR*) is 0.2 and the type of glass is clear. The absorption coefficient of the external wall surface is 0.8, and the solar heat gain coefficient (*SHGC*) of the glass is 0.7.

A smart wireless sensor block was installed in the room to record the indoor air temperature with the interval of 10 minutes. The wireless sensor block includes temperature, humidity, ambient light intensity, presence detection, Presence Detection (Bluetooth LE 4.0 – iBeacon), as listed in Table 4.1. The working diagram of the designed wireless sensor block is shown in Figure 4.4. The data are uploaded in defined intervals, i.e. every 10 minutes in this study, to the Internet Gateway via the wireless network with the protocol Zigbee HA 1.2. The recorded data are saved in XML format and then uploaded to the Cloud Server for storage and further analysis.

For the outdoor weather data, both outdoor air temperature and horizontal global solar radiation are obtained from the nearby Hong Kong Observatory with the interval of 1 minute.

Table 4.1 Specifications of the wireless sensor block

Sensor Type	**Range of measurement**	**Resolution**
Temperature + Humidity	-40-125℃ / 0-100%RH	0.01℃ / 0.04%RH
Ambient Light Intensity	Visible light & Infrared	0.06LUX
Presence Detection (PIR)	6 meter at 120°view angle	-
Presence Detection (Bluetooth LE 4.0 - iBeacon)	10 meter indoor	-

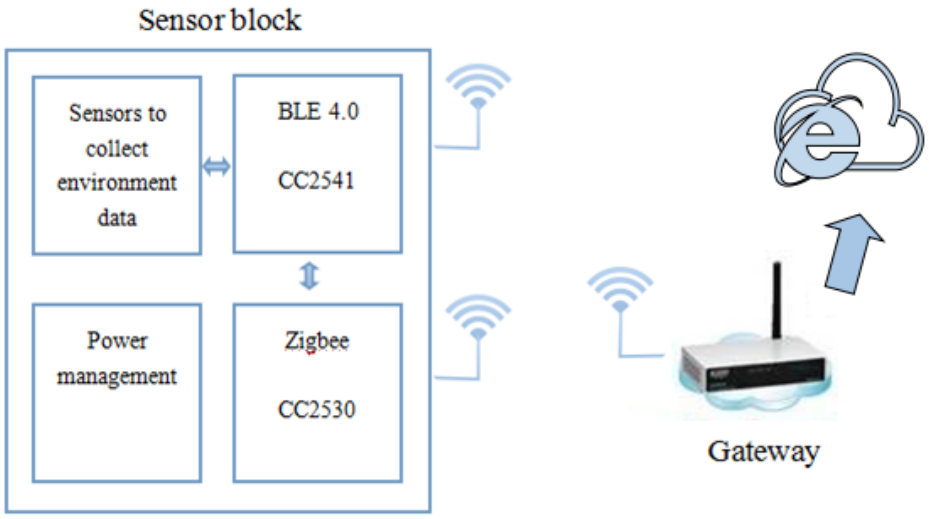

Figure 4.4 Working diagram of the wireless sensor block

Parameter pre-estimations are first conducted using the specific geometric parameters and general building thermal parameters in Hong Kong, as listed in Table 4.2. The

search range of each parameter is set as 1±50% of the corresponding estimated value. To improve the search efficiency, the estimated *R* and *C* are transformed to r and c, ranging from 0 to 1, by a diagonal matrix, as shown in Equation (4.14).

Table 4.2 Pre-estimations of R and C based on prior knowledge.

	C_w (J/K)	C_{in} (J/K)	C_m (J/K)	R_{win} (K/W)	R_w (K/W)	$R_{w,o}$ (K/W)	$R_{w,in}$ (K/W)	$R_{in,m}$ (K/W)
Estimated values	1,850,688	187,868	25,488,000	0.0643	0.0463	0.0033	0.0106	0.0014
Orders of magnitudes	1E+07	1E+06	1E+08	1E-01	1E-01	1E-02	1E-01	1E-02

$$OM = \begin{pmatrix} 10^{7} & & & & & & & \\ & 10^{6} & & & & & & \\ & & 10^{8} & & & & & \\ & & & 10^{-1} & & & & \\ & & & & 10^{-1} & & & \\ & & & & & 10^{-2} & & \\ & & & & & & 10^{-1} & \\ & & & & & & & 10^{-2} \end{pmatrix}_{8\times 8} \quad (4.14)$$

Three optimization solvers, i.e., TRA, GA and PSO, are used to identify the parameters. A six-day (26 - 31 July 2015) indoor air temperature profile is used for the identification. Noted that the time step of the prediction is 1minute and the predicted profile is reinitialized to the sampled value in the midnight of each day to reduce the accumulative error. The identification results (*R* and *C*) of the three optimization methods are listed in Table 4.3. The values of *f* in three cases are almost

the same: $f_{solar,w}$ = 0.7999; $f_{solar,m}$ = 0.1855; $f_{inter,in}$ = 0.7191; and $f_{inter,m}$ = 0.1034. Then, another six-day (1 - 6 August 2015) indoor air temperature profile is forwardly predicted using the developed grey-box model and the identified *R* and *C*.

Table 4.3 Identification results using different optimization solvers.

Solver	Identification results							
	C_w (J/K)	C_{in} (J/K)	C_m (J/K)	R_{win} (K/W)	R_w (K/W)	$R_{w,o}$ (K/W)	$R_{w,in}$ (K/W)	$R_{in,m}$ (K/W)
TRA	1,306,623	62,900	31,673,741	0.0579	0.0324	0.0026	0.0084	0.0020
GA	1,475,300	69,972	35,327,243	0.0608	0.0330	0.0031	0.0094	0.0018
PSO	1,301,978	62,623	33,158,823	0.0579	0.0327	0.0027	0.0084	0.0020

In order to quantify the deviations of the predicted data from the measured data during both training session and validation session, three indices are used to evaluate the deviations, as defined in Equations (4.15) - (4.17). Table 4.4 lists the indoor air temperature deviations of the modeled data from the measured data using different optimization solvers.

Mean Absolute Error

$$MAE = \frac{1}{n}\sum_{i=1}^{n}\left|T_{model,i} - T_{sample,i}\right| \quad (4.15)$$

Mean Absolute Percentage Error

$$MAPE = \frac{1}{n}\sum_{i=1}^{n}\left|\frac{T_{model,i}-T_{sample,i}}{T_{sample,i}}\right| \quad (4.16)$$

Root Mean Square Error

$$RMSE = \sqrt{\frac{1}{n}\sum_{i=1}^{n}(T_{model,i}-T_{sample,i})^2} \quad (4.17)$$

Comparing the optimization results in Table 4.4, it can be seen that the optimal parameter values by different optimization methods are almost the same. The runtimes in the cases of TRA, GA and PSO are 0.37, 4.70 and 6.09 mins, respectively. The deviations between the modeled data and measured data are smaller when TRA and PSO are used. It is worth mentioning that when the room thermal model is represented in the form of ODE, the runtimes in the cases of TRA, GA and PSO are 7.8, 87.7 and 24.3 mins, respectively (Hu et al., 2017). When the state space room thermal model is used instead of the ODE model, the runtimes are significantly reduced.

Table 4.4 Deviations of the modeled data from the measured data using different optimization solvers.

Optimization solver	Runtime (minute)	Training session			Validation session		
		MAE	MAPE	RMSE	MAE	MAPE	RMSE
TRA	0.37	0.1851	0.60%	0.2344	0.1005	0.32%	0.1215
GA	4.70	0.1929	0.62%	0.2429	0.1059	0.33%	0.1316
PSO	6.09	0.1833	0.59%	0.2307	0.0959	0.30%	0.1175

The sampled and modeled profiles of indoor air temperature using the PSO optimization during the training and validation sessions are shown in Figure 4.5 and Figure 4.6, respectively.

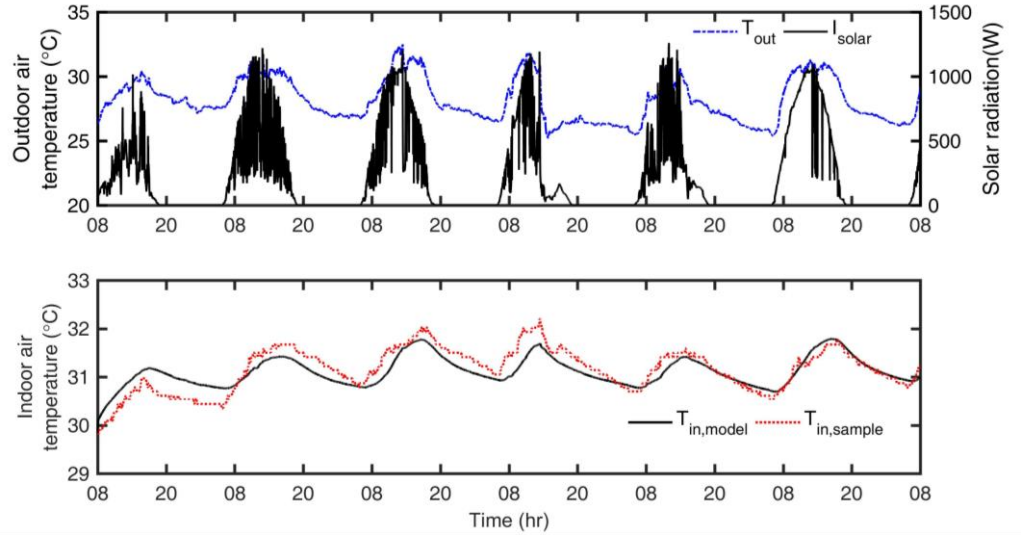

Figure 4.5 Weather conditions, predicted and sampled indoor air temperature profiles during the training session (26 - 31 July 2015).

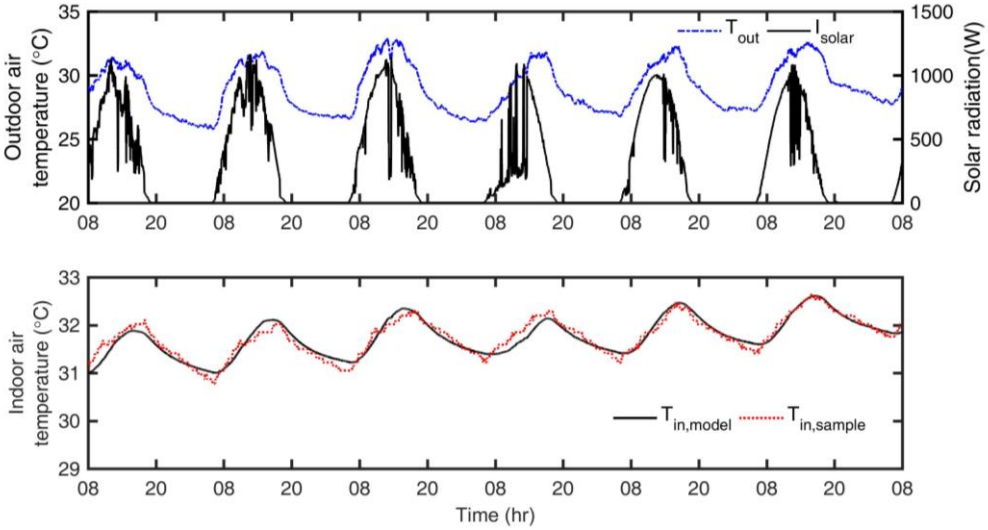

Figure 4.6 Weather conditions, predicted and sampled indoor air temperature profiles during the validation session (1 - 6 August 2015).

To better understand the function played by each component in the grey-box model physically, the room thermal dynamics on a typical summer day (1 August 2015) are simulated and shown in Figure 4.7. The temperature of the external wall surface ($T_{w\text{-}ex}$) in the daytime is higher than the outdoor air temperature (T_{out}) due to the effects of solar radiation, while at night without the solar radiation it is closer to the outdoor air temperature. The temperatures of the internal thermal mass (T_{mass}) and internal wall surface ($T_{w\text{-}in}$) hardly change simultaneously with the outdoor weather conditions due to the thermal capacitances. It is why the cooling output and hence the power consumption of air conditioners can be reduced during the DR period without significantly affecting the thermal comfort of residents. Figure 5.7 shows that the model outputs ($T_{in\text{-}model}$) and the sampled indoor air temperature ($T_{in\text{-}sample}$) agree very well, which means the model can predict the indoor air temperature in a high degree of accuracy.

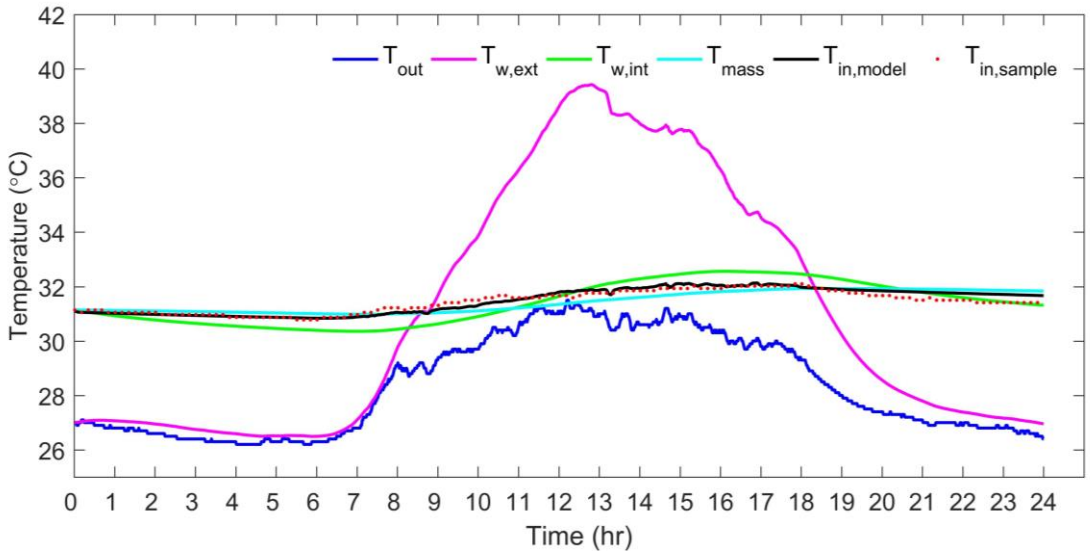

Figure 4.7 Comparison of modeled and sampled indoor air temperatures on a typical summer day.

4.5.2 Identification and Validation Using Simulation Data

Another room in a residential flat is modelled in TRNSYS (S. Klein et al., 2017). The prototype of the room is in Hong Kong. The residential room (L×W×H: 4.8m×3.6m×3m) has one south-facing exterior wall (3.6m×3m) and one east-facing exterior wall (4.8m×3m). Both exterior walls have single glazed windows and the window-wall-ratio of each wall is 0.2. The overall heat transfer coefficients of the exterior wall and the single glazed window are 2.57 and 5.69 W/(m^2·K), respectively. Instead of using the default TMY weather data, real historical weather data at 1-minute intervals from Hong Kong observatory are used in simulation tests. Four weeks (1 June to 29 June 2015) of indoor air temperature data at 1-minute intervals generated from TRNSYS are used to identify the room thermal model. The identification results are: C_w = 8,381,606 J/K, C_{in} = 871,887 J/K, C_m = 13,904,351 J/K, R_{win} = 0.0051 K/W, R_w = 0.0060 K/W, $R_{w,o}$ = 0.0010 K/W, $R_{w,in}$ = 0.0041 K/W, $R_{in,m}$ = 0.0023 K/W, $f_{solar,w}$ = 0.4834, $f_{solar,m}$ = 0.0012, $f_{inter,in}$ = 3.0367, $f_{inter,m}$ = 0.9976. Figure 4.8 shows the outdoor air temperatures and solar radiations as well as the indoor air temperature generated from TRNSYS ($T_{in,TRN}$) and the RC model ($T_{in,RC}$). The results show that the RC room thermal model is able to predict the indoor air temperature in a relatively high degree of accuracy.

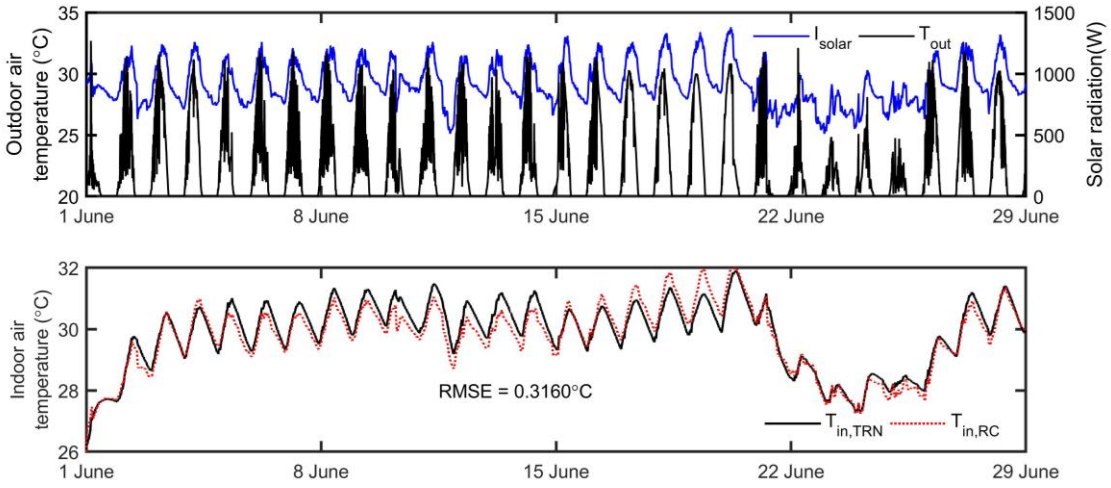

Figure 4.8 Weather conditions and indoor air temperature generated from TRNSYS and the RC model.

With the identified RC values and the sampling interval of 5-minute, the matrices in the discrete-time state-space model, i.e., Equations (4.6) – (4.7), can be determined as follows:

$$A_d = 10^{-2}\begin{pmatrix} 95.809 & 0.5757 & 0.0023 & 0.0001 \\ 0.5757 & 98.573 & 0.7543 & 0.0600 \\ 0.0223 & 7.2508 & 73.899 & 13.012 \\ 0.0001 & 0.0362 & 0.8159 & 99.119 \end{pmatrix}_{4\times4};$$

$$E_d = 10^{-4}\begin{pmatrix} 361.21 & 3.4146 & 0.0001 \\ 3.7494 & 0.0101 & 0.0415 \\ 581.53 & 0.0004 & 9.0293 \\ 2.8933 & 0.0013 & 0.2591 \end{pmatrix}_{4\times3};$$

$$B_d = 10^{-5}(0.0003 \quad 0.1367 \quad 29.686 \quad 0.1477)^T;$$

$$C_d = (0 \quad 0 \quad 1 \quad 0).$$

4.6 Summary

This chapter introduces the development of simplified dynamic room thermal model for model-based online control purpose. The major work in this chapter is as follows.

- A semi-physical (grey-box) dynamic room thermal model is proposed for predicting the indoor air temperature under dynamic operating conditions which is represented in the form of ODE. The model parameters can be learnt by making effective use of the data available in the today's smart in-home sensors.
- To improve the computational efficiency of both offline parameter identification and online model predictive control, the ODE model is transformed to the state space model, which can explicitly express the relationships between the outputs and inputs. Moreover, it can be used to formulate convex optimization problems which in general can be conveniently solved by using state-of-the-art optimization techniques.
- We propose the pre-estimation and scaling approaches to pre-process the model parameters, which help to improve the accuracy and computational efficiency of the parameter identification process. We also compare three popular optimization techniques including TRA, GA and particle PSO for parameter identification.
- Case studies are carried out to validate the simplified room thermal model using both field test and simulation data.

To conclude, due to the simple structure and moderate computation load, the developed dynamic room thermal model is suitable for online applications. It can be used in the HEMSs for model-based AC load scheduling in response to DR signals. It is also valuable for electric utilities to evaluate the impacts of DR programs on large populations of residential ACs and make appropriate incentive policies.

CHAPTER 5 DEVELOPMENT OF A SIMPLIFIED ENERGY PERFORMANCE MODEL OF VARIABLE-SPEED AIR CONDITIONERS

Although AC power consumption estimation and model-based control have been extensively studied, the residential ACs in the literature were single-speed ACs with on-off control method. The on-off control has a big disadvantage of undesired current peaks during state transitions (Aswani et al., 2012). The single-speed ACs are also gradually replaced by the variable-speed ACs which have gained an increasing market share in recent years due to its improved efficiency at part-load conditions (Qureshi & Tassou, 1996). Hence further studies should be conducted to explore the DR potential and control methods of variable-speed ACs. One of the major challenges is the lack of a simple yet accurate variable-speed AC model. A major difference between single-speed ACs and variable-speed ACs is that the performances of variable-speed ACs are influenced by not only the indoor and outdoor environmental conditions, but also the operating compressor frequencies. Thus, the previous steady-state models are not applicable to variable-speed ACs.

In the present chapter, we aim to develop a simplified energy performance model of variable-speed ACs and apply the AC model for model-based DR control. Figure 5.1 shows the flow chart of the development of the simplified energy performance model of residential variable-speed ACs. First, a simplified energy performance model structure of variable-speed ACs is proposed in the form of piecewise polynomial functions to characterize the performances of variable-speed ACs under various

operating frequencies and environmental conditions. However, the AC manufacturers seldom provide enough data for coefficient identification. Thus, a steady-state physical model of variable-speed ACs is developed to generate enough performance data to identify the simplified AC model. Then, the generated performance data are used to identify the coefficients in the piecewise polynomial functions.

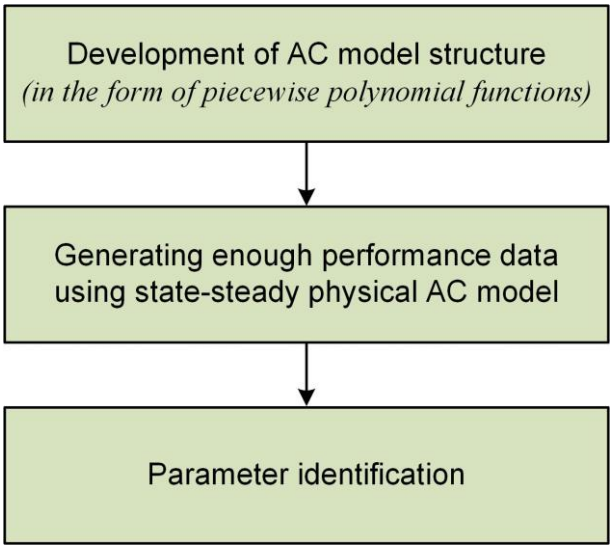

Figure 5.1 Flow chart of the development of the simplified energy performance model of residential variable-speed ACs

5.1 Simplified Energy Performance Model of Variable-speed Air Conditioners

Energy performance model of residential ACs can be used for two main purposes: DR potential estimation at individual and aggregate level and model-based DR control of an individual AC. Considering the computational efficiency, a simplified AC energy performance model is needed for both aforementioned purposes. For a single-speed AC, energy performances are normally characterized using dimensionless factors (Q^*

and COP^*) of cooling capacity (Q) and coefficient of performance (COP), which are the ratios of the performance data on a given environmental condition (Q_{real} and COP_{real}) to the nominal performance data (Q_{nom} and COP_{nom}). Environmental conditions are supposed to include dry-bulb and wet-bulb temperatures of both indoor air ($T_{in,db}$ and $T_{in,wb}$) and outdoor air ($T_{out,db}$ and $T_{out,wb}$). Experimental studies show that the thermal and energy performances of single-speed AC are mainly influenced by the outdoor air dry-bulb temperature ($T_{out,db}$) and indoor air wet-bulb temperature ($T_{in,wb}$) (Cherem-Pereira & Mendes, 2012; Meissner et al., 2014; York & Tucker, 1980). Thus, as shown in Equations (5.1) - (5.2), Q^* and COP^* are normally represented as the polynomial functions of indoor air wet-bulb temperature ($T_{in,wb}$) and outdoor air dry-bulb temperature ($T_{out,db}$) (Cherem-Pereira & Mendes, 2012; Meissner et al., 2014; York & Tucker, 1980). The nominal environmental conditions are: $T_{in,wb}$ = 19.4 ℃ ($T_{in,db}$ = 27 ℃) and $T_{out,db}$ = 35 ℃ (ANSI/AHRI, 2008). Previous research results show that the polynomial performance model can fit the performance data accurately even without the quadratic items, i.e., $a_3 = a_4 = b_3 = b_4 = 0$.

$$Q^* = \frac{Q_{real}}{Q_{nom}} = a_0 + a_1 T_{in,wb} + a_2 T_{out,db} + a_3 T_{in,wb}^2 + a_4 T_{out,db}^2 \quad (5.1)$$

$$COP^* = \frac{COP_{real}}{COP_{nom}} = b_0 + b_1 T_{in,wb} + b_2 T_{out,db} + b_3 T_{in,wb}^2 + b_4 T_{out,db}^2 \quad (5.2)$$

The major difference between single-speed AC and variable-speed AC is that energy performances of variable-speed ACs are influenced by the indoor and outdoor environmental conditions as well as the rotational speed of compressor. The thermal and energy performance model of variable-speed AC can be seen as the collection of a sequence of sub-models at different operating frequencies. Depending on the

operating frequency, the performance model of variable-speed AC switches among the sub-models for different operating frequencies. Like the performance model of single-speed AC, each sub-model can be mathematically represented in the form of polynomial function. Therefore, we can use piecewise polynomial model to characterize the energy performance of variable-speed ACs under different operating frequencies.

The dimensionless factor of cooling capacity and COP of variable-speed ACs under various operating frequencies can be described as shown in Equations (5.3) - (5.4). In contrast with the nominal operating condition of single-speed AC, the nominal operating condition of variable-speed AC includes not only the nominal environmental variables but also the nominal operating frequency such as 50 Hz in our study. Thus, the nominal operating condition of variable-speed AC is N_{comp} = 50Hz, $T_{in,wb}$ = 19.4 ℃ and $T_{out,db}$ = 35 ℃.

$$\mathrm{Q}^* = \frac{Q_{real}}{Q_{nom}} = \begin{cases} \underbrace{\begin{pmatrix} a_0^{N_0} & a_1^{N_0} & a_2^{N_0} \\ a_0^{N_1} & a_1^{N_1} & a_2^{N_1} \\ \vdots & \vdots & \vdots \\ a_0^{N_i} & a_1^{N_i} & a_2^{N_i} \\ \vdots & \vdots & \vdots \\ a_0^{N_K} & a_1^{N_K} & a_2^{N_K} \end{pmatrix}}_{A} \begin{pmatrix} 1 \\ T_{in,wb} \\ T_{out,db} \end{pmatrix} & \begin{matrix} N_{comp} = N_0 \\ N_{comp} = N_1 \\ \vdots \\ N_{comp} = N_i \\ \vdots \\ N_{comp} = N_K \end{matrix} \end{cases} \tag{5.3}$$

$$\mathrm{COP}^* = \frac{COP_{real}}{COP_{nom}} = \begin{cases} \underbrace{\begin{pmatrix} b_0^{N_0} & b_1^{N_0} & b_2^{N_0} \\ b_0^{N_1} & b_1^{N_1} & b_2^{N_1} \\ \vdots & \vdots & \vdots \\ b_0^{N_i} & b_1^{N_i} & b_2^{N_i} \\ \vdots & \vdots & \vdots \\ b_0^{N_K} & b_1^{N_K} & b_2^{N_K} \end{pmatrix}}_{B} \begin{pmatrix} 1 \\ T_{in,wb} \\ T_{out,db} \end{pmatrix} & \begin{matrix} N_{comp} = N_0 \\ N_{comp} = N_1 \\ \vdots \\ N_{comp} = N_i \\ \vdots \\ N_{comp} = N_K \end{matrix} \end{cases} \tag{5.4}$$

where Q^* and COP^* denote the dimensionless factor of cooling capacity and COP, respectively; A and B denote the coefficient matrices of dimensionless factors of cooling capacity and COP, respectively; N_{comp} denotes the operating frequency of compressor; N_i denotes the typical operating frequency, e.g., [*20, 30, 40, …, 100*] Hz in our case study. The piecewise polynomial model of variable-speed AC including Q^* and COP^* are grey-box models. The coefficient matrices of cooling capacity and COP (A and B) need to be identified using a large number of performance data under various environmental conditions ($T_{in,wb}$ and $T_{out,db}$) and operating frequencies (N_{comp}). Either experimental tests from AC manufacturers or physics-based modeling technique can be used for the identification. Since AC manufacturers seldom provide enough data for coefficient identification, the first method is infeasible. Considering the universal physical principles, physics-based modeling of typical ductless split variable-speed AC is preferred in our study.

5.2 Steady-state Physical Modeling of Variable-speed Air Conditioners

AC models can be generally classified into transient models and steady-state models. The refrigerant dynamics in residential ACs are much quicker than the thermal dynamics of the room. The refrigerant re-distributions in different AC components normally accomplish in a short period, around 100 seconds (He et al., 1997; B. P. Rasmussen, 2005). Therefore, a steady-state AC model is developed to predict the coupled dynamic behaviors of the room and the AC under time-varying internal and external conditions. The steady-state performances of variable-speed AC in terms of cooling capacity and COP can be determined from compressor frequencies (N_{comp}) as

well as indoor and outdoor air temperature ($T_{air,out}$ and $T_{air,in}$). For simplification of modeling, only the four major components, i.e., condenser, evaporator, variable- speed compressor, and EEV, are modeled in this paper. Other minor components such as accumulator, refrigerant pipeline, sub-cooler and receiver are not considered here.

5.2.1 Variable-speed Compressor

Refrigerant mass flow rate and enthalpy at the compressor outlet are the key outputs of the compressor module. The refrigerant mass flow rate through the compressor and the refrigerant enthalpy at the compressor outlet are given by Equations (5.5) - (5.6), respectively.

$$\dot{m}_{comp} = N_{comp} V_{comp} \rho_{comp} \eta_v \tag{5.5}$$

$$h_{comp,o} = h_{comp,i} + (h_{comp,o,is} - h_{comp,i})/\eta_{is} \tag{5.6}$$

where N_{comp}, V_{comp}, ρ_{comp} are the rotational speed of compressor motor in Hz, effective displacement volume, and refrigerant density at the inlet, respectively; $h_{comp,i}$, $h_{comp,o}$ are the enthalpies at the compressor inlet and outlet; $h_{comp,o,is}$ is the enthalpy at the compressor outlet under an isentropic compression; η_v and η_{is} are compressor volumetric efficiency (Kapadia et al., 2009; Koury et al., 2001) and isentropic efficiency (Leducq et al., 2003; B. P. Rasmussen, 2005; R. Zhou et al., 2010) which can be approximately calculated by Equations (5.7) - (5.8), respectively.

$$\eta_v = 1 + c_{comp} - c_{comp}(P_{comp,o}/P_{comp,i})^{c_v/c_p} \tag{5.7}$$

$$\eta_{is} = c_0 + c_1 N_{comp} + c_2 N_{comp}^2 + c_3 P_r + c_4 P_r^2 \tag{5.8}$$

where $P_{comp,o}$ and $P_{comp,i}$ are the refrigerant pressures at the compressor outlet and inlet, respectively; P_r is the ratio of compressor outlet pressure to the inlet pressure; c_{comp} is the compressor clearance ratio; c_v and c_p are the constant volume and constant pressure specific heats at the compressor inlet, respectively; c_0- c_4 are coefficients which can be empirically identified from the actual compressor.

5.2.2 Electronic Expansion Valve

Expansion devices are used in the refrigeration systems to regulate the refrigerant mass flow rate into the evaporator and maintain the refrigerant superheat at the evaporator outlet. In recent years, due to its superior performance in control, EEV has been implemented in the variable-speed ACs or heat pumps to control the cooling capacity and superheat instead of the conventional expansion devices such as capillary tubes and thermostatic expansion valves (Choi & Kim, 2003). Refrigerant mass flow rate through an EEV can be modeled using Equation (5.9). Since refrigerant expansion process in EEV can be considered as being adiabatic, the enthalpy at the EEV outlet therefore can be given by Equation (5.10).

$$\dot{m}_v = C_v A_v \sqrt{\rho_v (P_c - P_e)} \tag{5.9}$$

$$h_{v,o} = h_{v,i} \tag{5.10}$$

where C_v, A_v, ρ_v are the orifice coefficient, valve opening area, refrigerant density, respectively; P_c and P_e are refrigerant pressures at the condenser and evaporator, respectively; $h_{v,o}$ and $h_{v,i}$ are the refrigerant enthalpies at the EEV inlet and outlet, respectively.

5.2.3 Heat Exchangers

Heat exchangers, including the condenser and the evaporator, are responsible to conduct the heat transfer between the refrigeration system and the surroundings. Based on the fundamental principles of mass, momentum and energy conservations, the dynamics of the two-phase flow in heat exchangers can be represented by a set of elaborated, nonlinear partial differential equations (Leducq et al., 2003). The heat exchangers are assumed to be one-dimensional, and the pressure drops are assumed to be negligible.

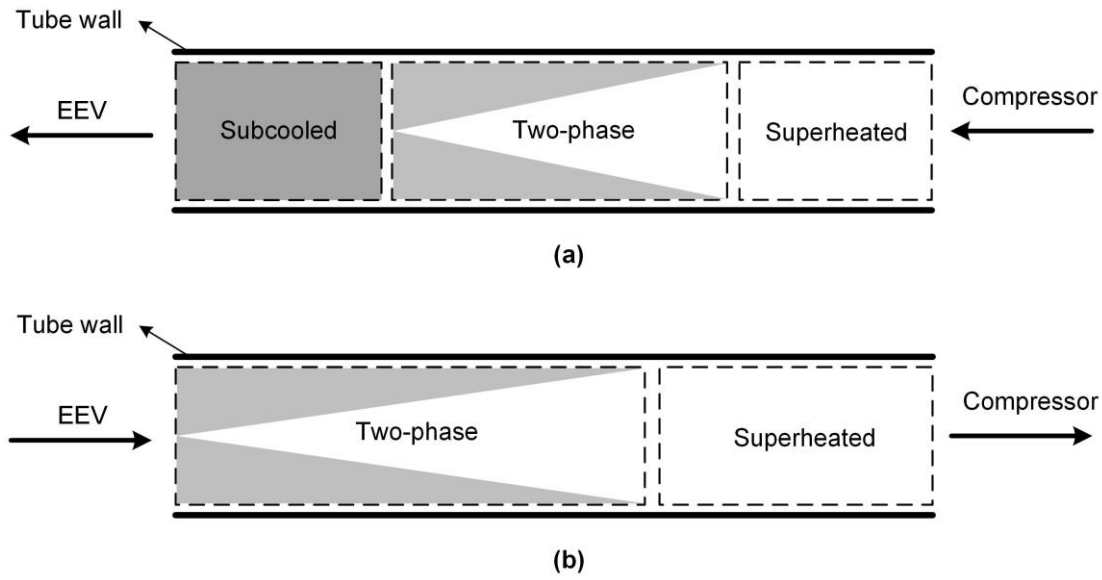

Figure 5.2 Diagram of the moving-boundary heat exchangers: (a) condenser with three fluid zones; (b) evaporator with two fluid zones.

The moving boundary approach is widely adopted for both transient modeling (Grald & MacArthur, 1992; He et al., 1997; He et al., 1998; B. P. Rasmussen, 2005; Bryan P. Rasmussen & Alleyne, 2004) and steady-state modeling (Zakula et al., 2011; R. Zhou et al., 2010) of heat exchangers. The method is able to capture the characteristics of

multiple fluid phase heat exchangers while preserving the simplicity of lumped parameter models. As shown in Figure 5.2, the condenser is normally divided into three zones based on the refrigerant state, i.e., de-superheated, two-phase, and subcooled zones, and the evaporator is divided into two zones, i.e., two-phase and superheated zones. With these assumptions, the one-dimensional steady state model of each zone can be represented by the conservation equations of mass and energy, which only contain the derivatives to the length of the zones. After integration along the length, the steady state model of a heat exchanger zone can then be transformed into the two algebraic equations as follows:

$$\dot{m}_{ex,o} = \dot{m}_{ex,i} \tag{5.11}$$

$$h_{ex,o} = h_{ex,i} + Q_{ref,air}/\dot{m}_{ex,i} \tag{5.12}$$

where $\dot{m}_{ex,i}$ and $\dot{m}_{ex,o}$ are the mass flow rates at the inlet and outlet of the zone, respectively; $h_{ex,i}$ and $h_{ex,o}$ are the enthalpy at the inlet and outlet of the zone, respectively; $Q_{ref,air}$ is the heat exchanged between the refrigerant and the air in that zone (negative value for the condenser). The heat transfer rates, $Q_{ref,air}$, in heat exchangers are calculated by effectiveness-number of transfer units (ε-NTU). In the ε-NTU method, the actual heat transfer between the refrigerant and air for each zone can be calculated by Equations (5.13) - (5.23).

$$C_{ref} = \dot{m}_{ref} c_{ref} \tag{5.13}$$

$$C_{air} = \dot{m}_{air} c_{air} \tag{5.14}$$

$$C_{min} = \min(C_{ref}, C_{air}) \tag{5.15}$$

$$C_{max} = \max(C_{ref}, C_{air}) \tag{5.16}$$

$$c_r = \frac{C_{min}}{C_{max}} \tag{5.17}$$

$$A_{sur} = \pi D_o L \tag{5.18}$$

$$U_{ov} = 1/(\frac{1}{\alpha_{ref}} + \frac{1}{2}\frac{D_o}{\lambda_w} ln\frac{D_o}{D_i} + \frac{1}{r\alpha_{air}}) \tag{5.19}$$

$$NTU = U_{ov}A_{sur}/C_{min} \tag{5.20}$$

$$\varepsilon = (1 - e^{-NTU(1-c_r)})/(1 - c_r e^{-NTU(1-c_r)}) \tag{5.21}$$

$$Q_{max} = C_{min}|T_{ref,in} - T_{air,in}| \tag{5.22}$$

$$Q_{ref,air} = \varepsilon Q_{max} \tag{5.23}$$

where C_{ref} and C_{air} are the refrigerant and air thermal capacitance rates, W/K; U_{ov} is the tube overall heat transfer coefficient from the refrigerant side to the air side, W/(m^2•K); *NTU* is the number of transfer unit; ε is the heat transfer effectiveness; α_{ref} and α_{air} are the heat transfer coefficients at the refrigerant and air sides, W/(m^2•K). The heat transfer coefficients (HTCs) are critical parameters in the heat exchanger modeling. For different zones in the heat exchangers, the correlations used for calculating HTCs at the refrigerant and air sides are different, as shown in Table 5.1.

Table 5.1 Correlations for the calculations of heat transfer coefficients.

Regions		Correlations for HTCs	
		Refrigerant side	Air side
Condenser	De-superheated zone	Petukhov correlation (Petukhov, 1970)	Wang et al. (C-C Wang et al., 1999) (Dry condition)
	Two-phase zone	Cavallini correlation (Cavallini et al., 2006)	
	Subcooled zone	Gnielinski correlation (Gnielinski, 1976)	
Evaporator	Two-phase zone	Kandlikar correlation (Kandlikar, 1990)	
	Superheated zone	Petukhov correlation (Petukhov, 1970)	Wang et al. (Chi-Chuan Wang et al., 2000) (Wet condition)

How to determine the length of each zone is a critical issue for steady-state heat exchanger modeling using moving boundary approach. Details of the numerical solution for heat exchanger modeling is introduced in Section 5.3.4. Similar to the heat exchanger models, the solution for the modeling of the whole refrigeration system is implicit and can only be solved by a numerical method which shown in Section 5.3.5.

5.2.4 Numerical Solution for Heat Exchanger

A one-dimensional optimization technique is adopted in this study to determine the length of each zone in the heat exchangers and obtain the refrigerant enthalpy at the heat exchanger outlet. The heat transfer from the refrigerant to the air can be calculated by forwardly using the ε-NTU method, Equations (5.13) - (5.23). The length of each zone can be determined using the ε-NTU method inversely, as shown in Equations (5.24) - (5.25). The flow chart for numerical solution of heat exchangers is shown in Figure 5.3.

$$L = \frac{C_{min}}{U_{ov}\pi D_o(c_r-1)} ln \frac{Q_{max}-Q_{ref,air}}{Q_{max}-rQ_{ref,air}} \quad (5.24)$$

$$Q_{ref,air} = \dot{m}_{ex,i}(h_{ex,o} - h_{ex,i}) \quad (5.25)$$

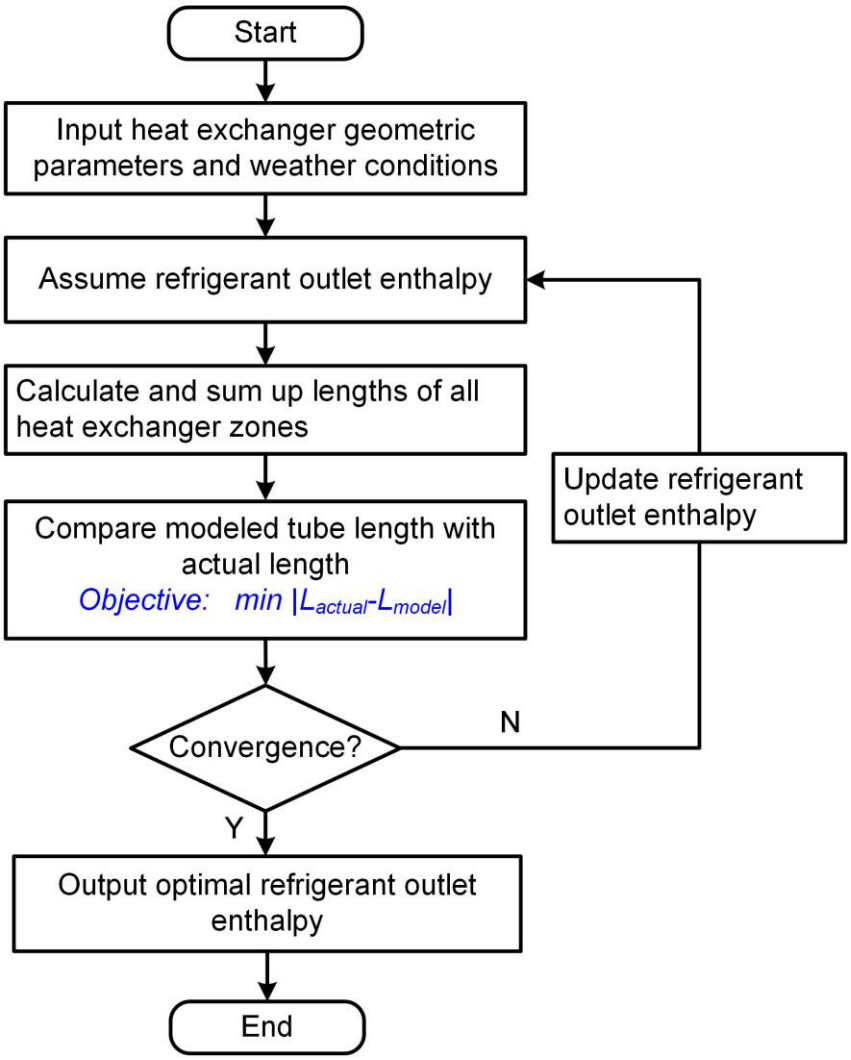

Figure 5.3 Flow chart for numerical solution of heat exchangers.

5.2.5 Numerical Solution for Whole Refrigeration System

Figure 5.4 shows the flowchart of the numerical solution of the whole refrigeration system. First, we input the geometric parameters of all components and operating conditions including the actuator signal, i.e., compressor rotational speed (N_{comp}) and

environmental disturbances ($T_{air,out}$ and $T_{air,in}$). In the steady-state modeling of variable-speed AC, the condenser airflow rate and evaporator airflow rate are assumed to be constants under all operating conditions and are not manipulated in any situations. The EEV opening degree N_v, condenser pressure P_c, evaporator pressure P_e , sub-cooling degree at the condenser outlet SC, and superheat at the evaporator outlet SH under the specific operating conditions, i.e., $T_{air,out}$, $T_{air,in}$ and N_{comp}, are determined by a constrained nonlinear optimization, as shown in Figure 6.2. The reference values for sub-cooling (SC_{ref}) and superheat (SH_{ref}) are both 4.5℃ which normally occurs in the real case. Given a set of N_v, P_c, P_e, SC and SH the nonlinear optimizer sequentially calls the modules of the compressor, condenser, EEV and evaporator and computes the value of the objective function as shown in Equation (5.26).

$$\min_{N_v,P_c,P_e,SC,SH} \left(\frac{\dot{m}_{comp}-\dot{m}_v}{\dot{m}_{comp}}\right)^2 + \left(\frac{SC-SC_{ref}}{SC_{ref}}\right)^2 + \left(\frac{SH-SH_{ref}}{SH_{ref}}\right)^2 \quad (5.26)$$

The outputs of the nonlinear optimization are then brought back to the refrigeration system from compressor to condenser, EEV and evaporator. To the end, the cooling capacity and COP under specific operating conditions can be calculated. In this study, all the sub-models of the refrigeration system and optimizations are carried out in MATLAB (MathWorks, 2012). The thermo-physical properties of refrigerant are calculated with the assistance of CoolProp tool (Bell et al., 2014).

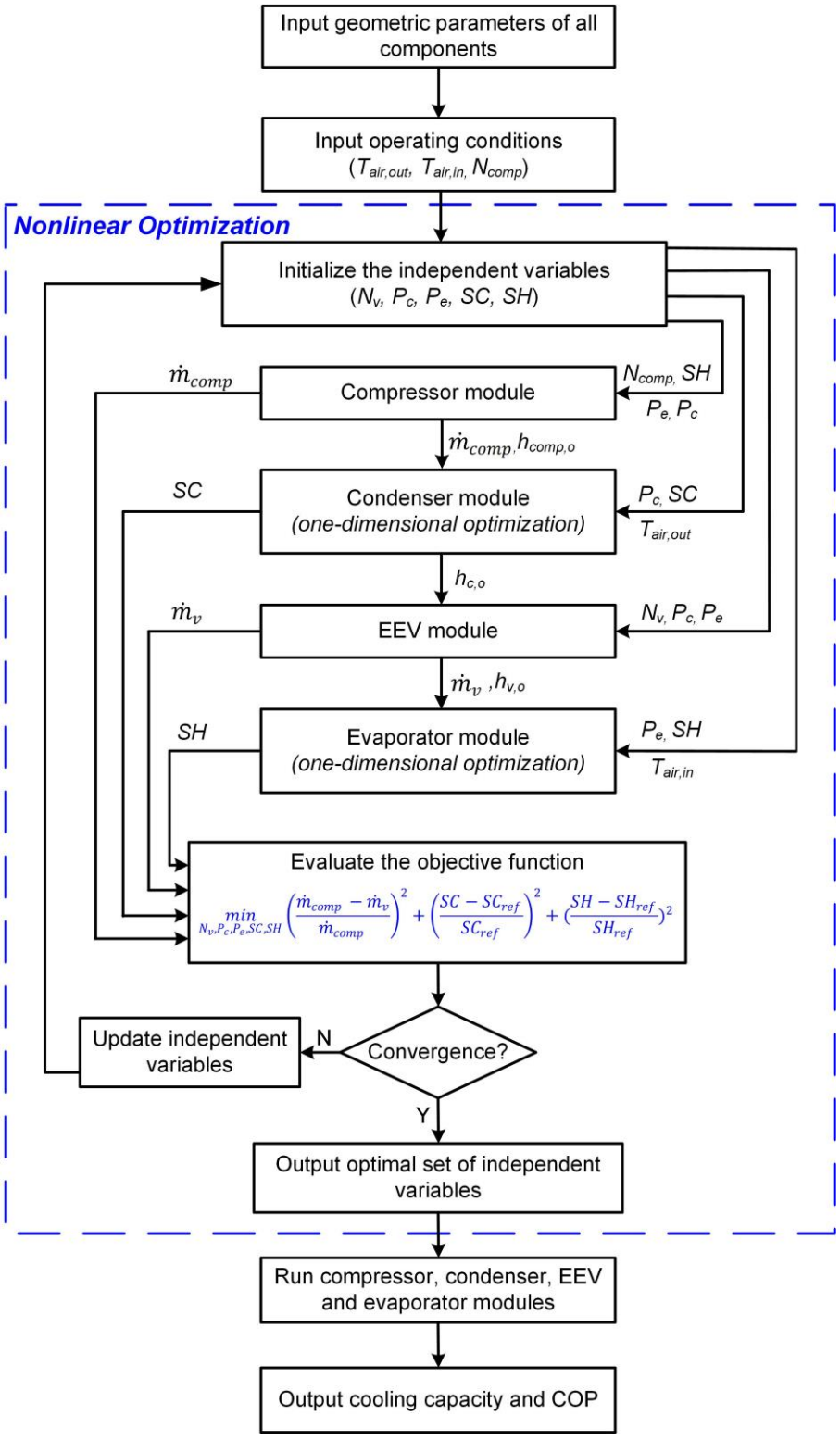

Figure 5.4 Flow chart for numerical solution of whole refrigeration system.

5.3 Parameter Identification and Model Validation

5.3.1 AC Description and Parameter Identification

There have been a number of experimental studies of steady-state performances of ACs (Cherem-Pereira & Mendes, 2012; Gayeski, 2010; Meissner et al., 2014). Gayeski (Gayeski, 2010) carried out quite elaborate experiments for a Mitsubishi split-type variable-speed air conditioner with a rated cooling capacity of 2.5kW. It is one of the most popular types of residential variable-speed ACs and the main specifications are listed in Table 5.2. The experimental results in (Gayeski, 2010), however, did not contain the complete performance data. The same split-type variable-speed air conditioner was chosen for performance identifications under a wide range of typical operating conditions using physical modeling techniques. The typical operating conditions are the combinations of typical compressor rotational speeds ($N_{comp,ty}$ = [20, 30, … , 100]), typical dry-bulb temperature of outdoor air ($T_{out,db,ty}$ = [23, 26, 29, 32, 35, 38]) and typical wet-bulb temperature of indoor air ($T_{in,wb,ty}$ = [14.6, 17.1, 19.4, 22.0, 24.5, 27.0]). The typical wet-bulb temperature of indoor air is determined by the corresponding typical dry-bulb temperature ($T_{in,db,ty}$ = [21, 24, 27, 30, 33, 36]).

Table 5.2 Main specifications of the variable-speed AC.

Item		Specification
Refrigeration		R410A
Compressor	type	rotary piston type
	piston displacement volume (cm^3)	10
EEV	type	step motor
	inner diameter (mm)	4
Evaporator	dimension (L×W×H) (m)	0.62×0.03×0.34
	row number	2
	loop number	2
	tube number per row	16
	tube length per row (m)	0.62
	tube outer diameter (mm)	6.8
	tube inner diameter (mm)	5.2
	fin number	488
	fin pitch (mm)	1.17
	fin thickness (mm)	0.102
Condenser	dimension (L×W×H) (m)	0.86×0.5×0.022
	row number	1
	loop number	2
	tube number per row	12
	tube length per row (m)	0.86
	tube outer diameter (mm)	6.5
	tube inner diameter (mm)	4.9
	fin number	610
	fin pitch (mm)	1.34
	fin thickness (mm)	0.0762

The dimensionless factors of cooling capacity and COP (Q^* and COP^*) of the target variable-speed AC under typical operating conditions, as shown in Figure 5.5, are obtained using the steady-state physical modeling technique. Figure 5.6 shows the performances of the variable-speed AC at the compressor speeds of 30Hz, 60Hz and 90Hz predicted by the model. It can be found that the cooling capacity and COP of variable-speed AC mainly depend on the compressor speed. The cooling capacity increases with the increase of compressor speed, but the COP decreases with the increase of compressor speed. The cooling capacity increases with the increase of indoor air temperature and decreases with the increase of the outdoor air temperature. Compared to the indoor air temperature, the outdoor air temperature has a larger effect on the COP. The trends predicted by the steady-state model are reasonable and typical for variable-speed ACs, therefore, the steady-state model does not suffer from the overfitting issue and can predict the change of performance with the operating conditions.

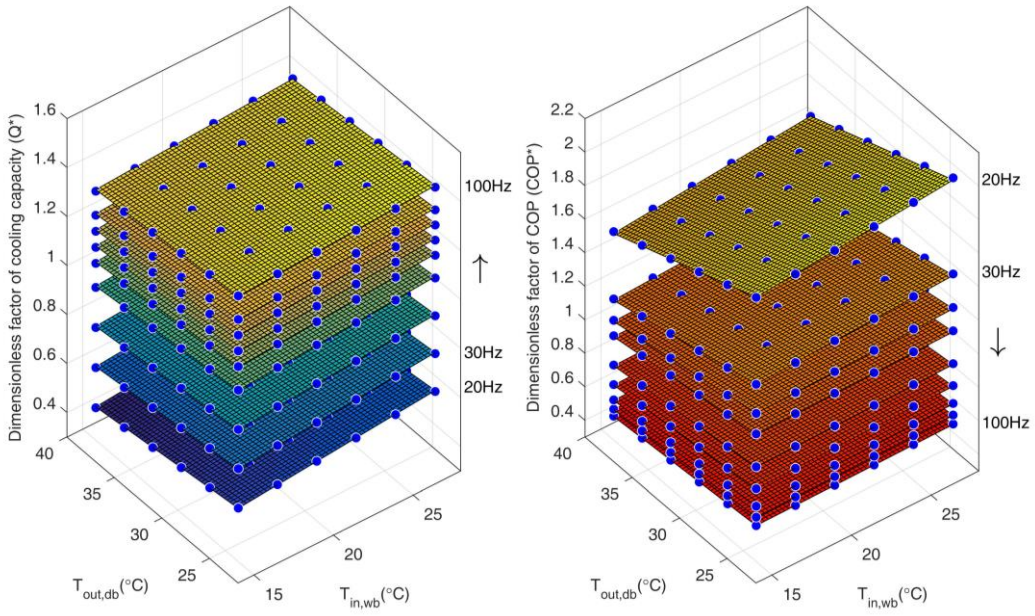

Figure 5.5 Performances (dimensionless factors of cooling capacity and COP) of the variable-speed AC under typical operating conditions.

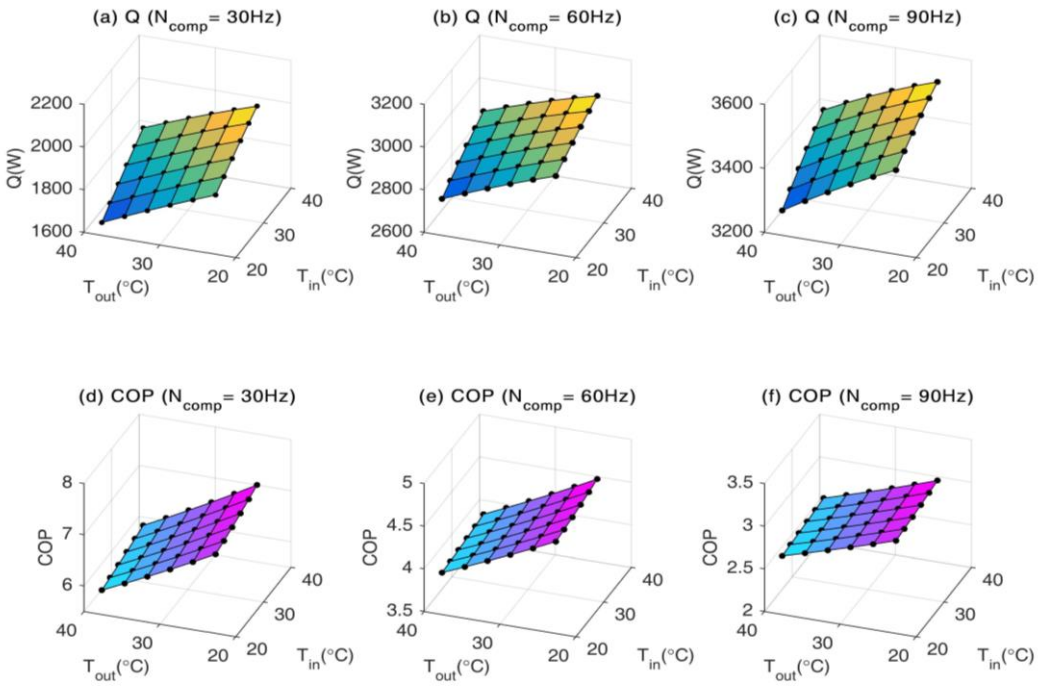

Figure 5.6 Performances of the variable-speed AC at the compressor speeds of 30Hz, 60Hz and 90Hz, respectively.

With the performance data under typical operating conditions, the simplified piecewise polynomial performance model of variable-speed AC then can be identified. The identified coefficients, i.e., matrices *A* and *B* in Equations (5.3) - (5.4), are listed in Table 5.3 and Table 5.4, respectively. Coefficient of determination R^2 is used to evaluate the goodness of fit of the model.

Table 5.3 Coefficients of the piecewise polynomial model for cooling capacity of variable-speed AC.

Operating frequency (Hz)	a_0	a_1	a_2	R^2
20	0.585843	0.006222	-0.005484	0.9988
30	0.746835	0.005789	-0.005232	0.9982
40	0.907888	0.005348	-0.004979	0.9975
50	1.068738	0.004910	-0.004723	0.9966
60	1.165241	0.004647	-0.004570	0.9958
70	1.229575	0.004472	-0.004467	0.9953
80	1.293910	0.004297	-0.004365	0.9947
90	1.358245	0.004121	-0.004262	0.9936
100	1.454747	0.003859	-0.004108	0.9923

Table 5.4 Coefficients of the piecewise polynomial model for COP of variable-speed AC.

Operating frequency (Hz)	b_0	b_1	b_2	R^2
20	2.3251606	0.0088524	-0.0230007	0.9989
30	1.6822462	0.0047449	-0.0149859	0.9987
40	1.4649414	0.0027292	-0.0118164	0.9984
50	1.3133828	0.0014556	-0.0097436	0.9981
60	1.0795743	0.0015988	-0.0081978	0.9986
70	0.9242602	0.0016845	-0.0071883	0.9989
80	0.8001989	0.0015814	-0.0062748	0.999
90	0.7225063	0.0013145	-0.0055670	0.999
100	0.6621846	0.0010672	-0.0049823	0.9989

5.3.2 Model Validation

To validate the simplified piecewise polynomial model of variable-speed AC, 40 sets of experimental data provided by Gayeski (Gayeski, 2010) are compared with the modeled data under the same operating conditions. The ranges of $T_{in,wb}$, $T_{out,db}$ and N_{comp} are 17.5-26.7 ℃, 24-36 ℃, and 19-95 Hz, respectively. Figure 5.7 shows the comparisons between the modeled data and the experimental data. The deviations mainly locate in the range of ±15%. The mean absolute percentage errors (MAPEs) between the predicted and tested cooling capacity and COP are 5.65% and 11.94%, respectively.

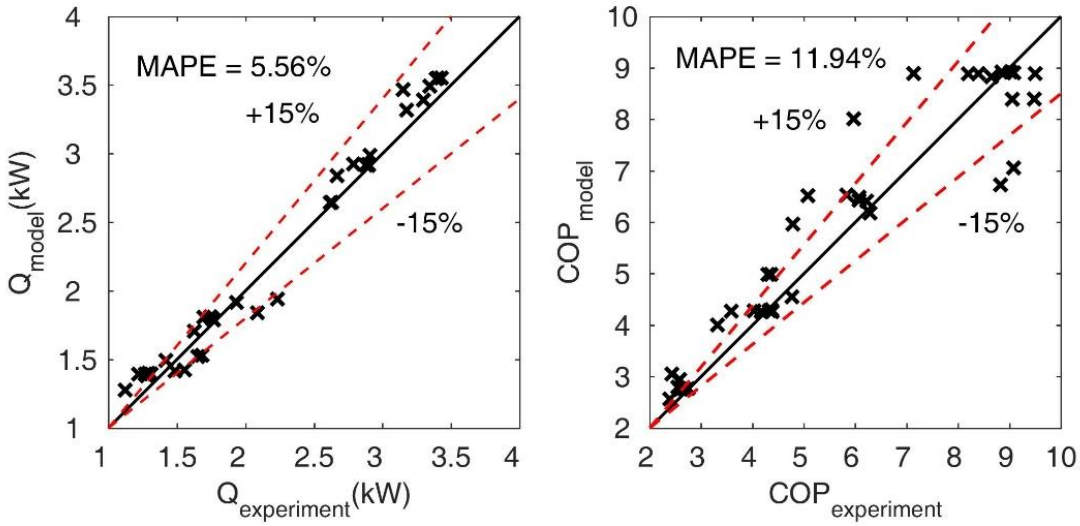

Figure 5.7 Comparisons between the modeled data and experimental data.

5.4 Summary

As the major contributors to home electricity bills and peak power demands in electrical grids, residential air conditioner (AC) has drawn increasing attention to the exploitation of its DR resource. In order to investigate DR potential of ACs at individual and aggregate level and to conduct model-based DR control of an individual AC, a simply structured energy performance model of ACs is needed by electrical engineers and researchers for the purpose of computational efficiency. However, recent studies on DR management of ACs mainly focused on the on-off (single-speed) ACs rather than variable-speed (variable-speed) ACs due to the lack of a simplified yet accurate energy performance model of variable-speed ACs.

In this chapter, we aim to develop a simplified energy performance model of variable-speed ACs to characterize the AC performances under various operating frequencies and environmental conditions. The essence of the simplified AC model is a grey-box

model which needs to be identified using performance data from either experimental tests from AC manufacturers or physics-based modeling technique. Since AC manufacturers seldom provide enough data for coefficient identification, physics-based modeling of typical variable-speed AC is considered in our study. For this reason, a steady-state physical model of variable-speed ACs is developed to generate performance data under typical operating frequencies and environmental conditions. The proposed simply structured energy performance model of variable-speed ACs can be readily used by electrical researchers and engineers for either model-based DR control in smart HEMSs or DR potential estimation of a single variable-speed AC or a large population of variable-speed ACs.

CHAPTER 6 INDIRECT MODEL-BASED OPTIMAL CONTROL METHOD IN RESPONSE TO DAY-AHEAD PRICING

The rapid developments of advanced metering infrastructure and dynamic electricity pricing provide great opportunities for residential electrical appliances, especially air conditioners (ACs), to participate in DR programs to reduce peak power consumptions and electricity bills. One of the biggest challenges faced by residential DR participants is the lack of intelligent DR control methods which enable residential ACs to automatically respond to dynamic electricity prices. Most existing studies on DR control of residential ACs focus on single-speed ACs. However, variable-speed ACs which have higher part-load efficiencies have been extensively installed in today's residential buildings.

This chapter presents a novel model-based DR control method for residential variable-speed ACs to automatically and optimally respond to day-ahead electricity prices. The proposed control-oriented room thermal model and steady-state energy performance model of variable-speed ACs in last two chapters are integrated to predict the coupled thermal response of the room and AC for the purpose of model-based control. Optimal scheduling of indoor air temperature set-points is formulated as a nonlinear programming problem which seeks the preferred trade-offs among electricity costs, thermal comfort and peak power reductions. Genetic algorithm (GA) is used to search the optimal solution of the nonlinear programming problem.

6.1 Outline of the Proposed Model-based Optimal Control Method

6.1.1 Local Control Loop

Figure 6.1 depicts the block diagram of the integrated thermal response models and frequency-based control method of variable-speed AC. A room temperature controller plays the function of connecting the room thermal dynamics with the variable-speed AC. The variable-speed AC controller in the present study is designed using a PID control structure. After detecting the temperature difference from the set-point, the PID controller computes and outputs the actuating signal of rotational speed to the variable-speed compressor motor. Under the specific compressor rotational speed and weather disturbances, the cooling capacity and COP of variable-speed AC can be determined using the developed AC model. The variable-speed AC then delivers the cooling capacity into the air-conditioned room removing the heat gains caused by the disturbances including outdoor air temperature, solar radiation, and internal heat gains.

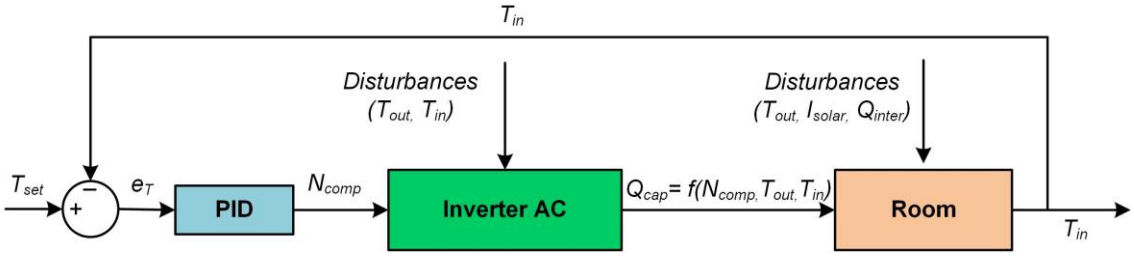

Figure 6.1 Block diagram of the integrated thermal response models and frequency-based control method of variable-speed AC.

6.1.2 Model-based Supervisory/Optimal Control

The basic idea of the model-based optimal control is to use the integrated model to predict the performances of variable-speed AC based on the predictions of weather

conditions, occupancy and day-ahead electricity prices. GA is used to search the optimal control signal, i.e., indoor air temperature set-point schedule.

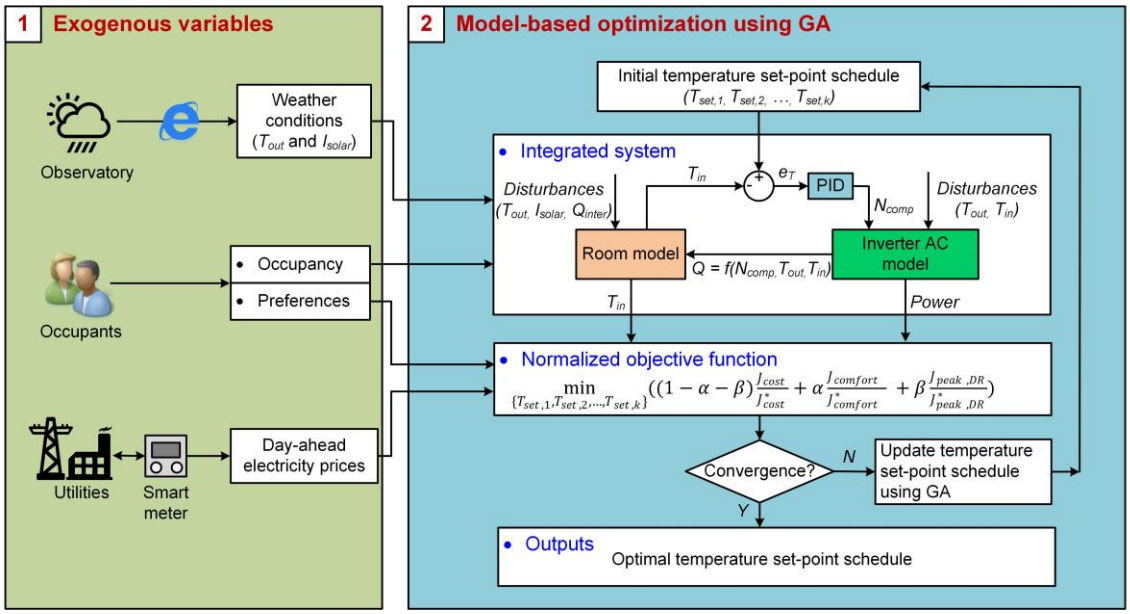

Figure 6.2 Framework of the model-based optimal load control methodology of variable-speed ACs.

As shown in Figure 6.2, the whole process of the model-based optimal DR control of variable-speed AC includes two major steps: preparation/prediction of exogenous input variables and model-based optimization using the GA solver. Weather conditions including outdoor air temperature and solar radiation are required for the predictions of the room thermal dynamics and AC performance, which may come from local observatory or from prediction models (Q. Zhou et al., 2008). The presence of occupant will influence the room thermal response and hence it is an influential variable in the room thermal model. With the aid of advanced infra-red sensing technology, the presence of occupant can be determined conveniently. However, considering the number of residents in a room is small and more or less the same, it

can be pre-defined. Dynamic electricity prices are available from smart meters. The integrated thermal response models of an air-conditioned room and an variable-speed AC are used to predict the AC power consumption and indoor air temperature with the inputs. In the end, an optimization problem is formulated and solved using GA to find the day-ahead optimal schedule of indoor air temperature set-point.

6.2 Problem Formulation and Set Point Optimization using GA

6.2.1 Problem Formulation

The optimization problem in this study is a multi-objective optimization problem, which includes three objectives, i.e., minimization the total electricity cost (J_{cost} as defined by Equation (6.2)), the thermal comfort deviation ($J_{comfort}$, as defined by Equation (6.3)) considering home residents and minimization of the peak power demand during DR hours ($J_{peak,DR}$, as defined by Equation (6.4)) considering the power grids. The total electricity cost (J_{cost}) is the sum of the products of the hourly energy consumption of variable-speed AC (E_i) and the hourly electricity price (C_i). The total comfort deviation ($J_{comfort}$) is the root mean square error of the indoor air temperatures to the temperature set-points. The peak power demand ($J_{peak,DR}$) is the maximum power consumption of the variable-speed AC during DR hours. The time steps of energy consumption (E_i) and electricity price (C_i) are 1 hour and the time intervals of the indoor air temperature ($T_{in,j}$) and the power consumption (P_l) are both 1 minute. The optimization processes of each objective function are subject to the comfort constraint, Equation (6.5), which limits the temperature set-point between a lower bound ($T_{set,lb}$) and an upper bound ($T_{set,ub}$). The three objectives, i.e., Equations (6.2) -

(6.4), are not independent but conflicting. For example, when minimizing the thermal comfort deviation, it may result in the increase of the electricity cost and the increase of the peak power demand. When minimizing the peak power demand, the deviation of thermal comfort may increase.

$$\min_{\{T_{set,1},T_{set,2},\dots,T_{set,k}\}}((1-\alpha-\beta)\frac{J_{cost}}{J^*_{cost}}+\alpha\frac{J_{comfort}}{J^*_{comfort}}+\beta\frac{J_{peak,DR}}{J^*_{peak,DR}}) \tag{6.1}$$

$$J_{cost}=\sum_{i=1}^{m}E_iC_i; \tag{6.2}$$

$$J_{comfort}=\sqrt{\frac{1}{n}\sum_{j=1}^{n}(T_{in,j}-T_{in,exp,j})^2}; \tag{6.3}$$

$$J_{peak,DR}=max\{P_1,P_2,\dots,P_l\}; \tag{6.4}$$

$$\textit{Subject to}\qquad T_{set.lb}\le T_{set,k}\le T_{set,ub} \tag{6.5}$$

where $J^*_{cost}=min\{J_{cost}\}$; $J^*_{comfort}=min\{J_{comfort}\}$ and $J^*_{peak,DR}=min\{J_{peak,DR}\}$.

The methods of multi-objective optimization problem can be divided into classical methods and evolutionary methods. Classical methods include the weighted sum method, epsilon constraint method, weighted metric method, value function method and so on. Evolutionary methods are methods based on evolutionary algorithms such as genetic algorithm(Deb et al., 2002) and particle swarm optimization algorithm(Hamid Reza Baghaee et al., 2012; H. R. Baghaee et al., 2016). The weighted sum method (Grodzevich & Romanko, 2006), which is simple and readily applicable to engineering practice, is adopted in this study to formulate a compound single-objective optimization problem as shown in Equation (6.1). The compound single objective function is mathematically expressed as a sum of weighted individual

objective functions. The weightings can be assigned by the users. Considering different objective functions may have different magnitudes, the individual objective function (J_{cost}, $J_{comfort}$ and $J_{peak,DR}$) is normalized by its own optimal value (J^*_{cost} , $J^*_{comfort}$ and $J^*_{peak,DR}$). After the normalization, all dimensionless objective functions are multiplied with corresponding weightings, i.e., thermal comfort weighting α, peak power weighting β, and cost weighting (1- α - β). Given a set of indoor air temperature set-point schedule $\{T_{set,1}, T_{set,2}, \ldots, T_{set,k}\}$, the indoor air temperature and power consumption can be predicted using the integrated thermal models. Note that due to the nonlinear characteristics of dynamics of the integrated thermal response models, the optimization problem is a nonlinear programming problem and an advanced optimization solver is needed to search the optimal schedule of the indoor air temperature set-points.

6.2.2 Optimization Using GA

Conventional optimization techniques depend strongly on the initial values and are apt to get a local optimization. GA is an evolutionary search algorithm inspired by the process of natural selection. It makes a population of individual solutions "evolve" toward an optimal solution by successive modifications. During each modification, three main types of rules, i.e., selection, crossover and mutation, are used to create the next generation from the current generation. GA can address a variety of optimization problems that standard gradient descent methods are incompetent to solve, such as the problems in which the objective function is discontinuous, stochastic, or highly nonlinear. GA (Tuhus-Dubrow & Krarti, 2010; S. Wang & Xu, 2006) has been used to solve the optimization problems in the domain of HVAC. The major reason for

applying GA in this study is that the algorithm is gradient free and the target problem is a nonlinear programming problem. Population-Size, Max-Generations and Function-Tolerance are three important parameters in the GA optimization, which indicate the number of individuals in each generation, the maximum number of iterations before the algorithm halts and the termination tolerance, respectively. In this study, they are assigned with the values of 100, 160 and 1×10^{-6}, respectively. The GA optimization is solved by using MATLAB on a desktop computer with Intel Core i7-4790 (3.60 GHz), 16 GB of memory, under Windows 10 64-bit operating system. The runtime of the GA optimization in our case study is around 80 minutes. As the model-based DR control method for residential variable-speed ACs developed in this study is to respond to day-ahead electricity pricing which is forecasted by the utility or third-party load aggregator and delivered to the end-users one day ahead, the runtime is acceptable.

6.3 Case Studies and Analysis

6.3.1 Test Conditions

Dynamic electricity pricing is one key component in the implementation of DR programs. DAP and RTP are the most commonly used dynamic electricity pricings used by Independent System Operators (ISO) or Regional Transmission Operators (RTO) such as Electricity Reliability Council of Texas (ERCOT), PJM or New York ISO. Figure 6.3 shows the historical DAP data of the PJM energy market from June to July 2016 (PJM Interconnection, 2017). The average DAP profile is used for case

studies. Weather forecast data from local observatory, pre-defined occupancy profiles and day-ahead electricity prices from electric utilities are used as the inputs.

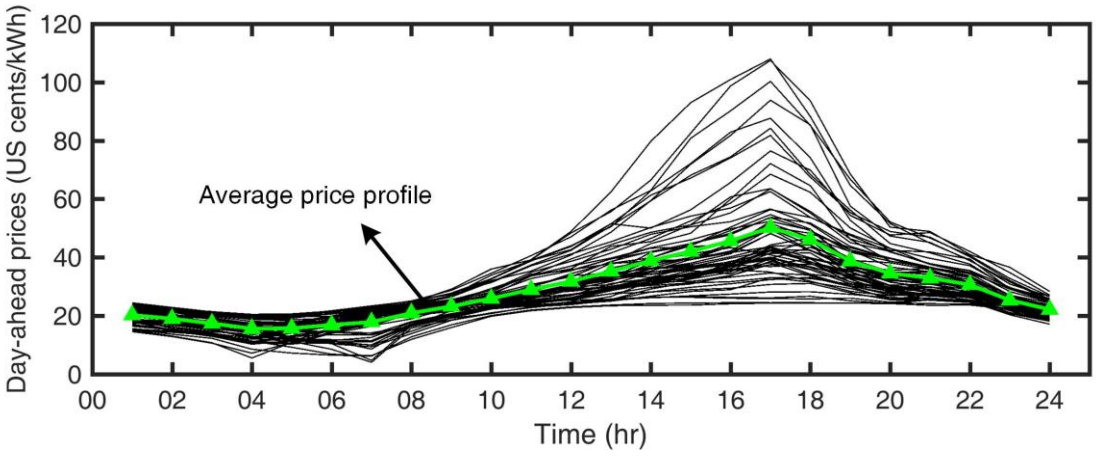

Figure 6.3 Day-ahead pricing data of the PJM energy market from June to July 2016.

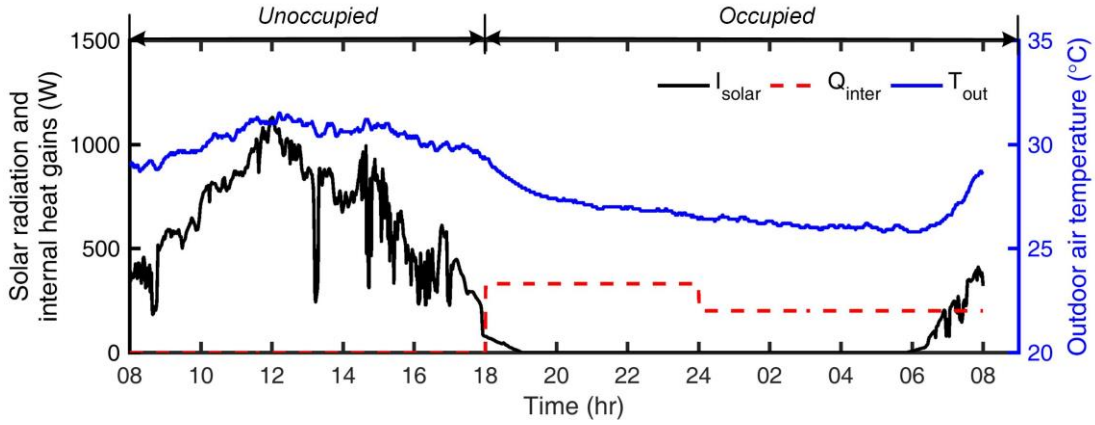

Figure 6.4 Outdoor weather conditions and internal heat gains on a typical hot summer day.

Case studies in this study are carried out on a typical hot summer day. Figure 6.4 shows the outdoor weather conditions and internal heat gains from 8:00 to 8:00 on the next day. The room is unoccupied from 8:00 to 18:00 considering the occupants are out for school or work during day time. Signals of DR events, which normally last for

2 to 4 hours, are determined and delivered by the electric utilities. The DR event here is assumed to start at 16:00 to end at 20:00, which is the typical time period when the residential buildings are occupied and the regional electricity consumption is high. The simulation starts from 8:00 in the morning. It is assumed that the room thermal response is stabilized after one-night AC operation and control, therefore, the AC temperature set-point is used as the initial value of indoor air temperature in the simulation. The time step for simulation is set as 1 minute.

6.3.2 Reference Case without DR Control

A reference case without DR is tested for comparison purpose. The indoor air temperature set-point from 18:00 to 08:00 on the next day is fixed as 24℃ in the baseline case. The PID controller parameters are tuned manually in this study with K_p = 5, K_i = 1 and K_d = 5. Average hourly power consumption, hourly electricity cost and indoor air temperature are shown in Figure 7.5 - Figure 7.10 for comparisons with the GA-based cases.

6.3.3 DR Cases

Different from the baseline case, the pre-cooling strategy is adopted in the GA-based cases which means the AC is allowed to be turned on from 16:00 to 18:00 before the room is occupied. The energy consumptions and electricity costs from 16:00 to 08:00 on the next day are also taken into account when calculating the objective function of Equation (6.2), i.e., m = 16 hours. The temperature deviations are considered only when the room is occupied, i.e., 18:00 to 8:00 on the next day and n = 840 minutes in Equation (6.3). The peak power demand during DR hours in Equation (6.4) is the

maximum value of power from 16:00 to 20:00, i.e., l = 240 minutes. To satisfy the thermal comfort of occupants, the temperature set-points are searched in the range of 22℃ - 26℃ with a constant interval of 0.5 ℃.

The optimal temperature set-point schedule searched by the GA-based method is affected by both thermal comfort weighting α and peak power weighting β. Three groups of cases are tested for investigating the impacts of the weightings on the optimization results. In each group of cases (e.g., Case 1), the peak power weightings are 0.3, 0.4 and 0.5 respectively (i.e., Case 1-a, 1-b and 1-c) while the thermal comfort weightings are the same. Different groups of cases adopt different thermal comfort weightings, i.e., 0.2 for Case 1, 0.3 for Case 2 and 0.5 for Case 3. Table 6.1 shows the whole-day indoor air temperature set-point schedules in the baseline case and GA-based cases. The schedules in the GA-based cases are the optimized results. Table 6.2 compares the performances of the GA-based cases with the baseline case in terms of peak power reductions, electricity cost savings and temperature deviations. Mean absolute error (MAE) and root mean square error (RMSE) are used to quantify the temperature deviations from the temperature set-points. Some common features in all GA Cases can be found as follows. Compared with the baseline case, the peak power consumptions and total electricity costs in all GA-based cases have certain reductions. In terms of thermal comfort, the indoor air temperatures in the GA-based cases have larger temperature deviations, but they still remain in the comfort constraint of 22℃ - 26℃.

Table 6.1 Indoor air temperature set-point schedules in baseline case and GA-based cases

Time of day		Indoor air temperature set-point schedules (°C)									
Start	End	Baseline Case	GA Cases								
			Case 1-a	Case 1-b	Case 1-c	Case 2-a	Case 2-b	Case 2-c	Case 3-a	Case 3-b	Case 3-c
08:00	16:00	off	off	off	off	off	off	off	off	off	off
16:00	17:00	off	25.5	26	26	25.5	25.5	26	25.5	25.5	26
17:00	18:00	off	25.5	26	26	25.5	25.5	26	25.5	25.5	25.5
18:00	19:00	24	25.5	26	26	25	25	25.5	24.5	25	25
19:00	20:00	24	25	26	26	24.5	25	25.5	24.5	24.5	24.5
20:00	21:00	24	24.5	23	25	24	24	25	24.5	24	24
21:00	22:00	24	24	25	26	24	24.5	24.5	24	24	24
22:00	23:00	24	24	25	26	24	24	24.5	24.5	24.5	24
23:00	00:00	24	25	25	24	25	25	24.5	24	24	24.5
0:00	01:00	24	24.5	25	25.5	24.5	24	24.5	24	24	24
01:00	02:00	24	24.5	24.5	25	24.5	24	23.5	24	24	24
02:00	03:00	24	24.5	24.5	25	24	23.5	25	24	24	24.5
03:00	04:00	24	25.5	23.5	25.5	24	24	24.5	24.5	24	23.5
04:00	05:00	24	25.5	23.5	25	24	24	24.5	25	24.5	23.5
05:00	06:00	24	25	26	26	23.5	24	24	24.5	23.5	24.5
06:00	07:00	24	23.5	24	24.5	23.5	25	25	24	24	23.5
07:00	08:00	24	26	25	25	25	24	25	24.5	25	24.5

Table 6.2 Performance comparison in baseline case and GA-based cases

Cases	Comfort weighting	Peak weighting	Peak power demand during DR hours (W)	Peak power reduction (%)	Electricity cost (Cents)	Cost saving (%)	Temperature deviation (°C)	
							MAE	RMSE
Baseline Case			1343.0	0	161.98	0	0.05	0.37
GA Case 1-a	0.2	0.3	566.2	57.84%	131.43	18.86%	0.50	0.65
GA Case 1-b	0.2	0.4	444.9	66.87%	133.47	17.60%	0.79	0.99
GA Case 1-c	0.2	0.5	444.9	66.87%	101.22	37.51%	1.01	1.19
GA Case 2-a	0.3	0.3	566.2	57.84%	142.22	12.20%	0.34	0.48
GA Case 2-b	0.3	0.4	566.2	57.84%	139.92	13.62%	0.31	0.50
GA Case 2-c	0.3	0.5	444.9	66.87%	121.97	24.70%	0.57	0.73
GA Case 3-a	0.5	0.3	702.6	47.68%	145.17	10.37%	0.20	0.29
GA Case 3-b	0.5	0.4	566.2	57.84%	144.66	10.69%	0.22	0.36
GA Case 3-c	0.5	0.5	549.4	59.09%	143.98	11.11%	0.31	0.43

6.3.3.1. Sensitivity analysis of peak power weighting

Three sets of GA-based cases (i.e., Case 1, 2 and 3) are studied to investigate the sensitivity of the optimization method to the peak power weighting. In each set of cases, the thermal comfort weightings remain fixed as 0.2, 0.3 and 0.5, respectively, and the peak power weightings are set as 0.3, 0.4 and 0.5 in each set. Average hourly power consumption, electricity cost and indoor air temperature in all cases are shown in Figure 6.5 - Figure 6.7. It can be found that when the thermal comfort weighting is fixed, peak power consumptions during DR hours and total electricity costs decrease with the increase of the peak power weighting. This is because the increase of the peak power weighting means the peak power reduction is considered to be more important

in searching the optimal solution using GA. As shown in Table 6.2, the maximum peak power reductions are achieved with the largest peak power weightings in each set of GA-based cases, i.e., 66.87% in Case 1-c, 66.87% in Case 2-c and 59.09% in Case 3-c, respectively. The minimum temperature deviations (RMSE) occur with the smallest peak power weighting in each set of GA-based cases, i.e., 0.65℃ in Case 1-a, 0.48℃ in Case 2-a, and 0.29℃ in Case 3-a, respectively. The results show that the objective function is sensitive to the peak power weighting, and the peak power weighting reasonably influences the optimization results to achieve the optimization purpose.

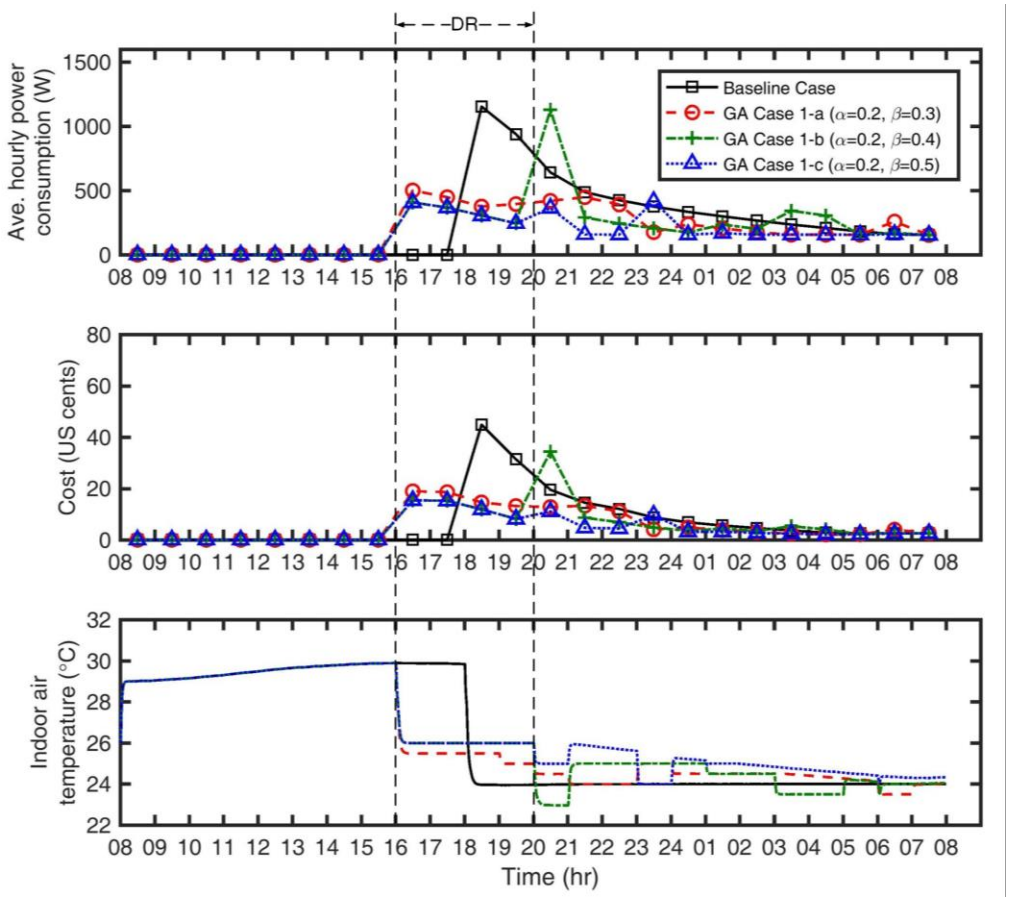

Figure 6.5 Energy consumption, cost and indoor air temperature in the baseline case and GA-based cases (α = 0.2, β = 0.3/0.4/0.5).

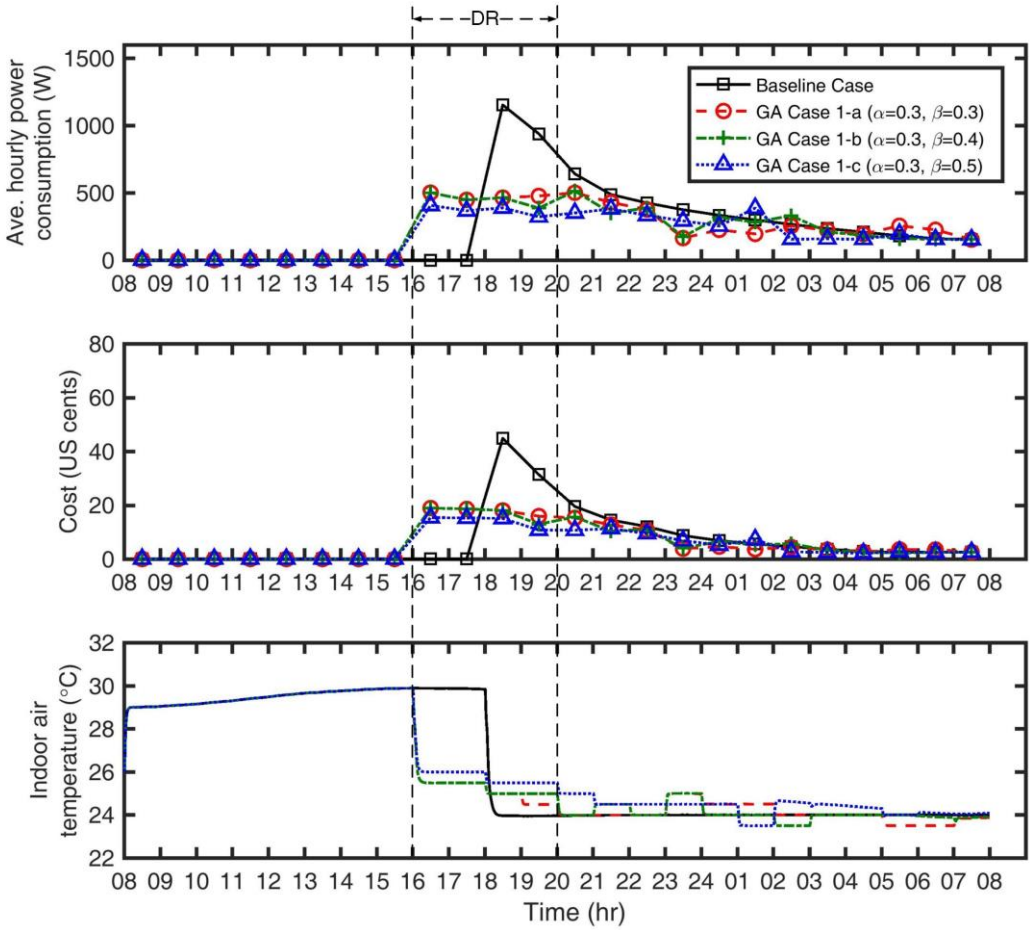

Figure 6.6 Energy consumption, cost and indoor air temperature in the baseline case and GA-based cases ($\alpha = 0.3$, $\beta = 0.3/0.4/0.5$).

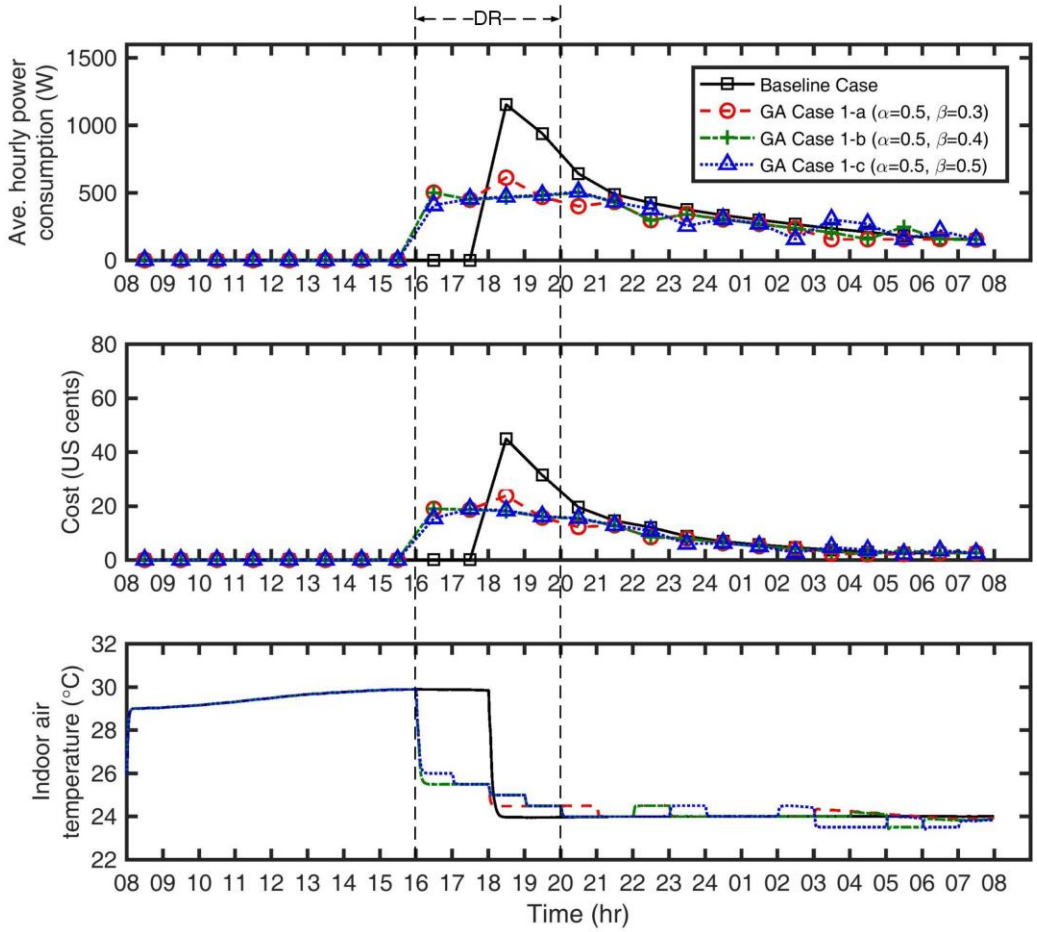

Figure 6.7 Energy consumption, cost and indoor air temperature in the baseline case and GA-based cases ($\alpha = 0.5$, $\beta = 0.3/0.4/0.5$).

6.3.3.2. Sensitivity analysis of thermal comfort weighting

In order to investigate the impacts of the thermal comfort weighting on the optimization results, the simulation results are presented in a different way where the peak power weightings remain fixed at 0.3, 0.4 and 0.5 while the thermal comfort weightings are 0.2, 0.3 and 0.5 in each set of GA-based cases. Figure 6.8 - Figure 6.10 show the profiles of average hourly power consumption, electricity cost and indoor air temperature in all cases. It can be seen that when the peak power weighting is fixed, peak power consumptions during DR hours and total electricity costs increase with

the increase of the thermal comfort weighting. This is because the increase of the thermal comfort weighting means occupants consider maintaining thermal comfort is more important in searching the optimal solution using GA. The maximum peak power reductions are achieved with the smallest thermal comfort weighting in each set of GA-based cases, i.e., 57.84% in GA Case 1-a, 66.87% in GA Case 1-b and 66.87% in GA Case 1-c, respectively. The minimum temperature deviations (RMSE) occur with the largest thermal comfort weighting in each set of GA-based cases, i.e., 0.29℃ in GA Case 3-a, 0.36℃ in GA Case 3-b, and 0.43℃ in GA Case 3-c, respectively. The results show that the objective function is sensitive to the peak power weighting, and the peak power weighting reasonably influences the optimization results to achieve the optimization purpose.

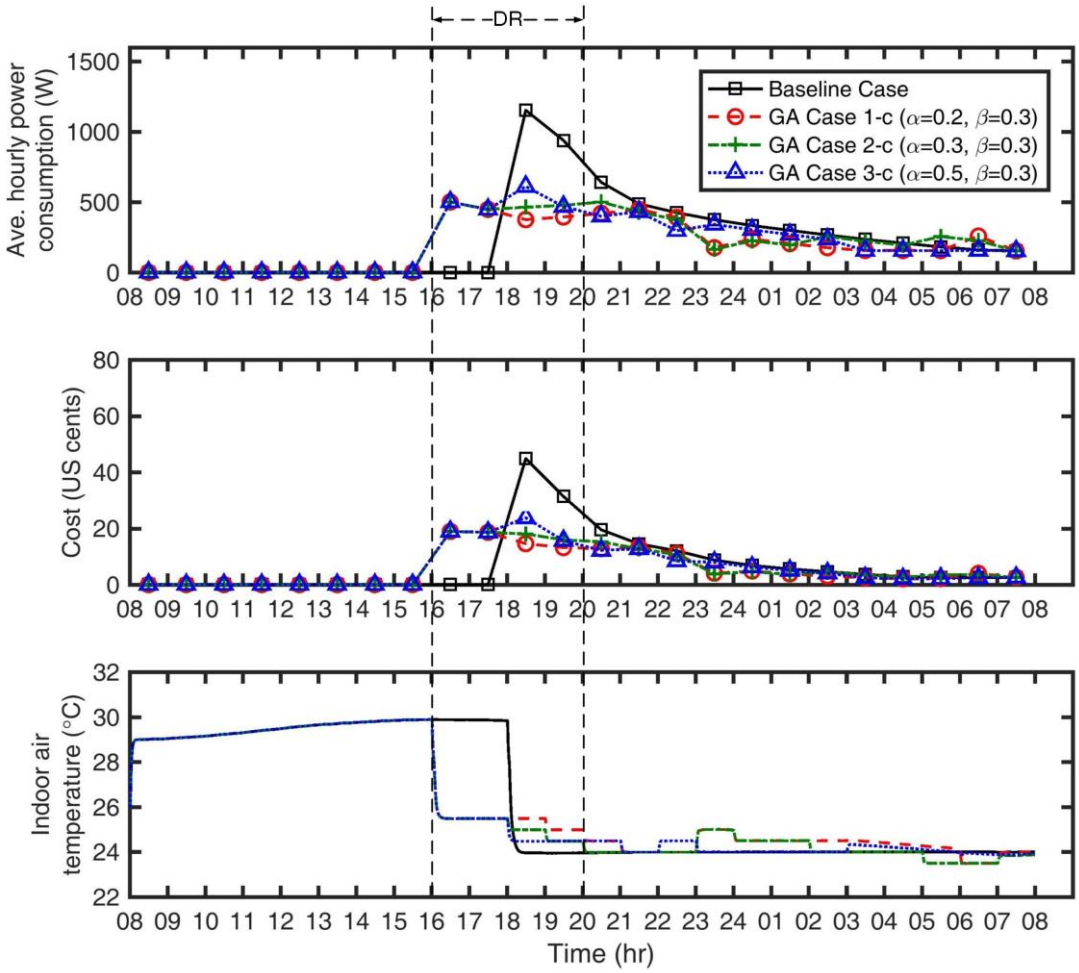

Figure 6.8 Energy consumption, cost and indoor air temperature in the GA-based cases (α = 0.2/0.3/0.5, β = 0.3).

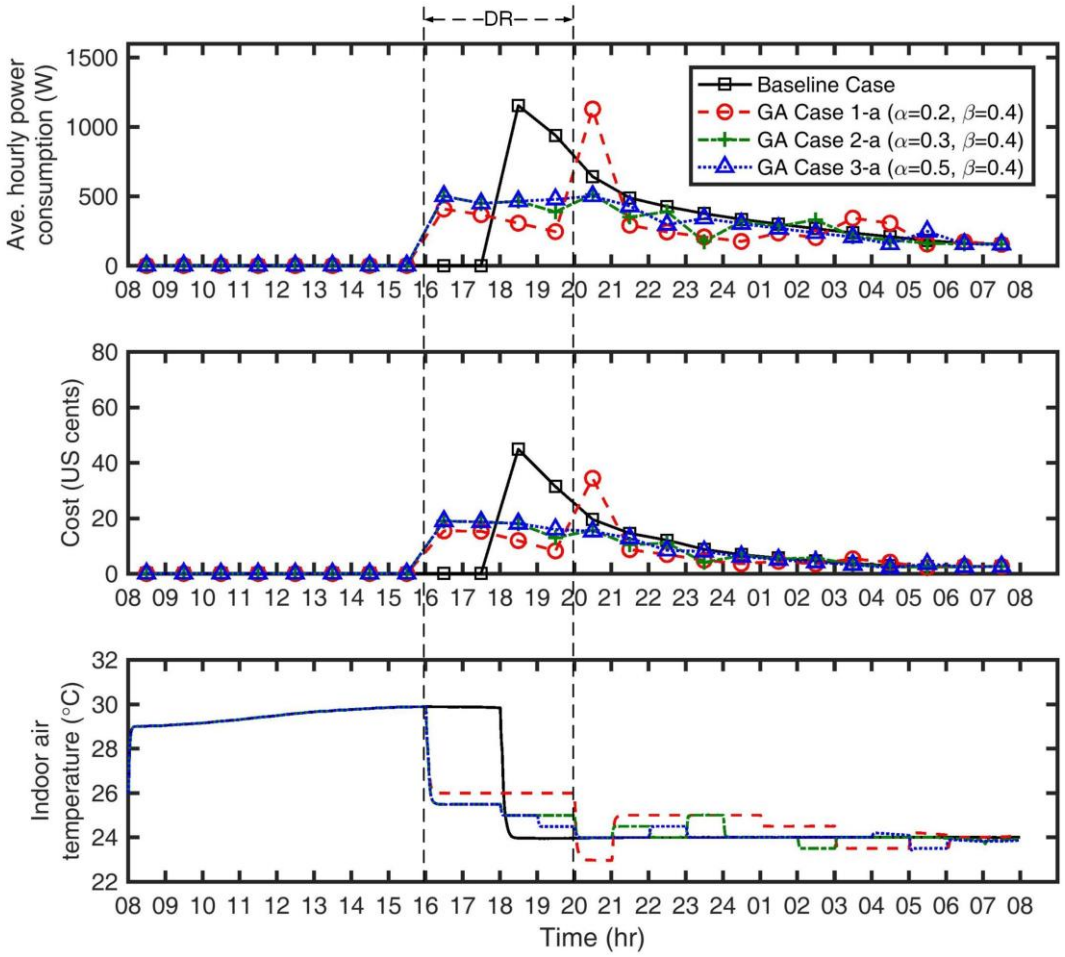

Figure 6.9 Energy consumption, cost and indoor air temperature in the GA-based cases (α = 0.2/0.3/0.5, β = 0.4).

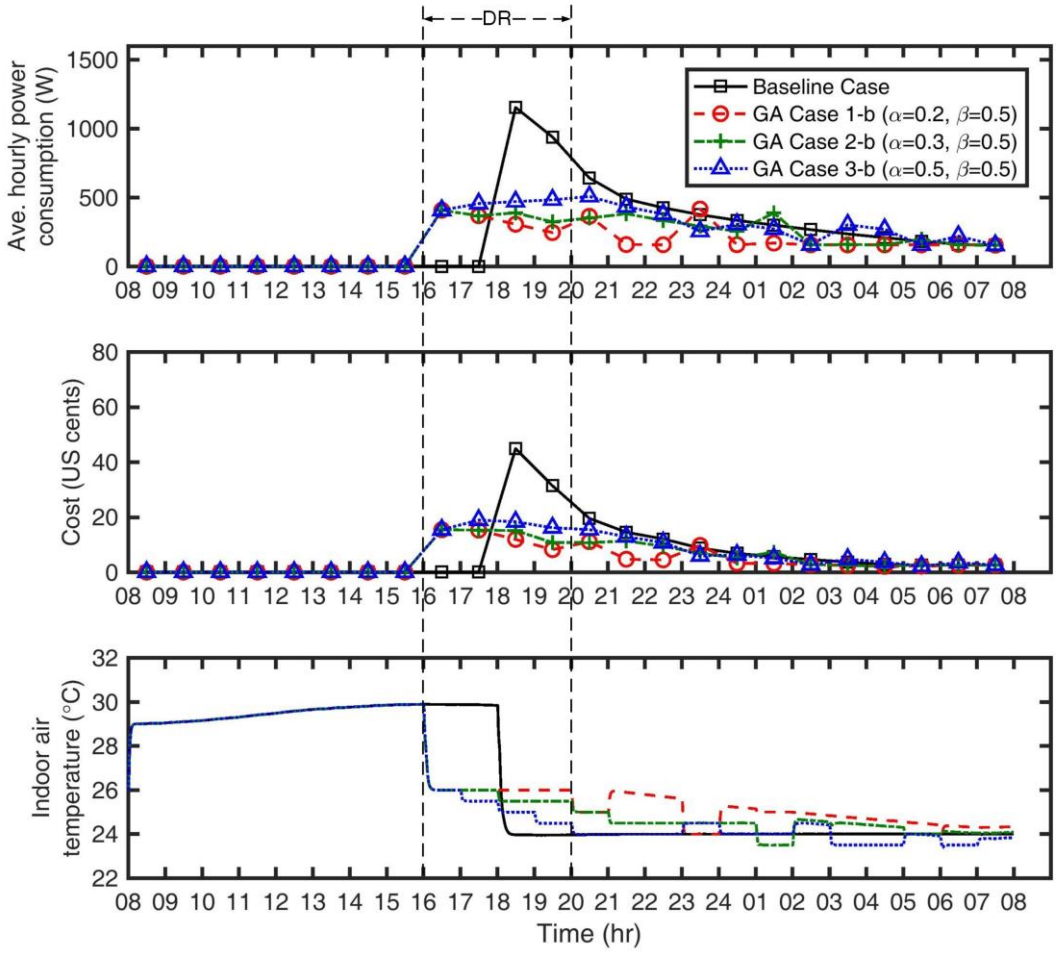

Figure 6.10 Energy consumption, cost and indoor air temperature in the GA-based cases (α = 0.2/0.3/0.5, β = 0.5).

6.4 Summary

Dynamic electricity pricing is an effective DR program in smart grids to attract residential end-users to participate in it. It can bring about cost savings to residential homes while relieving power imbalance issue during on-peak hours. Intelligent DR control technologies for household appliances, especially ACs, are urgently required to encourage and enable wider participations. The chapter presents a model-based optimal DR control method for residential variable-speed ACs to achieve optimal

trade-offs among electricity costs, thermal comfort and peak power reductions in the dynamic electricity pricing environment.

For the purpose of computational efficiency, the simplified control-oriented room thermal model and energy performance model of variable-speed ACs are integrated for model-based control. We formulate the trade-offs among electricity costs, occupant comfort and peak power reductions during DR hours as a nonlinear programming problem using the weighted sum approach. The weightings in the compound objective function are user-definable, which indicate the preferences of participants. GA, as an advanced and effective optimization method, is used to solve the optimization problems.

Simulation results of case studies show that the proposed model-based optimal control method can reduce the peak power consumptions of variable-speed ACs and reduce the electricity costs while still satisfying the thermal comfort constraints. Sensitivity analyses of the weightings in the normalized objective function show that the objective function is reasonably formulated and sensitive to both peak power weighting and thermal comfort is weighting. Minimizing the comprehensive objective function can effectively achieve the optimal trade-offs among the electricity costs, occupant comfort and peak power reductions.

The proposed model-based optimal control method can be implemented in the smart HEMSs and enable the residential variable-speed ACs to automatically respond to the day-ahead dynamic electricity prices to achieve the optimal trade-offs. When a large number of residential ACs simultaneously respond to dynamic electricity prices from

utilities or third-party load aggregators, power consumptions in grid during on-peak hours can be significantly reduced.

CHAPTER 7 PRINCIPLES OF MODEL PREDICTIVE CONTROL AND ITS APPLICATIONS IN BUILT ENVIRONMENT CONTROL

In order to make response to 5-minute RTPs for variable-speed ACs, a frequency-based model-based optimal control method is needed, which also needs to simultaneously take account of the other influential variables including dynamic weather conditions and occupancy. Model predictive control (MPC), also called receding horizon predictive control, is a promising method for frequency-based DR control of residential variable-speed ACs.

Prior to applying MPC method to control variable-speed ACs, the fundamentals behind MPC are first briefly discussed in Section 7.1. Section 7.2 presents the state-of-the-art studies on MPC of built environment.

7.1 Principles of Model Predictive Control

7.1.1 General Control Procedure

MPC, also called receding horizon control, is an intuitive advanced control method of constrained control that has been successfully applied in many research areas over the last decades (Camacho & Alba, 2013; Oldewurtel, 2011). The major advantage of MPC is that it can simultaneously take account of all the influential variables at the controller design stage while satisfying the system operating constraints. Its main idea

is to use system models to predict the future evolution of the system under the predicted operating conditions.

Table 7.1 Procedure of model predictive control (Receding horizon control)

Algorithm of Model Predictive Control
Step 1. Measure the state x_t at time step t
Step 2. Obtain the optimal output $u_t^*(x_t) = \{u_{t\|t}^*, u_{t+1\|t}^*, \dots, u_{t+N-1\|t}^*\}$ by solving an optimization problem with prediction horizon N
Step 3. Apply the first command signal $u_{t\|t}^*$ to the system
Step 4. Proceed to time step t+1
Step 5. Go to Step 1

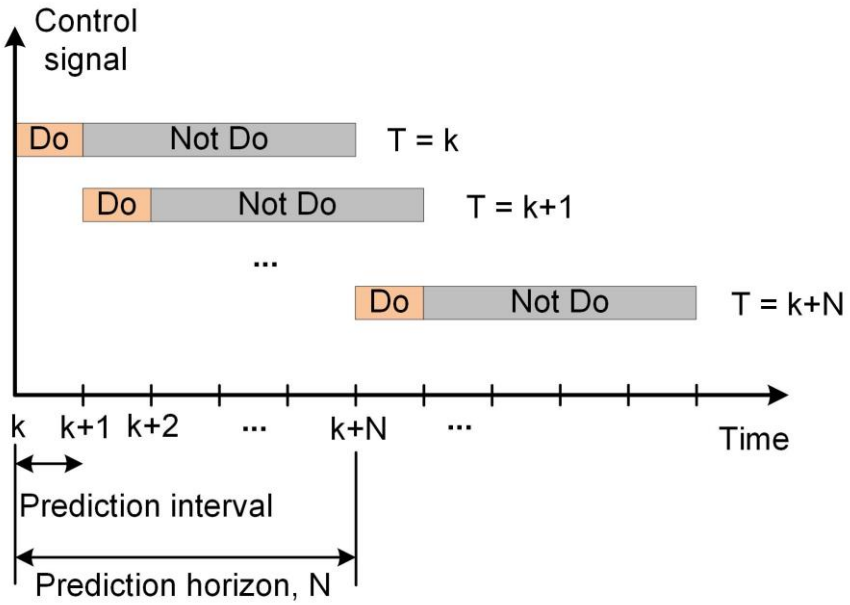

Figure 7.1 Scheme of receding horizon strategy. (Only the first control signal is adopted at each optimization step, while the rest of the output trajectory is discarded).

Table 7.1 summarizes the whole procedure of MPC. During each discrete time interval, starting at the current state, an optimal control problem is formulated and solved over a finite horizon. The optimization result is a trajectory of future control inputs satisfying the dynamics and time-varying constraints of the system. However, only the first control signal will be adopted by the system at the next sampling time, while the rest of the sequence is disposed, as shown in Figure 7.1. In order to compensate for modeling deviations and/or disturbances, a new measurement is taken at the next time step and the whole procedure is repeated with prediction horizon shifted forwards by one time step. The purpose of receding horizon is to introduce the feedback into the system.

7.1.2 Critical Components

The design efforts of an MPC controller consist of specifying some dynamics, constrains of the control problem and a cost function that encapsulate the preferences of the user towards some particular behavior of the control signals. At each sampling interval, the components, including cost function, dynamics, constraints and current state, are combined and converted into an optimization problem. A generic MPC framework is given by the following finite-horizon optimization problems, i.e., Equations (7.1) – (7.4).

$$\min_{u^*_{t|t},u^*_{t+1|t},\ldots,u^*_{t+N-1|t}} \sum_{k=0}^{N-1} f_k(x_{t+k|t}, u_{t+k|t}) \qquad \text{Cost function} \qquad (7.1)$$

$$\text{subject to} \quad x_{t+k+1|t} = g(x_{t+k|t}, u_{t+k|t}) \qquad \text{Dynamics} \qquad (7.2)$$

$$\left(x_{t+k|t}, u_{t+k|t}\right) \in \mathbb{X} \times \mathbb{U} \qquad \text{Constraints} \qquad (7.3)$$

$$x_{t|t} = x_t \qquad \text{Current state} \qquad (7.4)$$

In order to distinguish between the prediction of a state and the actual state, we use $x_{t+k|t}$ to denote the prediction for the actual state x_{t+k} at time *t*; *N* is the prediction horizon; $\mathbb{X}$ and $\mathbb{U}$ are the constraint sets for states and inputs, respectively.

The cost function and constraints are the major components of the MPC design. The dynamics of the system have to be modeled to a reasonable precision to achieve a good control performance. The current state is used as the initial state for predicting the future evolution of the system. In the following, the significance of each of the four components is briefly introduced.

Cost Function

The cost function depicts the desired behavior of the target system. Generally, it serves two purposes, i.e., stability and performance target.

- **Stability**. To achieve the stability of the control, Lyapunov functions are usually chosen as cost functions for the closed loop system. In practice, this requirement is normally relaxed for the systems with slow dynamics, such as

buildings. For MPC designers, this increases the freedom to select the cost function strictly on the basis of performance.

- **Performance target**. The cost function is generally, but not always, used to express a preference for one closed-loop behavior over another. For instance, minimizing energy consumption or maximizing thermal comfort in built climate control.

The majority of cost functions in use are convex, resulting in a simple optimization problem to solve using state-of-art solvers. Common options of cost functions are listed in Table 7.2.

Table 7.2 Common types of cost function in MPC controllers

Cost function type	Mathematical description
Quadratic cost	$J_k(x_{t+k\|t,}u_{t+k\|t}) = x_{t+k\|t}^T Q x_{t+k\|t} + u_{t+k\|t}^T R u_{t+k\|t}$
Linear cost	$J_k(x_{t+k\|t,}u_{t+k\|t}) = \|Q x_{t+k\|t}\|_1 + \|R u_{t+k\|t}\|_1$
Probabilistic cost	$J_k(x_{t+k\|t,}u_{t+k\|t}) = P[g(x_{t+k\|t,}u_{t+k\|t})]$

- **Quadratic cost**. The relative weighting between the states and the command inputs, i.e., the determination of the matrices Q and R, provides a trade-off between the regulation quality and the energy of the inputs. If a system is unconstrained, or the constraints are inactive, then the problem is reduced to a classic Linear Quadratic Regulator (LQR). In the area of built climate control, this type of cost function is usually used as a low-level controller which tracks the set-points given by the high-level controllers.

- **Linear cost**. If the control objective is to minimize the amount of the used energy/operating cost instead of doing a trade-off using quadratic costs, then the linear cost function is a suitable choice. 1-norm cost would be a common choice for minimizing the energy consumption in buildings.
- **Probabilistic cost**. This cost function is usually chosen for systems subject to random disturbances. It is able to take account of the stochastic nature of certain phenomena, and minimize some expected values of some events, such as the bound violations of room thermal comfort.

Dynamics

Given the initial condition of states, numerical optimizers need a system model to predict the future evolution of the states. Modeling the dynamics of the system plays a critical role in the MPC controller, since the control performance depends on the quality of the model. The most common models used in MPC controllers are listed in Table 7.3.

Table 7.3 Common types of dynamic models in MPC controllers.

Dynamic model type	Mathematical description
Linear model	$x_{t+k+1\|t} = Ax_{t+k\|t} + Bu_{t+k\|t}$
Input-affine model	$x_{t+k+1\|t} = f(x_{t+k\|t}) + g(x_{t+k\|t})u_{t+k\|t}$
Piecewise affine (PWA) model	$x_{t+k+1\|t} = \begin{cases} A_1 x_{t+k\|t} + B_1 u_{t+k\|t} & if\ x_{t+k\|t} = P_1 \\ \vdots & \vdots \\ A_n x_{t+k\|t} + B_n u_{t+k\|t} & if\ x_{t+k\|t} = P_n \end{cases}$
Non-linear model	$x_{t+k+1\|t} = f(x_{t+k\|t}, u_{t+k\|t})$

- **Linear model**. Linear model is the most common type of model in use. More importantly, it is the only one type which results in convex and easily solvable optimization problems. For multiple input multiple output (MIMO) systems, the state space model is commonly used to describe system dynamics.
- **Input-affine model**. It can be used to model a large number of complicated systems, but it is very difficult to handle at the same time. Under some circumstances, some mathematical tricks can be made to efficiently manage the dynamics of the system.
- **Piecewise affine (PWA) model**. This class of model contains a mixture of discrete and continuous components, such as switches or valves in combination with continuous systems. It is extremely general and can be used to approximate any smooth system to an arbitrary degree of accuracy. Optimization problems for this type of system are usually formulated as mixed-integer optimization problems, which are in general difficult to be solved, although many well-tested methods are available for some special cases.
- **Non-linear model**. Non-linear models are very common in real cases. Due to their generality, they are significantly more difficult to handle and thus not considered for MPC purposes.

Constraints

The key strength of the MPC method is the ability to specify constraints in the MPC formulation and to handle them directly using optimization routines. Instead of using the concept of specific set point of the controlled variables, specified constraints of

optimization problem are chosen to fulfill the control targets. Various types of constraints are used in practice, an overview of common types suitable for built climate control is given in Table 7.4.

Table 7.4 Common types of constraints in MPC controllers.

Constraint type	Mathematical description
Linear constraint	$Ax_{t+k\|t} \leq b$
Convex quadratic constraint	$\left(x_{t+k\|t} - \bar{x}\right)^T Q\left(x_{t+k\|t} - \bar{x}\right) \leq 1$
Second order cone constraint	$\left\|Ax_{t+k\|t} + b\right\|_2 \leq Cx_{t+k\|t} + d$
Chance constraint	$\mathrm{P}\left[Ax_{t+k\|t} \leq b\right] \geq 1 - \alpha, \alpha \in (0,1)$

- **Linear constraint**. This is the most common type of constraint, which is used to set upper and/or lower bounds on controlled variables. Linear constraints are the easiest to handle when solving optimization problems and can also be used to approximate any convex constraint to an arbitrary degree of accuracy.
- **Convex quadratic constraint**. This type of constraint is used to set variable bounds within ellipses. In building control, this type of constraint would arise, e.g., when formulating a bound on the total input energy produced by several actuators.
- **Second order cone constraint**. Under some special circumstances, second order cone constraints can result from reformulations of chance constraints. When $A = 0$, the constraint collapses to a linear constraint. When $C = 0$, the constraint collapses to a convex quadratic constraint.

- **Chance constraint**. This type of constraint is chosen when uncertainty needs to be taken into consideration. Since an optimization problem can only be solved if all variables are deterministic, chance constraints need to be transformed into deterministic constraints.

Current State

The system model needs to be initialized with the current (measured/estimated) state of the system and all future predictions of exogenous input variables. If some states cannot be measured, a Kalman filter is commonly used for state estimations (Bishop & Welch, 2001; Simon, 2006). The Kalman filter is an algorithm that provides a computationally efficient solution to estimate the state of a process in a way that minimizes the prediction mean squared error. The solution is recursive in such a way that each updated estimate of the state is computed from the previous estimate and the new measured data.

Prediction Horizon and Prediction Interval

Prediction horizon N and prediction interval Δt play significant roles in the performance of MPC controllers. The determination of the prediction horizon is a trade-off between the accuracy of the prediction of exogenous inputs and a sufficient length of the prediction horizon. Long horizon also increases the computation time of each optimization. For the MPC of radiant heating systems, the prediction horizon is normally set as 6 – 48 hours because the rooms have large thermal masses and respond to the heating system very slowly (Feng et al., 2015; Halvgaard et al., 2012; Hedegaard et al., 2018; Karlsson & Hagentoft, 2011; Široký et al., 2011). Prediction interval is

the frequency at which the optimization problem is solved and at which the actuator receives the command signal, which is affected by the thermal response time of the system.

7.2 MPC for Built Environment Control

MPC is a flexible and intuitive approach for constrained control, which was initially applied in the process industries such as petroleum refineries and chemical plants in the late 1970s and has been successfully developed in many other fields over the last decade (Camacho & Alba, 2013; Morari & Lee, 1999; Qin & Badgwell, 2003).

In recent years, MPC has received increasing attentions in the field of built environment control. As shown in Figure 7.2, the general procedure of MPC scheme in built environmental control is as follows: at the current time, a heating/cooling plan is formulated for the next several hours to days based on predictions of the upcoming weather conditions. Predictions of any other disturbances (e.g., internal gains), the to-be-controlled costs (e.g., dynamic electricity prices), and the constraints (e.g., thermal comfort range) can be readily included in the optimization. The first step of the control plan is applied to the building, determining the setting of all the heating, cooling, and ventilation actuators, then the process is repeated at the next time instant (Oldewurtel, 2011; Oldewurtel et al., 2012).

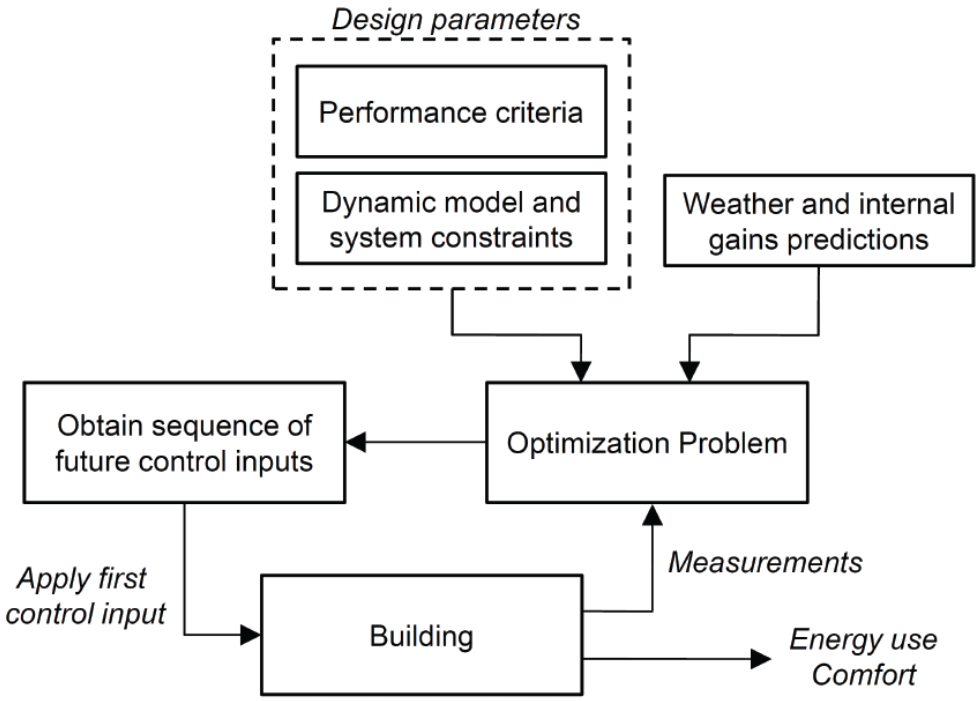

Figure 7.2 MPC scheme for built environment control (Oldewurtel et al., 2012).

Some major works on the MPC of built environment are listed as follows:

Privara et al. (Samuel Prívara et al., 2011) applied MPC to the temperature control of a real building heating system using both weather forecast and thermal model of a building. The MPC controller can utilize thermal capacity of a building and minimize energy consumption. It can also maintain inside temperature at desired level independent of outside weather conditions. The MPC controller was tested on a large university building during a heating season, achieving energy savings of 17–24% in comparison to the present controller.

Siroky et al. (Široký et al., 2011) applied MPC to a ceiling radiant heating system, in which heating beams were embedded into the concrete ceiling to utilize the thermal

capacity of the building. Simulation results showed that the energy savings for using MPC with weather predictions for the target building heating system were between 15% and 28%, which majorly depended on insulation level and outdoor temperature.

Ma et al. (J. Ma et al., 2012) developed an economic MPC method for a multi-zone commercial building equipped with of variable air volume cooling system. The Building Controls Virtual Test Bed (BCVTB) was used as middleware to provide real-time data exchange between EnergyPlus and MATLAB in which the MPC controller was developed. An economic objective function was used to account for the daily electricity costs. Precooling during off-peak periods and cooling discharge from the building thermal mass during on-peak periods can be observed from the simulation results. Compared with the open-loop control strategies, MPC helped to reduce the operating costs.

Ma et al. (Y. Ma, F. Borrelli, et al., 2012; Ma et al., 2015) used both deterministic and stochastic MPC approaches to control large building cooling systems equipped with thermal energy storage by using predictions of weather conditions and building loads. A simplified hybrid model was used to predict the main behavior of the overall system. An MPC controller was designed to optimize the scheduling and operation of the central plant to reduce the electricity costs and to improve the system performances. Experimental results showed that the MPC method enabled a 19.1% improvement of the COP of the plant in comparison to the original baseline case.

Halvgaard et al. (Halvgaard et al., 2012) developed an economic MPC controller to control a ground source heat pump for heating residential buildings with a water-based floor heating system. The thermal capacity of the building was used to shift the energy

consumption to low-price periods, making the residential building become a flexible power consumer. Both dynamic weather conditions and electricity pricing were included in the model. Simulation studies demonstrated that compared to traditional operation of heat pumps, the optimized operating strategy saves 25-35% of the electricity cost.

Unlike the other studies which focused on a particular case, Oldewurtel et al. (Oldewurtel et al., 2012) investigated the potential of energy saving in a large-scale simulation study for a large number of different cases varying in the building type, HVAC system, and weather conditions. Simulation results showed that for many cases, MPC has a significant energy savings potential. Besides, stochastic MPC was shown to outperform the conventional control method in terms of non-renewable primary energy usage, thermal comfort statistics, and advantageous room temperature dynamics.

Feng et al. (Feng et al., 2015) applied MPC to radiant slab systems with evaporative cooling sources. A first-order dynamical model was developed for implementation in the MPC controller and it was shown to be able to predict the system performance reasonably well. Model predictive control (MPC) was tested against a fine-tuned rule based heuristic control method for this complex control problem. Test results showed that the MPC controller was able to maintain zone operative temperatures at thermal comfort level more than 95% of the occupied hours for all zones. Compared to the heuristic method, MPC reduced the energy consumption of the cooling tower by 55% and pumping power consumption by 25%.

To conclude, existing studies demonstrate the superiority of MPC in energy-efficient/cost-effective based optimal control of building energy systems especially when several influential variables need to be considered.

7.3 Summary

The main idea of MPC is to use system models to predict the future evolution of the system under the predicted operating conditions. Unlike the conventional model-based optimal control method using one-shot optimization, MPC is intrinsically a feedback control, which incorporates iterative optimizations over moving prediction horizons.

The formulations of cost function, system dynamics, and constraints play significant roles in the performance of an MPC scheme. To obtain simple optimization problems, the majority of cost functions, which describe the desired performance, are convex, such as quadratic costs and linear costs. Instead of using the concept of specific set point of the controlled variables, specified constraints of optimization problem are chosen to fulfill the control targets. Due to the computational simplicity, linear constraint is the most common type of constrain. For multiple input multiple output (MIMO) systems, the state space model is commonly used to describe system dynamics.

MPC has been applied in the field of built environment control in recent years. Existing studies demonstrate the superiority of MPC in energy-efficient/cost-effective based optimal control of building energy systems especially when several influential variables need to be considered.

CHAPTER 8 DIRECT MODEL PREDICTIVE CONTROL IN RESPONSE TO REAL-TIME PRICING

Two types of dynamic electricity pricings are widely used by most utilities in the United States, i.e., day-ahead pricing and real-time pricing (Federal Energy Regulatory Commission, 2014). For day-ahead pricing, the prices at hourly intervals are announced to the end-consumers one day ahead. For real-time pricing, the electricity prices are offered every 5 minutes based on the current electricity supply and demand of grid nodes. The indirect model-based control method is used to respond to day-ahead pricing via temperature set-point adjustment. There is a lack of real-time optimal DR control methods in response to real-time pricing for variable-speed ACs.

The model-based optimal control method in the literature usually adopted a two-level hierarchy structure in which the command signals for actuators such as rotational speed of compressor and opening degree of valve were sent by local controllers, e.g., the on-off controller and PID controller. The high-level controller, i.e., the supervisory controller, was used to set the optimal set points for the low-level local controllers. Due to the thermal mass, indoor temperature changes in buildings is much slower than the response speed of a controller. To respond to real-time pricing at 5-minute intervals, direct control of the compressor frequency, which closely relates to the power consumption, is more effective in shifting power consumption than adjusting the temperature set points of a local controller every 5 minutes. Thus, in this chapter we aim to use model predictive control method to directly regulate the operating

frequencies of the compressors in variable-speed ACs in response to the real-time pricing.

8.1 Outline of the Proposed Model Predictive Control Method

For purposes of comparison, two types of MPC controllers are designed for variable-speed ACs including an ordinary MPC controller without DR function and a DR-enabled MPC controller with automatic response capability to RTP. As shown in Figure 8.1, for both MPC controllers, three major steps are included in each time step of MPC: (1) preparation/prediction of the exogenous input variables, including the weather, occupancy, and RTP; (2) solution of the optimization problem based on the predicted exogenous inputs and updated current state filtered by the Kalman filter; (3) control implementation and measurement. Figure 8.1 illustrates the flows of both MPC controller without DR function and the DR-enabled MPC controller. The RTP-related blocks (in yellow) are involved only in the DR-enabled MPC controller.

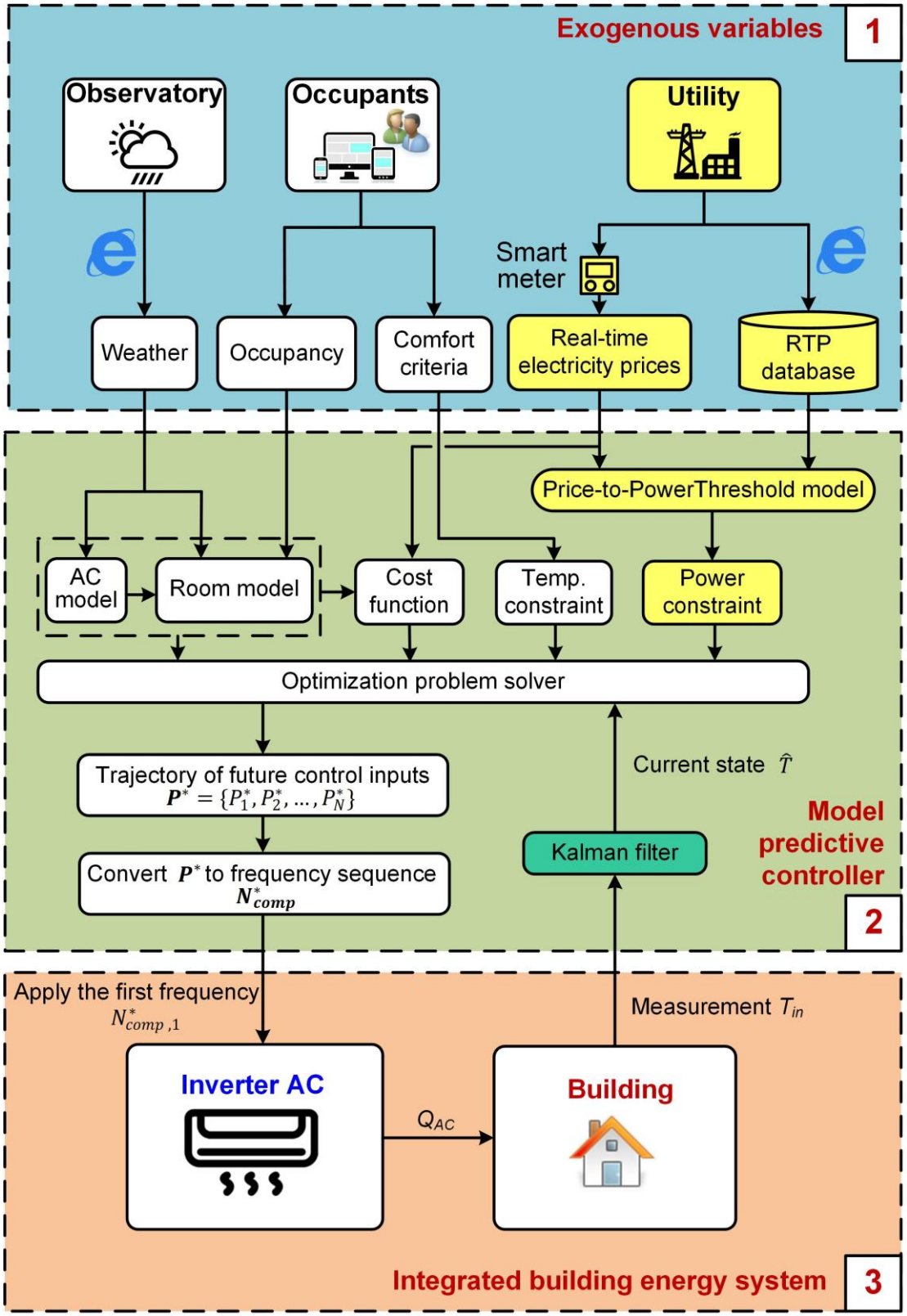

Figure 8.1 Flow chart of online MPC for variable-speed ACs.

8.2 DR-enabled MPC Controller

8.2.1 Step 1: Preparation/Prediction of Exogenous Input Variables

Weather Conditions and Occupancy

Weather conditions, such as outdoor air temperature and solar radiation, influence a room's thermal dynamics and AC performances. These data may come from a local observatory or from prediction models (Q. Zhou et al., 2008). The integrated building system model used in the MPC controllers in this study makes predictions regarding system dynamics based on local weather forecasts. Occupancy prediction plays a significant role in model-based building climate control. The occupancy pattern determines the internal heat gain and the control range of the indoor air temperature over the prediction horizon. In practical implementation, the occupancy information could be obtained from either Internet of Things (IoT) devices (B. Zhou et al., 2016) or on-site prediction models (Balvedi et al., 2018; Dong et al., 2018; W. Wang et al., 2018; W. Wang et al., 2017; Yao, 2018; Y. Zhang et al., 2018). In our simulation studies, the real-time weather forecast is obtained from the local observatory website, and the occupancy is pre-specified for the sake of simplicity.

RTP and Dynamic Power Thresholds

The typical RTP at 5-minute intervals is considered in the development of the online MPC controller for variable-speed ACs. Figure 8.2 shows the historical nodal dynamic RTPs of the Electric Reliability Council of Texas (ERCOT) in June 2016 (Electricity Reliability Council Of Texas (ERCOT)) to illustrate the large daily fluctuations in typical daily RTP profiles.

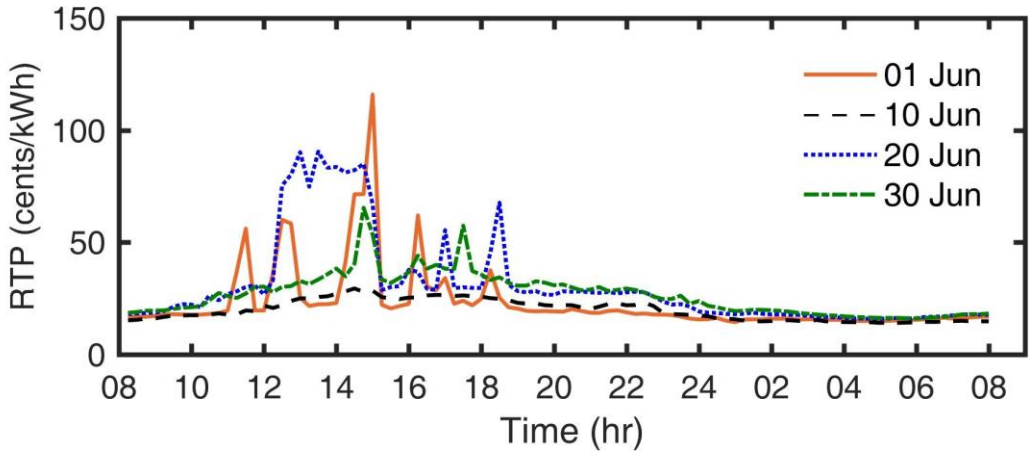

Figure 8.2 Daily RTP profiles in the ERCOT retail market on typical days of June 2016.

To achieve supply-demand balance in electrical grids, grid operators usually increase the RTP to prompt DR program participants to reduce power consumption during the peak demand periods. To obtain effective responses, a power constraint based on dynamic pricing is usually adopted in DR control methods for residential appliances. When the RTP is high, a low operating power threshold can be set for electric appliances to provide DR resources and reduce operating costs. In a similar way, when the RTP is low, a high operating power threshold can be adopted. Based on this idea, a "Price-to-Power Threshold" model for variable-speed ACs is formulated in this study. The cumulative probability distribution of RTP, which is obtained by analyzing the historical RTP database, can help us develop the model. The cumulative probability of RTP refers to the likelihood that the RTP is less than or equal to a specified value of RTP. Figure 8.3 shows the probabilities and cumulative probability distribution of RTPs in the ERCOT retail market in June 2016. Taking as an example the point denoted by the triangle symbol in Figure 8.3-b, the cumulative probability is

explained here. The point (24.97, 70%) means that the probability is 70% when the RTP is 24.97 cents/kWh or less (i.e., $RTP_{cp=0.7}$ = 24.97).

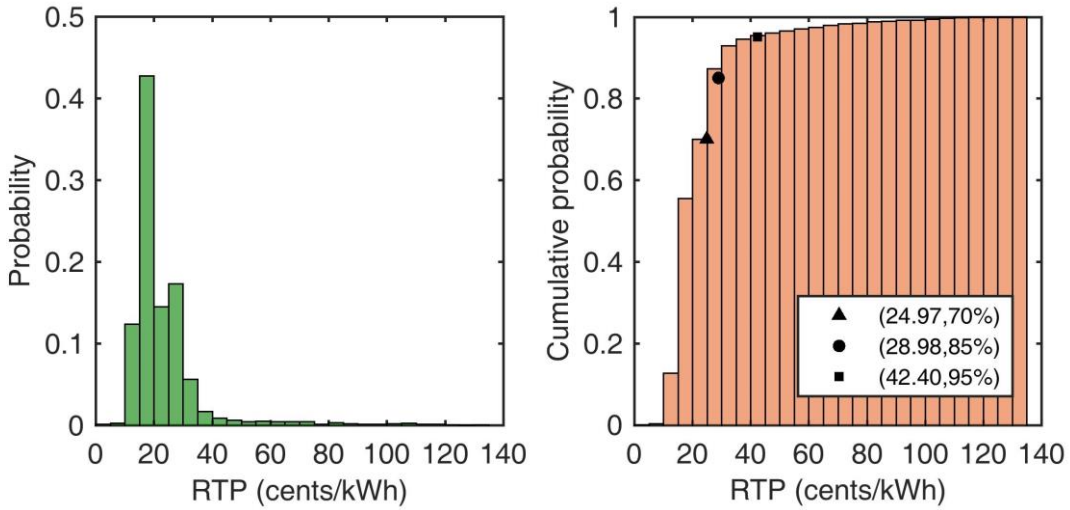

Figure 8.3 Probabilities (a) and cumulative probability distribution (b) of RTPs in the ERCOT retail market in June 2016.

Using the cumulative probability distribution of RTP, we propose a scheme to determine dynamic power thresholds for the DR-enabled MPC of variable-speed ACs that can be mathematically described by Equation (8.1).

$$P_{thsh,i} = \begin{cases} 100\% \cdot P_{max} & \text{if } RTP_i \leq RTP_{cp=0.7} \\ 85\% \cdot P_{max} & \text{if } RTP_{cp=0.7} < RTP_i \leq RTP_{cp=0.85} \\ 70\% \cdot P_{max} & \text{if } RTP_{cp=0.85} < RTP_i \leq RTP_{cp=0.95} \\ 55\% \cdot P_{max} & \text{if } RTP_i \geq RTP_{cp=0.95} \end{cases} \quad (8.1)$$

where P_{max} refers to the maximum operating power of an variable-speed AC; $P_{thsh,i}$ denotes the dynamic power threshold at time step i; and $RTP_{cp=0.7}$, $RTP_{cp=0.85}$, and $RTP_{cp=0.95}$ are the RTPs when the cumulative probabilities (cp) are 0.7, 0.85, and 0.95, respectively. The dynamic power thresholds are used as a time-varying constraint in

the DR-enabled MPC controller to limit the maximum operating power of AC during DR events.

8.2.2 Step 2: Formulation and Solving of Optimization Problem

A general MPC framework includes four parts: cost function, constraints, system dynamics and current state [32]. The cost function, constraints and system dynamics are introduced in Section 8.2.2.1. The method of updating current state using Kalman filter is presented in Section 8.2.2.2.

8.2.2.1 Cost Function, Constraints and System Dynamics

The objective of the DR-enabled MPC controller is to minimize the operating costs of the variable-speed AC over the prediction horizon N while keeping the indoor air temperature within a pre-specified range. The optimization problem is formulated as Equations (8.2) - (8.7).

$$\min_{P_1,P_2,\ldots,P_{N-1}} \sum_{k=1}^{N-1} P_k \Delta t \cdot RTP_k + \rho_e e_k \tag{8.2}$$

subject to

$$T_{k+1} = A_d \cdot T_k + B_d \cdot COP_k \cdot P_k + E_d \cdot d_k + w_k \tag{8.3}$$

$$y_k = C_d T_k + v_k \tag{8.4}$$

$$y_{lb,k} - e_k \leq y_k \leq y_{ub,k} + e_k \tag{8.5}$$

$$e_k \geq 0 \tag{8.6}$$

$$P_k = 0 \text{ or } P_{min} \leq P_k \leq P_{thsh,k} \tag{8.7}$$

where N is the prediction horizon; Δt is the prediction interval; P_k and COP_k are the AC power consumption and COP at time step k, respectively; $P_{thsh,k}$ is the dynamic power threshold; T_k, y_k, and d_k are the state vector, output vector, and disturbance vector in the state-space system model, respectively; w_k and v_k are the process and measurement noise, respectively, which are assumed to be independent and white and to have a normal distribution. A_d, B_d, C_d, and E_d are the state-space matrices of the discrete-time state-space model.

The objective function, Equation (8.2), aims to minimize the operating costs over the prediction horizon. If the constraints are not violated, the optimal power consumption remains at 0 kW, i.e., the AC is turned off.

Equation (8.3) - (8.4) depict the system dynamics in a state-space form. The input variable, the cooling capacity ($Q_{HVAC,k}$), is obtained by the product of COP_k and power consumption (P_k).

Equation (8.5) is a dynamic soft constraint that maintains the indoor air temperature within a certain range. During unoccupied hours, it is supposed that the AC is turned off and that the optimized power consumption is 0 kW. To achieve that goal, a wide temperature range is normally set, e.g., 20℃ to 30℃, as a result, the indoor air temperature is always within the range and AC remains off during the unoccupied period. When the room is occupied, a narrow temperature range is set to ensure thermal comfort (i.e., 22°C to 24°C when the occupants are awake and 24°C to 26°C while the occupants sleep).

However, the temperature constraint may not be satisfied in practice even if the AC runs at its full cooling capacity, such as on an extremely hot day. This situation may lead to a failure to solve the optimization problem. To address this issue, we can relax the MPC problem by introducing a slack variable e_k. The hard constraint is then converted to a soft constraint, which has a similar function as the dead-band plays in the on-off control. To ensure that the preset temperature range is met most of the time (i.e., $e_k = 0$), an especially large penalty ρ_e can be imposed on the slack variable e_k in the objective function.

Equation (8.7) is a time-varying hard constraint to limit the maximum power consumption of AC based on the RTP from electric utilities. A variable-speed AC has a minimum operating frequency (e.g., 20 Hz) and corresponding minimum power consumption P_{min}. Therefore, the power consumption should range between P_{min} and $P_{thsh,k}$, which can be determined by Equation (8.1) or equal zero when it is turned off.

The prediction horizon N and prediction interval Δt play significant roles in MPC controllers. The optimal prediction horizon is a trade-off between the accuracy of the predictions of exogenous inputs and a sufficient length of the prediction horizon. A long horizon also increases the computation time for each optimization step. For the MPC of radiant heating systems, the prediction horizon is normally set as 6 to 48 hours because the rooms have large thermal masses and respond very slowly to the heating system (Feng et al., 2015; Halvgaard et al., 2012; Hedegaard et al., 2018; Karlsson & Hagentoft, 2011; Široký et al., 2011). However, the room concerned in this study is located in a cooling-dominated district and has a relatively small thermal mass. In addition, the variable-speed AC delivers cooling to the space via heat convection,

which is a direct and quicker mode of heat transfer than heat radiation in a radiant heating system. Considering the short thermal response time of the target room to the cooling system, the prediction horizon *N* in this study is set to 3 hours, which is sufficient for the variable-speed AC to respond in advance to upcoming disturbances. The prediction interval is the frequency at which the optimization problem is solved and at which the actuator receives the control signal. Considering the room's thermal response time and the compressor motor's life expectancy, the compressor's rotational speed is allowed to change every 5 minutes (i.e., the prediction interval of the MPC controller in our study is 5 minutes).

8.2.2.2 Current State Estimation Using Kalman Filter

At the beginning of each step, current state is needed as the starting point for optimization. In our case, the system state includes four variables: $T = [T_{w,ext} \quad T_{w,int} \quad T_{in} \quad T_m]^T$. However, only the indoor air temperature T_{in} is measured in real applications. To address this issue, Kalman filter is commonly used to optimally estimate the immeasurable variables and to filter the noise in measurements (Bishop & Welch, 2001; Simon, 2006). The Kalman filter is an algorithm that provides a computationally efficient solution to estimate the state of a process in a manner that minimizes the prediction mean squared error. The solution is recursive in such a way that each updated estimate of the state is computed from the previous estimate and the new measured data. As shown in Figure 8.4, each Kalman filter cycle includes two steps: time update (priori estimate) and measurement update (posteriori estimate). *P*, *Q*, and *R* are the covariance matrices of the state estimate error, the process noise, and the measurement noise, respectively. $\hat{T}_k'$ denotes a priori state

estimate at time step k. $\hat{T}_k$ denotes the posteriori state estimate given measurement y_k (i.e., indoor air temperature T_{in}) at time step k. K_k is the Kalman gain determined by solving an algebraic Riccati equation. I is an identity matrix.

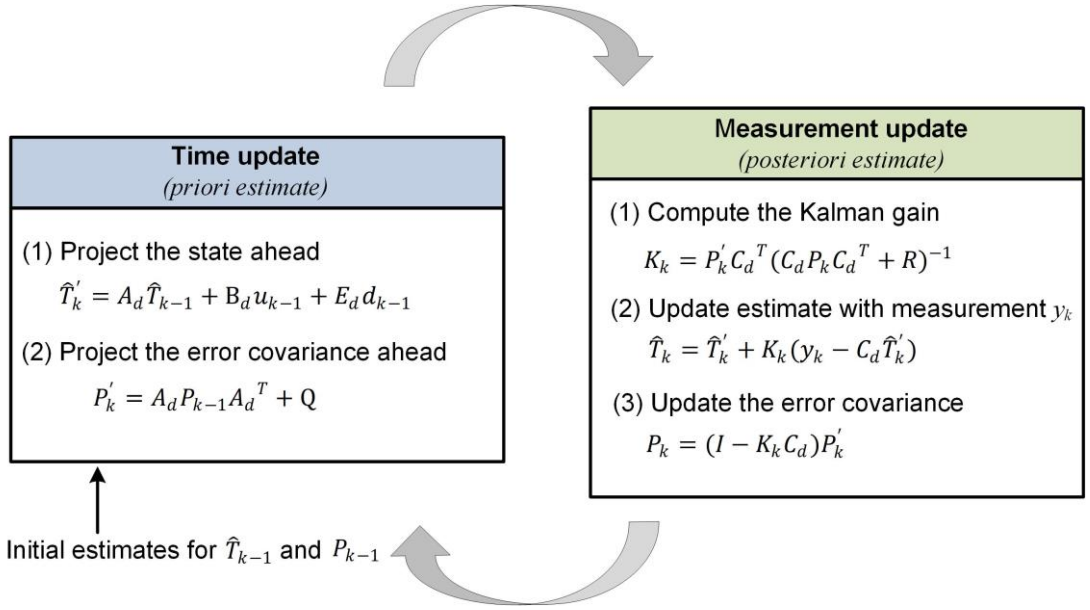

Figure 8.4 Kalman filter cycle for current state estimate in MPC

8.2.3 Step 3: Implementation of Frequency Signal from MPC controllers

The actuator in a variable-speed AC is the variable frequency driver of the compressor, which usually adopts the frequency as the control signal. In the development of the MPC controller for residential ACs, the AC power consumption, rather than the AC frequency, is chosen as the variable to be optimized because most incentives (e.g., DAP and RTP) for DR are set for power shifting and power shaving. It is more straightforward to use power consumption in the objective function. The optimization result (i.e., the power of the AC) must be converted into frequency signals to implement DR control. The performance maps of variable-speed ACs can be used in an inverse manner to determine the corresponding frequency.

MPC is intrinsically a feedback control, which incorporates iterative optimizations over moving prediction horizons. The optimization result at each time step is a trajectory of control signals. Only the first signal is implemented and the rest signals are disposed. At next time step, the optimization is repeated based on the updated current state.

8.3 Ordinary MPC Controller without DR Function

Compared with the DR-enabled MPC controller, the ordinary MPC controller without DR function does not consider the dynamic RTP in formulating the optimization problem. A general MPC framework includes four parts: cost function, constraints, system dynamics, and current state [32]. The differences of the two types of MPC controllers for variable-speed ACs only exist in the parts of cost function and constraints.

The optimization problem of the ordinary MPC scheme, which aims to save the energy use, can be described by the objective function Equation (8.8), and the constraints including Equations (8.3) – (8.6) and Equation (8.9). In contrast to the time-varying constraint, i.e., Equation (8.7) in the DR-enabled MPC controller, Equation (8.9) is a static constraint that limits power consumption in a constant power range.

$$\min_{P_1,P_2,\ldots,P_{N-1}} \sum_{k=1}^{N-1} P_k \Delta t + \rho_e e_k \tag{8.8}$$

$$P_k = 0 \text{ or } P_{min} \leq P_k \leq P_{max} \tag{8.9}$$

8.4 Case Studies and Analyses

8.4.1 TRNSYS-MATLAB Co-simulation Testbed and Test Conditions

Computer-based dynamic simulation is usually considered an effective and reliable approach to test control performance under various conditions. Building energy simulation programs like EnergyPlus and TRNSYS are commonly used to simulate a building's thermal performance and the energy performance of its HVAC system. However, the embedded controller models in these programs usually implement on-off control and PID control. In addition to the lack of advanced controllers, the simulation programs seldom provide frequency-based model of variable-speed AC and corresponding frequency-based control methods.

To solve these problems, TRNSYS and MATLAB are combined in this study, as illustrated in Figure 8.5. In the integrated building energy system, the air-conditioned room is coupled with a variable-speed AC. The building model (Type 56) in TRNSYS is used to characterize the building's thermal performance under the influences of weather, occupancy and AC cooling. The output of the controller is the operating frequency of the compressor motor. The variable-speed AC then uses the operating frequency to determine the corresponding cooling capacity and delivers it to the building component in TRNSYS. In this study, the component of Type 155 is used to establish the communication between the models in TRNSYS 18 (32-bit) and MATLAB 2014a (32-bit) in the Windows 10 64-bit operating system. The MPC controller is designed and implemented in MATLAB using the YALMIP optimization

toolbox (Löfberg, 2004) with the Gurobi optimization solver (Gurobi Optimization, 2016).

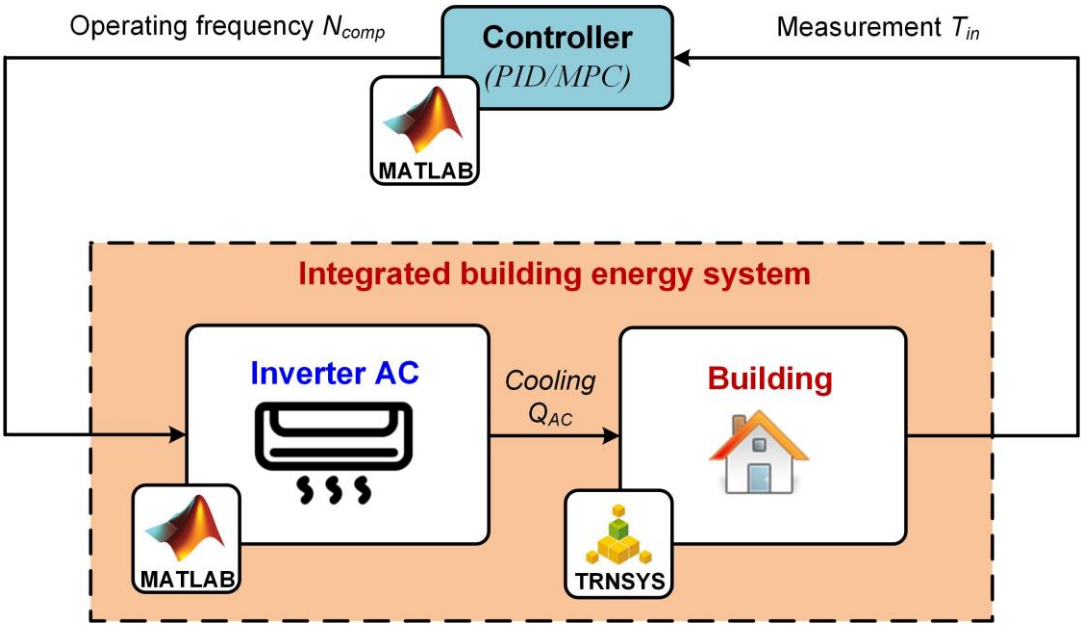

Figure 8.5 TRNSYS-MATLAB co-simulation testbed for building energy system

Weather forecast data from a local observatory, occupancy profiles, and RTPs from electric utilities are the exogenous inputs of the MPC controllers. The variables for three typical summer days are shown in Figure 8.6, and are used to test the performances of the MPC controllers in this study. It can be seen that RTP at 5-min intervals from ERCOT retail market varies throughout the day and normally reaches a peak around 16:00, which prompts DR from residential ACs. A fluctuant occupancy pattern is defined to simulate the time-changing occupancy patterns. The room is assumed to be occupied from 12:00 to 18:00 and from 20:00 to 08:00. The simulation begins at 08:00. It is assumed that the room's thermal response is stabilized after one night of AC operation at 08:00. Thus, the AC temperature set point is used as the initial value of the indoor air temperature in the simulation.

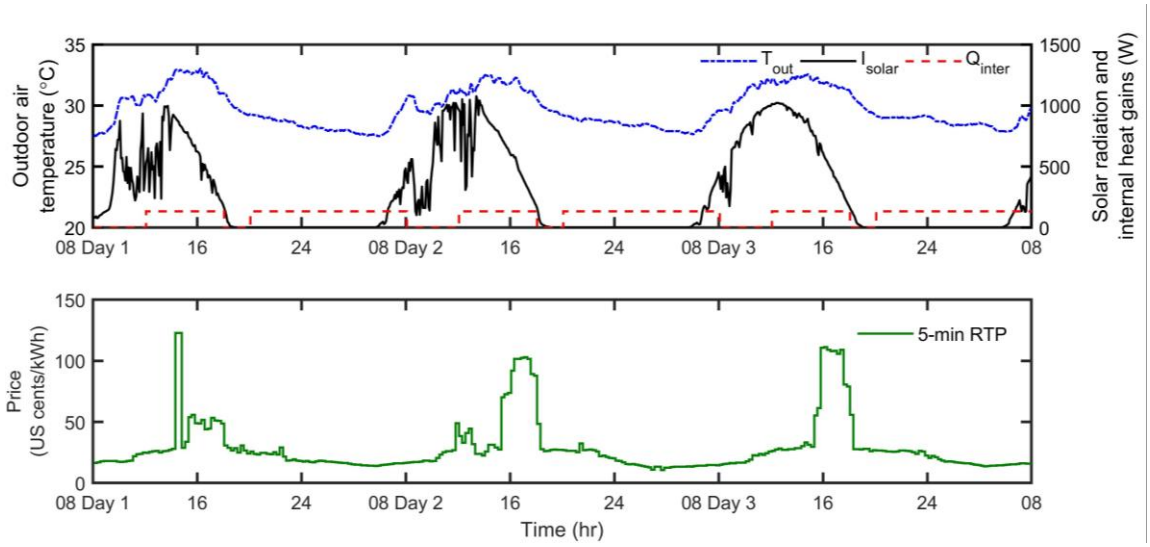

Figure 8.6 Weather conditions and RTP from ERCOT on three sequential typical summer days.

8.4.2 Reference Case Using Conventional PID Control

For comparison, the system performance using conventional PID control is tested first. A PID controller is chosen to control the variable-speed AC to maintain the indoor temperature at the set point. The indoor air temperature set point is 24℃ from 12:00 to 18:00 and from 20:00 to 24:00 and 26℃ from 24:00 to 08:00 to reflect the common practice of setting the indoor temperature higher at night. In this case, RTP is used only to calculate electricity costs and is not involved in the control algorithm. The simulation time step is 1 minute.

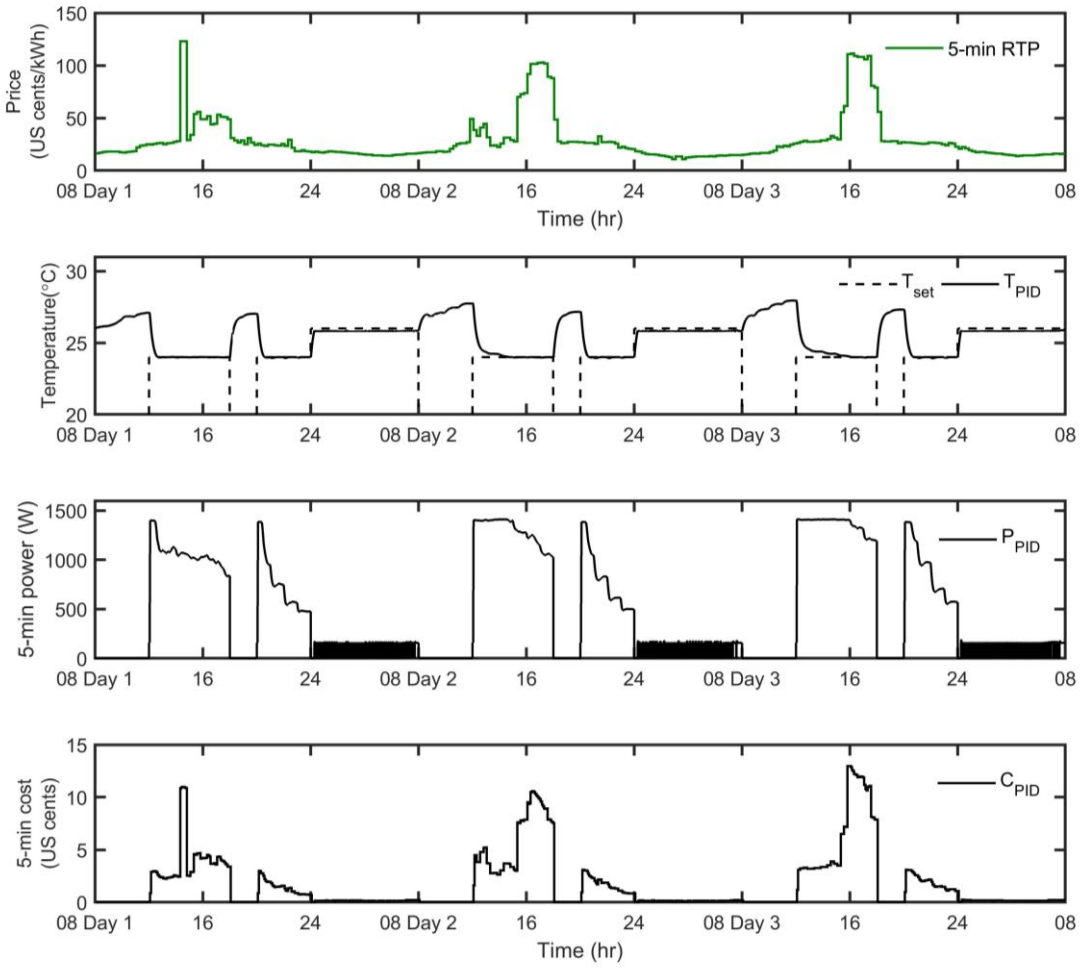

Figure 8.7 (a) RTPs and system performance under PID control, including (b) indoor air temperature, (c) power consumption, and (d) electricity costs.

Figure 8.7 shows the performances of the room and the AC under conventional PID control. Figure 8.7-b shows that the PID controller can maintain the indoor air temperature at its set point most of the time. The AC is off from 18:00 to 20:00 and from 08:00 to 12:00 because it is assumed that no one is in the room. When the room changes from unoccupied to occupied, the variable-speed AC takes time to counter the accumulated heat gain and bring the indoor temperature back to the set point. The variable-speed AC runs at high frequencies when RTP is high around 16:00. It is a

disadvantage to the power grid considering the large population of residential ACs operating at the same time. It is also a disadvantage to residential users due to the high electricity cost.

8.4.3 Cases Using MPC Controllers

The simulation tests with the two types of MPC controllers are conducted separately under conditions identical to those used in the reference case. The simulation time step in TRNSYS is set as 5 minutes, and at each time step the MPC controller in MATLAB is called by TRNSYS, and the frequency control signal is sent to the variable-speed AC model.

8.4.3.1 Ordinary MPC controller without DR function

Figure 8.8 shows the system performances with the ordinary MPC without DR function. For easy comparison, the RTP and the performances under the PID control are shown in the same figure. Figure 8.8-b shows that the MPC controller, as a new optimal control method for variable-speed ACs, satisfactorily maintains the indoor air temperature between the upper and lower limits, although the temperature fluctuates due to the uncertain noise.

The results also show that the ordinary MPC controller naturally implements the precooling strategy, which obviously improves thermal comfort at the beginning of occupancy. On Day 1, the prediction made by the MPC controller at 10:00 indicates that the indoor air temperature will exceed the upper boundary (i.e., 24℃) at 12:00. Hence, the variable-speed AC begins to run at 10:00 to precool the room before it is occupied so that the indoor air temperature is at a comfortable level at the beginning

of occupancy. In the PID case, the temperature deviations from the set point evaluated by the mean absolute error (MAE) from 12:00 to 14:00 are 0.39℃, 0.78℃, and 0.96℃ on Days 1, 2 and 3, respectively, which are greater than those in the MPC case (i.e., 0.06°C, 0.17°C, and 0.18°C, respectively).

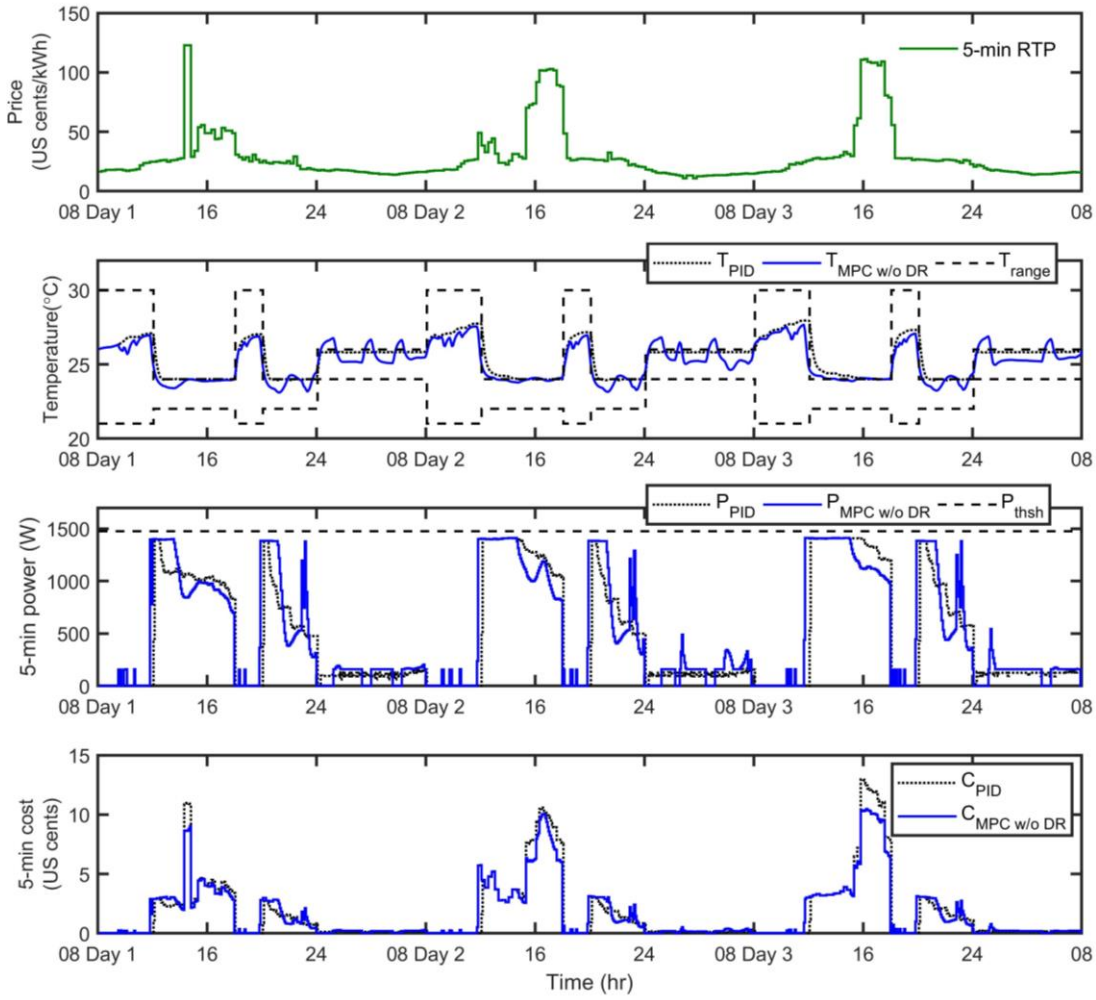

Figure 8.8 (a) RTPs and system performance under PID control and ordinary MPC without DR function, including (b) indoor air temperature, (c) power consumption, and (d) electricity costs.

Moreover, precooling is an optimal solution because the objective of the ordinary MPC is to minimize the energy consumption in the horizon. The ordinary MPC controller automatically implements precooling with different start-up times and durations on the three days because the weather conditions differ. In this way, the ordinary MPC controller solves the problem of determining the start-up time for precooling, which was challenging for most previous studies in which a precooling strategy was developed (Sun et al., 2012; Turner et al., 2015). Precooling may result in an increase in energy consumption, which can be observed in the test results shown in Figure 8.8-b. The AC under the ordinary MPC control consumes more energy than that under the PID control on these three days. However, the daily operating costs may be reduced, as shown in Figure 8.10-d, because the MPC controller allows a higher indoor air temperature than the PID controller.

8.4.3.2 DR-enabled MPC controller

The DR-enabled MPC controller considers the RTP in the optimization process. Dynamic power thresholds can be generated using Equation (8.1) according to the RTP signals from the electric utility. The dynamic power threshold acts as a time-varying constraint in the solution of the optimization problem.

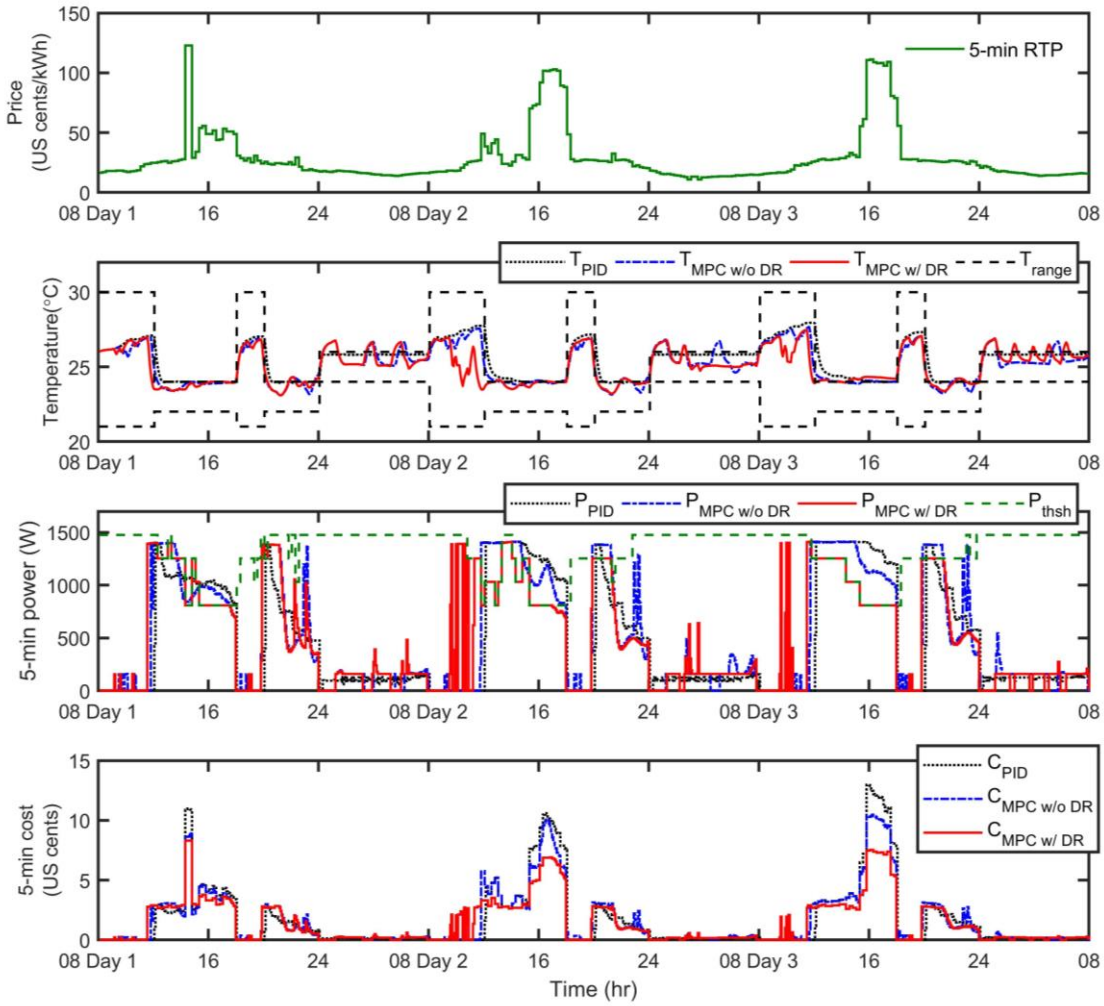

Figure 8.9 (a) RTPs and system performances under PID control, ordinary MPC without DR function, and DR-enabled MPC, including (b) indoor air temperature, (c) power consumption, and (d) electricity costs.

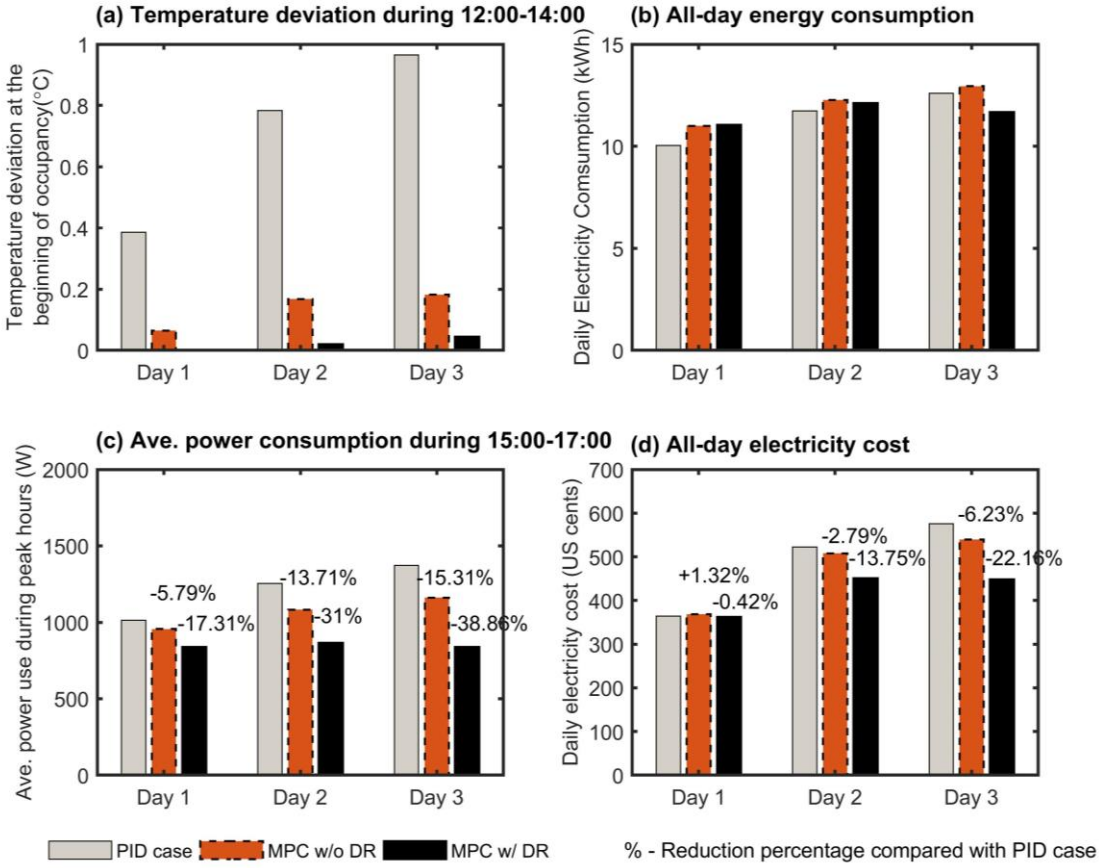

Figure 8.10 System performances under PID control, ordinary MPC without DR function, and DR-enabled MPC.

Figure 8.9 shows the system performances under the PID control, the ordinary MPC without DR function, and the DR-enabled MPC. Like the ordinary MPC controller without DR function, the DR-enabled MPC controller can implement automatic and optimal precooling. However, the DR-enabled MPC controller adopts longer and deeper precooling to limit power consumption during peak demand periods. It starts the variable-speed AC to precool the room to a lower temperature so that the AC power consumption and operating frequency can be limited around 16:00, when the

RTP is very high. Thermal comfort can be maintained due to the cooling energy stored in the thermal mass during the precooling period.

As can be seen from Figure 8.10-c that, compared with the PID case, the average power consumption from 15:00 to 17:00 is reduced by 17.31% on Day 1, 31.00% on Day 2, and 38.86% on Day 3, in the DR-enabled MPC control case.

Because the DR-enabled MPC controller effectively shifts power consumption from high-RTP periods to low-RTP periods, the all-day electricity costs are reduced by 0.42% on Day 1, 13.75% on Day 2, and 22.16% on Day 3. The electricity cost saving is influenced by the weather conditions and RTP profiles. For example, the weather on Day 1 is cooler than that on Days 2 and 3 and the RTP curve is flatter, so the electricity cost saving is less.

Meanwhile, as shown by Figure 8.10-b, the daily energy consumption of the AC under the DR-enabled MPC may exceed that under the PID control. This is the price paid to achieve power reductions during the peak demand hours via precooling. From the prospective of power grids, it is more important to provide a stable power reduction as required.

Figure 8.11 shows the computation time required to solve the optimization problem at each time step using a PC with Intel Core i7-4600U 2.70 GHz. The computation time is less than 5 seconds, which is shorter than the prediction interval of 5 minutes. Therefore, the MPC controllers are competent in real-time online control.

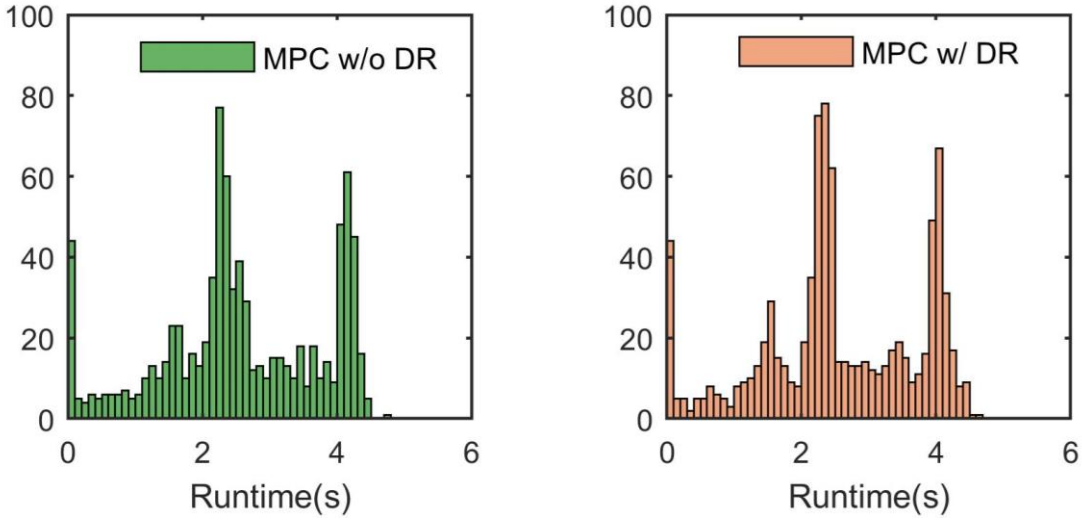

Figure 8.11 Computation time for MPC controller without DR function (left) and DR-enabled MPC controller (right) at each time step.

8.5 Summary

In this chapter, I present the developed advanced DR-enabled MPC controller for residential variable-speed ACs that directly controls the operating frequency of variable-speed ACs in response to RTP. Stochastic white noise is added to the dynamic room thermal model to make it more realistic and robust. The performance under the proposed DR-enabled MPC controller is compared with that under the conventional PID controller and the ordinary MPC controller without DR function using a TRNSYS-MATLAB co-simulation testbed.

The test results show that the DR-enabled MPC controller can reduce power consumption by 17.31% to 38.86% compared with the PID controller during peak demand periods and reduce all-day electricity costs by 0.42% to 22.16%. The percentages of peak power reduction and cost savings are influenced by the room's

thermal mass, the weather conditions, and the RTP profiles. The total energy consumption of variable-speed ACs under the MPC may exceed that under PID control because the MPC controller adopts precooling to shift power demands during peak demand periods. The thermal comfort, as evaluated by the indoor air temperature, is satisfactory under all three controllers. The thermal comfort at the beginning of occupancy under the MPC controllers is improved by automatic precooling. The test results also show that the computation time of the MPC controllers is suitable for online real-time control. In general, residential variable-speed ACs under the proposed frequency-based stochastic MPC are more grid-friendly and cost-efficient.

CHAPTER 9 CONCLUSIONS AND RECOMMENDATIONS

In this chapter, conclusions are made based on the work done. Main contributions of the thesis are summarized. Recommendations for the future work are also presented.

9.1 Conclusions

The simplified dynamic room thermal model

The proposed grey-box dynamic room thermal can accurately predict the indoor air temperature under dynamic operating conditions. The model transformation from ODE to state space form helps to improve the computational efficiency of both offline parameter identification and online model predictive control.

Test results show the runtime of GA optimization is largely reduced from 87.7 to 4.7 minutes after the state space model is used instead of the ODE model. When the state space model is used for online model predictive control, it helps to formulate convex optimization problems which in general can be conveniently solved by using state-of-the-art optimization techniques. Test results show that the computation time at each optimization step is less than 5 seconds, making the MPC controllers are competent to fulfill the online control.

A room thermal model with fixed parameter values is not applicable to various residential buildings in different cities because the building materials, architecture design and occupant habits are very different. Thus, a self-learning grey-box model is

needed to learn the thermal characteristics of the certain room. The unknown parameters in the developed model can be trained by making effective use of the data available in the today's smart in-home sensors. It can be embedded in smart HEMSs for optimal home load scheduling in response to DR signals. The electric utilities can also use the model to evaluate the potential benefits of DR programs on a large scale and make corresponding incentive policies before practical implementations of the DR programs.

The simplified energy performance model of variable-speed ACs

The developed simplified energy performance model of variable-speed ACs is able to characterize the AC performances under various operating frequencies and environmental conditions. The essence of the simplified AC model is a grey-box model which needs to be identified using performance data from either experimental tests from AC manufacturers or physics-based modeling technique. Since AC manufacturers seldom provide enough data for coefficient identification, physics-based modeling of typical variable-speed AC is considered in our study. For this reason, a steady-state physical model of variable-speed ACs is developed to generate performance data under typical operating frequencies and environmental conditions.

The proposed simply structured energy performance model of variable-speed ACs can be readily used by electrical researchers and engineers for either model-based DR control in smart HEMSs or DR potential estimation of a single variable-speed AC or a large population of variable-speed ACs.

Indirect model-based optimal control method in response to hourly day-ahead prices

The proposed model-based optimal control method can reduce the peak power consumptions of variable-speed ACs and reduce the electricity costs while still satisfying the thermal comfort constraints. Sensitivity analyses of the weightings in the normalized objective function show that the objective function is reasonably formulated, which is sensitive to both peak power weighting and thermal comfort weighting. Minimizing the comprehensive objective function can effectively achieve the optimal trade-offs among the electricity costs, occupant comfort and peak power reductions.

The proposed model-based optimal control method can be implemented in the smart HEMSs and enable the residential variable-speed ACs to automatically respond to the day-ahead electricity prices to achieve the optimal trade-offs. When a large number of residential ACs simultaneously respond to dynamic electricity prices from utilities or third-party load aggregators, power consumptions in grid during on-peak hours can be significantly reduced.

Direct model predictive control in response to 5-minute real-time prices

The developed MPC controller is able to directly control the operating frequency of variable-speed AC while considering all the influential variables including weather conditions, occupancy and RTP. The stochastic state-space room thermal model and the simplified energy performance model of variable-speed ACs are used for online predicting the future evolutions of the system.

Test results show that compared with the conventional PID control, the major advantage of the ordinary MPC controller without DR function is to implement

automatic and optimal precooling to improve the thermal comfort at the beginning of occupancy. The precooling duration depends on the weather conditions on different days. However, it cannot effectively shift the peak power demands from high-RTP to low-RTP period, neither significantly reduce the electricity costs. To make automatic response to RTP, RTP is considered in the DR-enabled MPC controller. Compared with the MPC controller without DR function, the DR-enabled MPC controller shows great improvements in terms of peak power reductions and electricity cost savings even if the AC may consume more energy than the PID case due to precooling. Compared with the MPC controller without DR function, the DR-enabled MPC controller is more grid-friendly and cost-efficient.

Challenges of implementing MPC for built environment control

- **System model for online applications.** An appropriate system model is the cornerstone of MPC, which is used to predict the future evolution of the system and to output the optimal control inputs. The model needs to predict the relevant variables, e.g., indoor air temperature, in a sufficient accuracy. Moreover, it needs to be simple enough for the optimization task to be computationally tractable and numerically stable. Normally, it is much more suitable to use Linear Time Invariant (LTI) models for the MPC controller design. This results in a convex optimization problem that in general can be well solved by state-of-the-art optimization software. Obtaining an appropriate LTI model of the controlled building is, however, a delicate and laborious task even for experienced and knowledgeable engineers. Black-box, white-box, and grey-box modeling approaches have all been applied for model-based control.

The black-box approach is conceptually simple but technically tricky, and it depends crucially on the availability of appropriate input data sets. The white-box models require availability and processing of a large amount of building-specific information. The grey-box models are the most commonly used models for MPC purpose, which are not only physically interpretable but they also use real-time collected data from smart in-home sensors. One of the biggest challenges of implementing grey-box model is the parameter identification.

- **Data availability and analytics**. Except for a feasible system model, a number of input data are also required at the beginning of each optimization. The required input data include the predictions of influential variables, such as solar radiation, ambient air temperature, occupancy profile and dynamic electricity prices, and the current state of the system. For the latter, Kalman filter is commonly used to optimally estimate the immeasurable variables and filter the noises in measurements. In order to obtain effective KF estimates, the sensor network in the real building and the building model need to be adjusted to each other. In general, effective collection, communication and analyses of the input data are very important for the implementation of MPC.
- **Hardware, software and communication.** The commonly used programmable logic controllers (PLCs) in building automation systems have been proved incompetent for MPC, because they lack sufficient memory, processor speed and software support for numerical optimization. At present, an external dedicated computational core is required to be connected to the building's automation system. In this way, some specifications are required

including the selection of the to-be-communicated signals, a communication protocol, and the implementation of mechanisms to handle communication and optimization problems (e.g., infeasibility or too long computation time).

9.2 Summary of Main Contributions

The present study aims at developing model-based optimal control strategies/methods for residential variable-speed ACs in response to two types of electricity pricings, i.e., DAP and RTP, with the assistance of advanced information and communication technologies and computational intelligence techniques in smart grids.

Main contributions are summarized as follows:

i. A semi-physical (grey-box) dynamic room thermal model is developed and validated for predicting the indoor air temperature under dynamic operating conditions. The model parameters can be learnt by making effective use of the data available in the today's smart in-home sensors. Due to the simple structure and moderate computation load, the developed room thermal model is suitable for the applications in the HEMSs, such as model-based optimal control of residential ACs in response to dynamic DR signals.

ii. A method is proposed to transform the dynamic room thermal model from ordinary differential equations to stochastic discrete-time state-space representation. Random white Gaussian noise is added in the system model to consider the uncertainty and make the model more realistic. The state space model explicitly expresses the relationships between the outputs and inputs. Moreover, it can be used to formulate convex optimization problems which in

general can be conveniently solved by using state-of-the-art optimization techniques.

iii. A simplified energy performance model of variable-speed ACs is developed and validated to characterize the AC performances under various operating frequencies and environmental conditions. The proposed simply structured energy performance model of variable-speed ACs can be readily used by electrical researchers and engineers for either model-based DR control in smart HEMSs or DR potential estimation of a single variable-speed AC or a large population of variable-speed ACs.

iv. In order to respond to hourly day-ahead prices, a model-based optimal control method is developed for variable-speed ACs, which adopts a two-level hierarchy structure. The high-level controller, i.e., the supervisory controller, is used to output the optimal set-point scheduling for the low-level local PID controller. The local PID controller is used to track the optimal set-points. The proposed model-based optimal control method enables the residential variable-speed ACs to achieve the optimal trade-offs among electricity costs, occupant comfort and peak power reductions during DR hours.

v. A frequency-based model predictive control method for variable-speed ACs is developed in response to 5-minute real-time prices. The advanced MPC method is intended to directly control the operating frequency of variable-speed AC while considering all the influential variables including weather conditions, occupancy and real-time prices. The test results show that compared to the conventional PID controller, the MPC controller can implement automatic and optimal precooling based on the predictions of

dynamic weather conditions and occupancy. Besides, the DR-enabled MPC controller demonstrates great improvements in both peak power reduction and electricity cost savings and is thus more grid-friendly and cost-efficient.

9.3 Recommendations for Future Work

Major efforts of the present thesis have been made on the development of model-based optimal control methods of residential variable-speed ACs in response to dynamic electricity pricings. It would be very desirable and valuable to make further efforts on the following aspects:

i. More rooms with different thermal characteristics in different cities are needed to test the adaptability of the grey-box room thermal model. For the same room, more measured real data in different seasons need to be collected to test the robustness of the model. Similarly, more types of residential variable-speed ACs could be experimentally tested to validate the simplified energy performance model.

ii. On-site implementation and validation of the proposed model-based optimal control methods for residential variable-speed ACs are needed when the real conditions can meet the requirements. The on-site test results are very important to update them and to achieve desirable and satisfactory performances in practical applications. A lot of efforts need to be paid to test and validate the proposed DR control method in the practical buildings in future studies.

iii. For simplification purpose, the occupancy profile in this study is predefined. An occupant behavior model is desirable to be used for online prediction with the assistance of occupancy sensing system. The effects of occupant behavior on the performance of MPC controllers are worth being investigated.

iv. Due to the simplified model structure, the room thermal model and the AC model can be used on a large scale to investigate the DR potential benefits of a large population of residential buildings. When a large number of residential ACs simultaneously respond to dynamic electricity prices from utilities or third-party load aggregators, power consumptions in grid during on-peak hours can be significantly reduced. If the residential micro-grid incorporates the renewable energy resources, the effects of DR control of residential ACs on the penetration of renewable energy resources are worthy being investigated.

v. In the design of the economic MPC controller, different levels of penalties can be imposed on the dynamic electricity prices, forming a quadratic cost function. In this way, the optimization solver can automatically help to shift the power consumption from high-price to low-price periods.

REFERENCES

Aalami, H., Yousefi, G. R., & Moghadam, M. P. (2008, 21-24 April 2008). *Demand Response model considering EDRP and TOU programs.* Paper presented at the 2008 IEEE/PES Transmission and Distribution Conference and Exposition.

Aalami, H. A., Moghaddam, M. P., & Yousefi, G. R. (2010). Demand response modeling considering Interruptible/Curtailable loads and capacity market programs. *Applied Energy, 87*(1), 243-250.

Afram, A., Janabi-Sharifi, F., Fung, A. S., & Raahemifar, K. (2017). Artificial neural network (ANN) based model predictive control (MPC) and optimization of HVAC systems: A state of the art review and case study of a residential HVAC system. *Energy and Buildings, 141*, 96-113.

Albadi, M. H., & El-Saadany, E. (2007). *Demand response in electricity markets: An overview.* Paper presented at the IEEE power engineering society general meeting.

Albadi, M. H., & El-Saadany, E. F. (2008). A summary of demand response in electricity markets. *Electric Power Systems Research, 78*(11), 1989-1996.

Amini, M. H., Nabi, B., & Haghifam, M.-R. (2013). *Load management using multi-agent systems in smart distribution network.* Paper presented at the Power and Energy Society General Meeting (PES), 2013 IEEE.

ANSI/AHRI. (2008). Standard for Performance Rating of Unitary Air-Conditioning and Air-Source Heat Pump Equipment. Arlington, VA: Air-Conditioning, Heating, and Refrigeration Institute.

Asakawa, K., & Takagi, H. (1994). Neural networks in Japan. *Communications of the ACM, 37*(3), 106-113.

ASHRAE. (2009). *ASHRAE Handbook: Fundamentals (SI Edition)*. Atlanta, GA: American Society of Heating, Refrigerating and Air-conditioning Engineers.

Aswani, A., Master, N., Taneja, J., Culler, D., & Tomlin, C. (2012). Reducing transient and steady state electricity consumption in HVAC using learning-based model-predictive control. *Proceedings of the IEEE, 100*(1), 240-253.

Avci, M., Erkoc, M., Rahmani, A., & Asfour, S. (2013). Model predictive HVAC load control in buildings using real-time electricity pricing. *Energy and Buildings, 60*, 199-209.

Bacher, P., & Madsen, H. (2011). Identifying suitable models for the heat dynamics of buildings. *Energy and Buildings, 43*(7), 1511-1522.

Baghaee, H. R., Mirsalim, M., Gharehpetian, G. B., & Kaviani, A. K. (2012). Security/cost-based optimal allocation of multi-type FACTS devices using multi-objective particle swarm optimization. *Simulation, 88*(8), 999-1010.

Baghaee, H. R., Mirsalim, M., Gharehpetian, G. B., & Talebi, H. A. (2016). Reliability/cost-based multi-objective Pareto optimal design of stand-alone wind/PV/FC generation microgrid system. *Energy, 115*, 1022-1041.

Balvedi, B. F., Ghisi, E., & Lamberts, R. (2018). A review of occupant behaviour in residential buildings. *Energy and Buildings, 174*, 495-505.

Bargiotas, D., & Birdwell, J. (1988). Residential air conditioner dynamic model for direct load control. *Power Delivery, IEEE Transactions on, 3*(4), 2119-2126.

Bell, I. H., Wronski, J., Quoilin, S., & Lemort, V. (2014). Pure and Pseudo-pure Fluid Thermophysical Property Evaluation and the Open-Source

Thermophysical Property Library CoolProp. *Industrial & Engineering Chemistry Research, 53*(6), 2498-2508.

Bishop, G., & Welch, G. (2001). An introduction to the Kalman filter. *Proc of SIGGRAPH, Course, 8*(27599-23175), 41.

Bode, J. L., Sullivan, M. J., Berghman, D., & Eto, J. H. (2013). Incorporating residential AC load control into ancillary service markets: Measurement and settlement. *Energy Policy, 56*, 175-185.

Braun, J., & Chaturvedi, N. (2002). An Inverse Gray-Box Model for Transient Building Load Prediction. *HVAC&R Research, 8*(1), 73-99.

BRE. (2012). *The Governments Standard Assessment Procedure for Energy Rating of Dwellings*. Retrieved from

California Energy Commission. (2000). California Energy Demand: 2000-2010. *California Energy Commission, Sacramento*.

Camacho, E. F., & Alba, C. B. (2013). *Model predictive control*: Springer Science & Business Media.

Camyab, A. (2015). Automated Demand Response, Smart Grid Technologies, and Sustainable Energy Solutions. 187-222.

Cappers, P., Goldman, C., & Kathan, D. (2010). *Demand response in US electricity markets: Empirical evidence*. Retrieved from

Cappers, P., MacDonald, J., Goldman, C., & Ma, O. (2013). An assessment of market and policy barriers for demand response providing ancillary services in U.S. electricity markets. *Energy Policy, 62*, 1031-1039.

Cavallini, A., Col, D. D., Doretti, L., Matkovic, M., Rossetto, L., Zilio, C., & Censi, G. (2006). Condensation in horizontal smooth tubes: a new heat transfer model for heat exchanger design. *Heat Transfer Engineering, 27*(8), 31-38.

Chassin, D. P., Stoustrup, J., Agathoklis, P., & Djilali, N. (2015). A new thermostat for real-time price demand response: Cost, comfort and energy impacts of discrete-time control without deadband. *Applied Energy, 155*, 816-825.

Che, J., Wang, J., & Wang, G. (2012). An adaptive fuzzy combination model based on self-organizing map and support vector regression for electric load forecasting. *Energy, 37*(1), 657-664.

Chen, J., Augenbroe, G., & Song, X. (2018). Lighted-weighted model predictive control for hybrid ventilation operation based on clusters of neural network models. *Automation in Construction, 89*, 250-265.

Chen, K., & Yu, J. (2014). Short-term wind speed prediction using an unscented Kalman filter based state-space support vector regression approach. *Applied Energy, 113*, 690-705.

Chen, Z., Wu, L., & Fu, Y. (2012). Real-time price-based demand response management for residential appliances via stochastic optimization and robust optimization. *Smart Grid, IEEE Transactions on, 3*(4), 1822-1831.

Cherem-Pereira, G., & Mendes, N. (2012). Empirical modeling of room air conditioners for building energy analysis. *Energy and Buildings, 47*, 19-26.

Chi, J., & Didion, D. (1982). A simulation model of the transient performance of a heat pump. *International Journal of Refrigeration, 5*(3), 176-184.

Chiou, C. B., Chiou, C. H., Chu, C. M., & Lin, S. L. (2009). The application of fuzzy control on energy saving for multi-unit room air-conditioners. *Applied Thermal Engineering, 29*(2-3), 310-316.

Choi, J. M., & Kim, Y. C. (2003). Capacity modulation of an inverter-driven multi-air conditioner using electronic expansion valves. *Energy, 28*(2), 141-155.

Crawley, D. B., Pedersen, C. O., Lawrie, L. K., & Winkelmann, F. C. (2000). EnergyPlus: energy simulation program. *ASHRAE journal, 42*(4), 49.

Cui, B., Gao, D.-c., Wang, S., & Xue, X. (2015). Effectiveness and life-cycle cost-benefit analysis of active cold storages for building demand management for smart grid applications. *Applied Energy, 147,* 523-535.

Deb, K., Pratap, A., Agarwal, S., & Meyarivan, T. (2002). A fast and elitist multiobjective genetic algorithm: NSGA-II. *IEEE transactions on evolutionary computation, 6*(2), 182-197.

Depuru, S. S. S. R., Wang, L., & Devabhaktuni, V. (2011). Smart meters for power grid: Challenges, issues, advantages and status. *Renewable and Sustainable Energy Reviews, 15*(6), 2736-2742.

Dodrill, K. (2011). Demand Dispatch—Intelligent Demand for a More Efficient Grid.

Domínguez-Muñoz, F., Cejudo-López, J. M., & Carrillo-Andrés, A. (2010). Uncertainty in peak cooling load calculations. *Energy and Buildings, 42*(7), 1010-1018.

Dong, B., Cao, C., & Lee, S. E. (2005). Applying support vector machines to predict building energy consumption in tropical region. *Energy and Buildings, 37*(5), 545-553.

Dong, B., Li, Z., Taha, A., & Gatsis, N. (2018). Occupancy-based buildings-to-grid integration framework for smart and connected communities. *Applied Energy, 219*, 123-137.

Ekren, O., Sahin, S., & Isler, Y. (2010). Comparison of different controllers for variable speed compressor and electronic expansion valve. *International Journal of Refrigeration, 33*(6), 1161-1168.

Electrical and Mechanical Services Department. (2017). *Hong Kong Energy End-use Data 2017*. Retrieved from Hong Kong:

Electricity Reliability Council Of Texas (ERCOT). (2017). Historical RTM Load Zone and Hub Prices. *Available from http://mis.ercot.com/misapp/GetReports.do?reportTypeId=13061&reportTitle=Historical%20RTM%20Load%20Zone%20and%20Hub%20Prices&showHTMLView=&mimicKey*.

Fang, X., Misra, S., Xue, G., & Yang, D. (2012). Smart grid—The new and improved power grid: A survey. *IEEE communications surveys & tutorials, 14*(4), 944-980.

Faruqui, A., Harris, D., & Hledik, R. (2010). Unlocking the €53 billion savings from smart meters in the EU: How increasing the adoption of dynamic tariffs could make or break the EU's smart grid investment. *Energy Policy, 38*(10), 6222-6231.

Federal Energy Regulatory Commission. (2010). *National action plan on demand response*. Retrieved from

Federal Energy Regulatory Commission. (2014). Assessment of demand response and advanced metering.

Federal Energy Regulatory Commission. (2018). Assessment of demand response and advanced metering.

Feng, J. D., Chuang, F., Borrelli, F., & Bauman, F. (2015). Model predictive control of radiant slab systems with evaporative cooling sources. *Energy and Buildings, 87*, 199-210.

Ferreira, P. M., Ruano, A. E., Silva, S., & Conceição, E. Z. E. (2012). Neural networks based predictive control for thermal comfort and energy savings in public buildings. *Energy and Buildings, 55*, 238-251.

Foucquier, A., Robert, S., Suard, F., Stéphan, L., & Jay, A. (2013). State of the art in building modelling and energy performances prediction: A review. *Renewable and Sustainable Energy Reviews, 23*, 272-288.

Gayeski, N. T. (2010). *Predictive pre-cooling control for low lift radiant cooling using building thermal mass.* Massachusetts Institute of Technology.

Gnielinski, V. (1976). New equations for heat and mass-transfer in turbulent pipe and channel flow. *International chemical engineering, 16*(2), 359-368.

Goddard, G., Klose, J., & Backhaus, S. (2014). Model Development and Identification for Fast Demand Response in Commercial HVAC Systems. *IEEE Transactions on Smart Grid, 5*(4), 2084-2092.

Grald, E. W., & MacArthur, J. W. (1992). A moving-boundary formulation for modeling time-dependent two-phase flows. *International Journal of Heat and Fluid Flow, 13*(3), 266-272.

Grodzevich, O., & Romanko, O. (2006). *Normalization and other topics in multi-objective optimization.* Paper presented at the Proceedings of the Fields–MITACS Industrial Problems Workshop.

Güngör, V. C., Sahin, D., Kocak, T., Ergüt, S., Buccella, C., Cecati, C., & Hancke, G. P. (2011). Smart grid technologies: communication technologies and standards. *Industrial informatics, IEEE transactions on, 7*(4), 529-539.

Gurobi Optimization, I. (2016). Gurobi optimizer reference manual. *URL http://www.gurobi.com*.

Halvgaard, R., Poulsen, N. K., Madsen, H., & Jørgensen, J. B. (2012). *Economic model predictive control for building climate control in a smart grid.* Paper presented at the Innovative Smart Grid Technologies (ISGT), 2012 IEEE PES.

He, X.-D., Liu, S., & Asada, H. H. (1997). Modeling of Vapor Compression Cycles for Multivariable Feedback Control of HVAC Systems. *Journal of dynamic systems, measurement, and control, 119*(2), 183-191.

He, X.-D., Liu, S., Asada, H. H., & Itoh, H. (1998). Multivariable control of vapor compression systems. *HVAC&R Research, 4*(3), 205-230.

Hedegaard, R. E., Pedersen, T. H., Knudsen, M. D., & Petersen, S. (2018). Towards practical model predictive control of residential space heating: Eliminating the need for weather measurements. *Energy and Buildings, 170*, 206-216.

Henze, G. P., Felsmann, C., & Knabe, G. (2004). Evaluation of optimal control for active and passive building thermal storage. *International Journal of Thermal Sciences, 43*(2), 173-183.

Herter, K., McAuliffe, P., & Rosenfeld, A. (2007). An exploratory analysis of California residential customer response to critical peak pricing of electricity. *Energy, 32*(1), 25-34.

Herter, K., & Wayland, S. (2010). Residential response to critical-peak pricing of electricity: California evidence. *Energy, 35*(4), 1561-1567.

Hirsch, J. (2010). eQUEST: Introductory tutorial, version 3.63. *Camarillo, CA*.

Hu, M., & Xiao, F. (2018). Price-responsive model-based optimal demand response control of inverter air conditioners using genetic algorithm. *Applied Energy, 219*, 151-164.

Hu, M., Xiao, F., & Wang, L. (2017). Investigation of demand response potentials of residential air conditioners in smart grids using grey-box room thermal model. *Applied Energy, 207*, 324-335.

Hubert, T., & Grijalva, S. (2012). Modeling for residential electricity optimization in dynamic pricing environments. *Smart Grid, IEEE Transactions on, 3*(4), 2224-2231.

Ipakchi, A., & Albuyeh, F. (2009). Grid of the future. *Power and Energy Magazine, IEEE, 7*(2), 52-62.

Kamyab, F., Amini, M., Sheykhha, S., Hasanpour, M., & Jalali, M. M. (2016). Demand response program in smart grid using supply function bidding mechanism. *IEEE Transactions on Smart Grid, 7*(3), 1277-1284.

Kandlikar, S. G. (1990). A general correlation for saturated two-phase flow boiling heat transfer inside horizontal and vertical tubes. *Journal of heat transfer, 112*(1), 219-228.

Kapadia, R., Jain, S., & Agarwal, R. (2009). Transient characteristics of split air-conditioning systems using R-22 and R-410A as refrigerants. *HVAC&R Research, 15*(3), 617-649.

Karlsson, H., & Hagentoft, C.-E. (2011). Application of model based predictive control for water-based floor heating in low energy residential buildings. *Building and Environment, 46*(3), 556-569.

Katipamula, S., & Lu, N. (2006). Evaluation of residential HVAC control strategies for demand response programs. *ASHRAE Transctions, 112*(1), 535.

Kavaklioglu, K. (2011). Modeling and prediction of Turkey's electricity consumption using Support Vector Regression. *Applied Energy, 88*(1), 368-375.

Kim, M.-H., & Bullard, C. W. (2001). Dynamic characteristics of a R-410A split air-conditioning system. *International Journal of Refrigeration, 24*(7), 652-659.

Klein, S., Beckman, W., Mitchell, J., Duffie, J., Duffie, N., & Freeman, T. (2017). TRNSYS 18: A Transient System Simulation Program, Solar Energy Laboratory, University of Wisconsin, Madison, USA.

Klein, S. A. (1979). *TRNSYS, a transient system simulation program*. Madison: Solar Energy Laborataory, University of Wisconsin--Madison.

Koury, R., Machado, L., & Ismail, K. (2001). Numerical simulation of a variable speed refrigeration system. *International Journal of Refrigeration, 24*(2), 192-200.

Kusiak, A., Xu, G., & Tang, F. (2011). Optimization of an HVAC system with a strength multi-objective particle-swarm algorithm. *Energy, 36*(10), 5935-5943.

Lam, J. C., Lun, I. Y., & Li, D. H. (2000). Long-term wind speed statistics and implications for outside surface thermal resistance. *Architectural Science Review, 43*(2), 95-100.

Lam, J. C., Tsang, C. L., Li, D. H. W., & Cheung, S. O. (2005). Residential building envelope heat gain and cooling energy requirements. *Energy, 30*(7), 933-951.

Leducq, D., Guilpart, J., & Trystram, G. (2003). Low order dynamic model of a vapor compression cycle for process control design. *Journal of food process engineering, 26*(1), 67-91.

Li, Q., Meng, Q., Cai, J., Yoshino, H., & Mochida, A. (2009a). Applying support vector machine to predict hourly cooling load in the building. *Applied Energy, 86*(10), 2249-2256.

Li, Q., Meng, Q., Cai, J., Yoshino, H., & Mochida, A. (2009b). Predicting hourly cooling load in the building: A comparison of support vector machine and different artificial neural networks. *Energy Conversion and Management, 50*(1), 90-96.

Li, S., & Zhang, D. (2014). *Developing smart and real-time demand response mechanism for residential energy consumers.* Paper presented at the Power Systems Conference (PSC), 2014 Clemson University.

Li, S., Zhang, D., Roget, A. B., & O'Neill, Z. (2014). Integrating home energy simulation and dynamic electricity price for demand response study. *Smart Grid, IEEE Transactions on, 5*(2), 779-788.

Li, X., & Malkawi, A. (2016). Multi-objective optimization for thermal mass model predictive control in small and medium size commercial buildings under summer weather conditions. *Energy, 112*, 1194-1206.

Lin, Y., Barooah, P., Meyn, S., & Middelkoop, T. (2015). Experimental Evaluation of Frequency Regulation From Commercial Building HVAC Systems. *IEEE Transactions on Smart Grid, 6*(2), 776-783.

Lin, Y., Middelkoop, T., & Barooah, P. (2012, 10-13 Dec. 2012). *Issues in identification of control-oriented thermal models of zones in multi-zone buildings.* Paper presented at the 2012 IEEE 51st IEEE Conference on Decision and Control (CDC).

Löfberg, J. (2004). *YALMIP: A toolbox for modeling and optimization in MATLAB.* Paper presented at the Computer Aided Control Systems Design, 2004 IEEE International Symposium on.

Lu, N. (2012). An evaluation of the HVAC load potential for providing load balancing service. *Smart Grid, IEEE Transactions on, 3*(3), 1263-1270.

Lujano-Rojas, J. M., Monteiro, C., Dufo-López, R., & Bernal-Agustín, J. L. (2012). Optimum residential load management strategy for real time pricing (RTP) demand response programs. *Energy Policy, 45*, 671-679.

Ma, J., Qin, J., Salsbury, T., & Xu, P. (2012). Demand reduction in building energy systems based on economic model predictive control. *Chemical Engineering Science, 67*(1), 92-100.

Ma, Y., Borrelli, F., Hencey, B., Coffey, B., Bengea, S., & Haves, P. (2012). Model predictive control for the operation of building cooling systems. *Control Systems Technology, IEEE Transactions on, 20*(3), 796-803.

Ma, Y., Kelman, A., Daly, A., & Borrelli, F. (2012). Predictive control for energy efficient buildings with thermal storage. *IEEE Control System Magazine, 32*(1), 44-64.

Ma, Y., Matuško, J., & Borrelli, F. (2015). Stochastic model predictive control for building HVAC systems: Complexity and conservatism. *IEEE Transactions on Control Systems Technology, 23*(1), 101-116.

MacArthur, J. W., & Grald, E. W. (1989). Unsteady compressible two-phase flow model for predicting cyclic heat pump performance and a comparison with experimental data. *International Journal of Refrigeration, 12*(1), 29-41.

MathWorks. (2012). MATLAB and Statistics Toolbox Release: Natick, MA: The MathWorks.

Meissner, J. W., Abadie, M. O., Moura, L. M., Mendonça, K. C., & Mendes, N. (2014). Performance curves of room air conditioners for building energy simulation tools. *Applied Energy, 129*, 243-252.

Messner, K., & Nadel, S. (2011). Joint Petition To ENERGY STAR To Adopt Stakeholder Agreement As It Relates To Smart Appliances. *Washington, DC: US Environmental Protection Agency. I*.

Molina, D., Lu, C., Sherman, V., & Harley, R. G. (2013). Model predictive and genetic algorithm-based optimization of residential temperature control in the presence of time-varying electricity prices. *Industry Applications, IEEE Transactions on, 49*(3), 1137-1145.

Morari, M., & Lee, J. H. (1999). Model predictive control: past, present and future. *Computers & Chemical Engineering, 23*(4), 667-682.

Motegi, N., Piette, M. A., Watson, D. S., Kiliccote, S., & Xu, P. (2007). Introduction to commercial building control strategies and techniques for demand response. *Lawrence Berkeley National Laboratory LBNL-59975*.

Mulroy, W., & Didion, D. (1985). Refrigerant migration in a split-unit air conditioner. Discussion. *ASHRAE transactions, 91*(1), 193-206.

Murphy, W. E., & Goldschmidt, V. (1985). Cyclic characteristics of a typical residential air conditioner-modeling of start-up transients. *ASHRAE transactions*, *91*(2A), 427-437.

Nocedal, J., & Wright, S. (2006). *Numerical optimization*: Springer Science & Business Media.

Oldewurtel, F. (2011). *Stochastic model predictive control for energy efficient building climate control.* Georgia Institute of Technology.

Oldewurtel, F., Parisio, A., Jones, C. N., Gyalistras, D., Gwerder, M., Stauch, V., . . . Morari, M. (2012). Use of model predictive control and weather forecasts for energy efficient building climate control. *Energy and Buildings*, *45*, 15-27.

Pacific Northwest National Laboratory. GridLAB-D software. Retrieved from http://gridlab-d.sourceforge.net/wiki/index.php/Main_Page

Paniagua-Tineo, A., Salcedo-Sanz, S., Casanova-Mateo, C., Ortiz-García, E. G., Cony, M. A., & Hernández-Martín, E. (2011). Prediction of daily maximum temperature using a support vector regression algorithm. *Renewable Energy*, *36*(11), 3054-3060.

Patteeuw, D., Bruninx, K., Arteconi, A., Delarue, E., D'haeseleer, W., & Helsen, L. (2015). Integrated modeling of active demand response with electric heating systems coupled to thermal energy storage systems. *Applied Energy*, *151*, 306-319.

Petukhov, B. (1970). Heat transfer and friction in turbulent pipe flow with variable physical properties. *Advances in heat transfer*, *6*, 503-564.

Piette, M. A., Sezgen, O., Watson, D. S., Motegi, N., Shockman, C., & Ten Hope, L. (2004). Development and evaluation of fully automated demand response in large facilities. *Lawrence Berkeley National Laboratory*.

Piette, M. A., Watson, D., Motegi, N., Kiliccote, S., & Xu, P. (2006). Automated Critical Peak Pricing field tests: Program description and results. *Lawrence Berkeley National Laboratory*.

PJM Interconnection. (2017). Hourly Real-Time & Day-Ahead Locational Marginal Pricing. Retrieved from http://www.pjm.com/markets-and-operations/energy/real-time/monthlylmp.aspx

Pratt, R. G., Conner, C. C., Drost, M. K., Miller, N. E., Cooke, B. A., Halverson, M. A., . . . Hauser, S. G. (1991). *Significant ELCAP analysis results: Summary report. [End-use Load and Consumer Assessment Program]* (PNL-6659; Other: ON: DE91009156 United States10.2172/6079039Other: ON: DE91009156Thu Dec 20 08:18:57 EST 2012OSTI; NTIS; GPO Dep.PNNL; EDB-91-051502; NTS-91-012032; ERA-16-014822English). Retrieved from http://www.osti.gov/scitech//servlets/purl/6079039/

Prívara, S., Cigler, J., Váňa, Z., Ferkl, L., & Šebek, M. (2010, 15-17 Dec. 2010). *Subspace identification of poorly excited industrial systems.* Paper presented at the 49th IEEE Conference on Decision and Control (CDC).

Prívara, S., Široký, J., Ferkl, L., & Cigler, J. (2011). Model predictive control of a building heating system: The first experience. *Energy and Buildings*, *43*(2-3), 564-572.

Qin, S. J. (2006). An overview of subspace identification. *Computers & Chemical Engineering*, *30*(10), 1502-1513.

Qin, S. J., & Badgwell, T. A. (2003). A survey of industrial model predictive control technology. *Control Engineering Practice, 11*(7), 733-764.

Qureshi, T., & Tassou, S. (1996). Variable-speed capacity control in refrigeration systems. *Applied Thermal Engineering, 16*(2), 103-113.

Rabl, A. (1988). Parameter estimation in buildings: methods for dynamic analysis of measured energy use. *Journal of Solar Energy Engineering, 110*(1), 52-66.

Rasmussen, B. P. (2005). *Dynamic modeling and advanced control of air conditioning and refrigeration systems.* (PhD), UIUC.

Rasmussen, B. P., & Alleyne, A. G. (2004). Control-Oriented Modeling of Transcritical Vapor Compression Systems. *Journal of dynamic systems, measurement, and control, 126*(1), 54-64.

Reynolds, J., Rezgui, Y., Kwan, A., & Piriou, S. (2018). A zone-level, building energy optimisation combining an artificial neural network, a genetic algorithm, and model predictive control. *Energy, 151*, 729-739.

Richardson, D., Jiang, H., Lindsay, D., & Radermacher, R. (2002). Optimization of vapor compression systems via simulation.

Richardson, D. H. (2006). An object oriented simulation framework for steady-state analysis of vapor compression refrigeration systems and components.

Ruan, Y., Liu, Q., Li, Z., & Wu, J. (2016). Optimization and analysis of Building Combined Cooling, Heating and Power (BCHP) plants with chilled ice thermal storage system. *Applied Energy, 179*, 738-754.

Seem, J. E. (1987). *Modeling of heat transfer in buildings.* Wisconsin Univ., Madison (USA).

Siano, P. (2014). Demand response and smart grids—A survey. *Renewable and Sustainable Energy Reviews, 30*, 461-478.

Simon, D. (2006). *Optimal state estimation: Kalman, H infinity, and nonlinear approaches*: John Wiley & Sons.

Široký, J., Oldewurtel, F., Cigler, J., & Prívara, S. (2011). Experimental analysis of model predictive control for an energy efficient building heating system. *Applied Energy, 88*(9), 3079-3087.

Smarra, F., Jain, A., de Rubeis, T., Ambrosini, D., D'Innocenzo, A., & Mangharam, R. (2018). Data-driven model predictive control using random forests for building energy optimization and climate control. *Applied Energy, 226*, 1252-1272.

Somasundaram, S., Pratt, R., Akyol, B., Fernandez, N., Foster, N., Katipamula, S., . . . Taylor, Z. (2014). Reference guide for a transaction-based building controls framework. *Pacific Northwest National Laboratory*.

Soyguder, S., Karakose, M., & Alli, H. (2009). Design and simulation of self-tuning PID-type fuzzy adaptive control for an expert HVAC system. *Expert Systems with Applications, 36*(3), 4566-4573.

Strbac, G. (2008). Demand side management: Benefits and challenges. *Energy Policy, 36*(12), 4419-4426.

Su, L., & Norford, L. K. (2015). Demonstration of HVAC chiller control for power grid frequency regulation—Part 2: Discussion of results and considerations for broader deployment. *Science and Technology for the Built Environment, 21*(8), 1143-1153.

Sun, Y., Wang, S., Xiao, F., & Huang, G. (2012). A study of pre-cooling impacts on peak demand limiting in commercial buildings. *HVAC&R Research, 18*(6), 1098-1111.

Tang, R., Wang, S., Gao, D.-C., & Shan, K. (2016). A power limiting control strategy based on adaptive utility function for fast demand response of buildings in smart grids. *Science and Technology for the Built Environment, 22*(6), 810-819.

Thomas, A. G., Jahangiri, P., Wu, D., Cai, C., Zhao, H., Aliprantis, D. C., & Tesfatsion, L. (2012). Intelligent residential air-conditioning system with smart-grid functionality. *Smart Grid, IEEE Transactions on, 3*(4), 2240-2251.

Torriti, J. (2012). Price-based demand side management: Assessing the impacts of time-of-use tariffs on residential electricity demand and peak shifting in Northern Italy. *Energy, 44*(1), 576-583.

Tree, D. R., & Weiss, B. W. (1986). Two time constant modeling approach for residential heat pumps.

Tuhus-Dubrow, D., & Krarti, M. (2010). Genetic-algorithm based approach to optimize building envelope design for residential buildings. *Building and Environment, 45*(7), 1574-1581.

Turner, W. J. N., Walker, I. S., & Roux, J. (2015). Peak load reductions: Electric load shifting with mechanical pre-cooling of residential buildings with low thermal mass. *Energy, 82*, 1057-1067.

U.S. Department of Energy. (2006). Benefits of demand response in electricity markets and recommendations for achieving them.

Van Overschee, P., & De Moor, B. (1994). N4SID: Subspace algorithms for the identification of combined deterministic-stochastic systems. *Automatica, 30*(1), 75-93.

Vanthournout, K., Dupont, B., Foubert, W., Stuckens, C., & Claessens, S. (2015). An automated residential demand response pilot experiment, based on day-ahead dynamic pricing. *Applied Energy, 155*, 195-203.

Vrettos, E., Lai, K., Oldewurtel, F., & Andersson, G. (2013). *Predictive control of buildings for demand response with dynamic day-ahead and real-time prices.* Paper presented at the European Control Conference (ECC), Zürich, Switzerland.

Wang, C.-C., Lee, C.-J., Chang, C.-T., & Lin, S.-P. (1999). Heat transfer and friction correlation for compact louvered fin-and-tube heat exchangers. *International Journal of Heat and Mass Transfer, 42*(11), 1945-1956.

Wang, C.-C., Lin, Y.-T., & Lee, C.-J. (2000). Heat and momentum transfer for compact louvered fin-and-tube heat exchangers in wet conditions. *International Journal of Heat and Mass Transfer, 43*(18), 3443-3452.

Wang, J., An, D., & Lou, C. (2006). *Application of fuzzy-PID controller in heating ventilating and air-conditioning system.* Paper presented at the Mechatronics and Automation, Proceedings of the 2006 IEEE International Conference on.

Wang, S. (2016). Making buildings smarter, grid-friendly, and responsive to smart grids. *Science and Technology for the Built Environment, 22*(6), 629-632.

Wang, S., & Ma, Z. (2008). Supervisory and Optimal Control of Building HVAC Systems: A Review. *HVAC&R Research, 14*(1), 3-32.

Wang, S., & Tang, R. (2016). Supply-based feedback control strategy of air-conditioning systems for direct load control of buildings responding to urgent requests of smart grids. *Applied Energy*.

Wang, S., & Xu, X. (2006). Parameter estimation of internal thermal mass of building dynamic models using genetic algorithm. *Energy Conversion and Management, 47*(13-14), 1927-1941.

Wang, S., Xue, X., & Yan, C. (2014). Building power demand response methods toward smart grid. *HVAC&R Research, 20*(6), 665-687.

Wang, W., Chen, J., & Hong, T. (2018). Occupancy prediction through machine learning and data fusion of environmental sensing and Wi-Fi sensing in buildings. *Automation in Construction, 94*, 233-243.

Wang, W., Chen, J., & Song, X. (2017). Modeling and predicting occupancy profile in office space with a Wi-Fi probe-based Dynamic Markov Time-Window Inference approach. *Building and Environment, 124*, 130-142.

Watson, D. S., Kiliccote, S., Motegi, N., & Piette, M. A. (2006). Strategies for demand response in commercial buildings. *Lawrence Berkeley National Laboratory*.

Wedekind, G., Bhatt, B., & Beck, B. (1978). A system mean void fraction model for predicting various transient phenomena associated with two-phase evaporating and condensing flows. *International Journal of Multiphase Flow, 4*(1), 97-114.

Winkelmann, F., Birdsall, B., Buhl, W., Ellington, K., Erdem, A., Hirsch, J., & Gates, S. (1993). *DOE-2 supplement: version 2.1 E*. Retrieved from

Xu, P., & Haves, P. (2006). Case study of demand shifting with thermal mass in two large commercial buildings. *ASHRAE transactions, 112*(1), 572.

Xu, P., Haves, P., Piette, M. A., & Braun, J. (2004). Peak demand reduction from pre-cooling with zone temperature reset in an office building. *Lawrence Berkeley National Laboratory*.

Xu, X., & Wang, S. (2007). Optimal simplified thermal models of building envelope based on frequency domain regression using genetic algorithm. *Energy and Buildings, 39*(5), 525-536.

Xuemei, L., Lixing, D., Yan, L., Gang, X., & Jibin, L. (2010). *Hybrid genetic algorithm and support vector regression in cooling load prediction.* Paper presented at the Knowledge Discovery and Data Mining, 2010. WKDD'10. Third International Conference on.

Yao, J. (2018). Modelling and simulating occupant behaviour on air conditioning in residential buildings. *Energy and Buildings, 175*, 1-10.

Yin, R., Xu, P., Piette, M. A., & Kiliccote, S. (2010). Study on Auto-DR and pre-cooling of commercial buildings with thermal mass in California. *Energy and Buildings, 42*(7), 967-975.

Yoon, J. H., Bladick, R., & Novoselac, A. (2014). Demand response for residential buildings based on dynamic price of electricity. *Energy and Buildings, 80*, 531-541.

York, D. A., & Tucker, E. F. (1980). *DOE-2 Reference Manual Part 1 Version 2.1* (LA-7689-M(Ver.2.1)(Pt.1); LBL-8706(Rev.1)(Pt.1) United StatesWed Feb 06 19:00:48 EST 2008NTIS, PC A99/MF A01.LANL; ERA-05-032444;

EPA-06-004261; EDB-80-101819English). Retrieved from Los Alamos, New Mexico:

Zakula, T., Gayeski, N. T., Armstrong, P. R., & Norford, L. K. (2011). Variable-speed heat pump model for a wide range of cooling conditions and loads. *HVAC&R Research, 17*(5), 670-691.

Zhang, F., & de Dear, R. (2015). Thermal environments and thermal comfort impacts of Direct Load Control air-conditioning strategies in university lecture theatres. *Energy and Buildings, 86*, 233-242.

Zhang, F., de Dear, R., & Candido, C. (2016). Thermal comfort during temperature cycles induced by direct load control strategies of peak electricity demand management. *Building and Environment, 103*, 9-20.

Zhang, W., Lian, J., Chang, C.-Y., & Kalsi, K. (2013). Aggregated modeling and control of air conditioning loads for demand response. *Power Systems, IEEE Transactions on, 28*(4), 4655-4664.

Zhang, Y., Bai, X., Mills, F. P., & Pezzey, J. C. V. (2018). Rethinking the role of occupant behavior in building energy performance: A review. *Energy and Buildings, 172*, 279-294.

Zhou, B., Li, W., Chan, K. W., Cao, Y., Kuang, Y., Liu, X., & Wang, X. (2016). Smart home energy management systems: Concept, configurations, and scheduling strategies. *Renewable and Sustainable Energy Reviews, 61*, 30-40.

Zhou, Q., Wang, S., Xu, X., & Xiao, F. (2008). A grey‐box model of next‐day building thermal load prediction for energy‐efficient control. *International Journal of Energy Research, 32*(15), 1418-1431.

Zhou, R., Zhang, T., Catano, J., Wen, J. T., Michna, G. J., Peles, Y., & Jensen, M. K. (2010). The steady-state modeling and optimization of a refrigeration system for high heat flux removal. *Applied Thermal Engineering, 30*(16), 2347-2356.